DANMARKS OG GRØNLANDS GEOLOGISKE UNDERSØGELSE RAPPORT 2016/50

PROMICE 2015

Report for the 2015 operational phase of the Programme for Monitoring of the Greenland Ice Sheet

Andersen, S.B., Ahlstrøm, A.P., Andersen, M.L., Box, J.,
Citterio, M., Charalampidis, C., Colgan, W.T.,
Fausto, R.S., Larsen, S.H., Machguth, H.,
Solgaard, A.M., As, D.v., Veicherts, M.,
Pedersen, D.,Nielsen, J.E.,
Hvidegaard, S.M., Simonsen, S.B.,
Sørensen, L.S. & Forsberg, R.

GEOLOGICAL SURVEY OF DENMARK AND GREENLAND
DANISH MINISTRY OF ENERGY, UTILITIES AND CLIMATE

GEUS

PROMICE 2015

Report for the 2015 operational phase of the Programme for Monitoring of the Greenland Ice Sheet

Andersen, S.B., Ahlstrøm, A.P., Andersen, M.L., Box, J.,
Citterio, M., Charalampidis, C., Colgan, W.T.,
Fausto, R.S., Larsen, S.H., Machguth, H.,
Solgaard, A.M., As, D.v., Veicherts, M.,
Pedersen, D.,Nielsen, J.E.,
Hvidegaard, S.M., Simonsen, S.B.,
Sørensen, L.S. & Forsberg, R.

GEOLOGICAL SURVEY OF DENMARK AND GREENLAND
DANISH MINISTRY OF ENERGY, UTILITIES AND CLIMATE

G E U S

PROMICE 2015

Report for the 2015 operational phase of the Programme for Monitoring of the Greenland Ice Sheet

Signe B. Andersen, Andreas P. Ahlstrøm, Morten L. Andersen, Jason E. Box, Michele Citterio, Charalampos Charalampidis, William Colgan, Robert S. Fausto, Signe Hillerup Larsen, Horst Machguth, Anne M. Solgaard, Dirk van As, Martin Veichert, GEUS

Dorthe Petersen, Asiaq

Jens Emil Nielsen, Sine Munk Hvidegaard, Henriette Skourup, Sebastian B. Simonsen, Louise Sandberg Sørensen, René Forsberg, DTU-Space

GEUS, 2016

Contents

Summary 5

Automatic weather stations 7

Ice velocity mapping 14

Airborne LiDAR campaign 2015 15

Airborne survey camera and spectrometer 18

Glacier mapping 20

Observations of runoff from the Greenland ice sheet 27

Collaboration with DMI modelling 33

Outreach 35

SWIPA input 37

Related projects 41

WMO CryoNet 42

References 44

Appendix A: Data ....

Appendix B: Newsletters ....

Appendix C: Publications from PROMICE ....

Appendix D: ROSA paper ....

Summary

The Programme for Monitoring of the Greenland Ice Sheet (PROMICE) is as an on-going effort to monitor changes in the mass budget of the Greenland Ice Sheet and is operated by the Geological Survey of Denmark and Greenland (GEUS) in collaboration with the National Space Institute (DTU Space) and the Greenland Survey (Asiaq) started in 2007.

A central part of PROMICE is the network of presently 22 automatic weather stations (AWS) situated in the ablation zone of the Greenland ice sheet. Combining these with airborne surveys of ice thickness and mapping of ice velocities makes it possible to estimate the mass loss of the Greenland ice sheet. Also mapping of individual glaciers and ice caps surrounding the ice sheet is done to assess the mass loss. The PROMICE data can be used directly as indicators of climate change - becoming more and more valuable as the monitoring period increases. Furthermore the programme contributes through observations to process-oriented studies to understand the mass loss as well as validation efforts to improve ice sheet models and future predictions.

PROMICE is committed to maintain an accessible, safe and thoroughly documented database for storing and disseminating the data free of charge to the climate research community.

This report updates on PROMICE activities for the year 2015. It is not intended to give a complete overview of the programme. More information about PROMICE may be found in the earlier PROMICE reports (Ahlstrøm et al., 2011, Andersen et al., 2013, Andersen et al., 2014, Andersen et al. 2015).

The mass loss from the Greenland ice sheet has increased significantly since the beginning of this century. For the year 2015 we find that melt was average on the southern half of the ice sheet, and even below average in the southwest. However, during the summer anomalously warm conditions occurred northwest of Greenland, resulting in record high temperatures observed at the PROMICE stations in Thule and above-average melting on the northern half of the ice sheet.

Some main achievements for 2015 are:

- Successful monitoring by 22 automatic weather stations on the Greenland ice sheet
- The first ice velocity maps from the European Sentinel-1 satellite were produced
- Airborne survey of ice elevation along the entire ice sheet margin was repeated by DTU Space
- The airborne survey also included a set of optical sensors for measuring spectral albedo
- Collaboration with DMI on evaluating and improving ice sheet models using PROMICE observations continued
- A glacier area change database was finalized and will be made freely available for download on the PROMICE website (see Newsletter no. 8, Appendix D)
- Study on the capacity of the Greenland ice sheet to store meltwater (Newsletter 9, Appendix D)
- The PROMICE team contributed to 21 peer reviewed ISI-tracked scientific journal publications in 2015. 13 of these directly incorporated PROMICE observations
- The Snow Water Ice Permafrost in the Arctic (SWIPA) update will include 20 publications using PROMICE data
- PROMICE contributed to Polar Portal, a website where Danish research institutions display the results of their monitoring of the Greenland ice sheet and the sea ice in the Arctic to the general public (polarportal.org)

Automatic weather stations

The network

The PROMICE station network currently consists of automatic weather station (AWS) transects in eight melt regions of the Greenland ice sheet (GrIS), adding up to 20 stations in total, of which 17 are on the ice sheet proper (Figure 1, Table 1). In each region, one station is located in the lower ablation zone close to the margin, and one or two in the middle/upper ablation zone, to obtain elevation gradients in the measured variables. Exceptions are KAN_U and KPC_U, located in the lower part of the accumulation zone; MIT and NUK_K, positioned on independent glaciers; and KAN_B, located on tundra at one kilometre from the ice sheet margin. The AWSs measure all important meteorological variables: air temperature (aspirated), pressure and humidity, wind speed, downward and upward solar (shortwave) and terrestrial (longwave) radiation. The AWSs also record temperature profiles in the upper 10 m of ice, GPS-derived location and diagnostic parameters such as station tilt, which is crucial for interpreting solar radiation measurements. A GEUS-developed pressure transducer and two sonic rangers measure snow and surface height change due to ablation and accumulation. Most variables are measured every ten minutes, with all data stored locally awaiting collection during maintenance visits. Hourly averages of the most transient variables are transmitted via satellite between days 100 and 300 of each year, while a selection of the remaining variables is transmitted at six-hour intervals. Transmissions have a lower (daily) frequency in the winter period to save battery power and transmission costs. All data and metadata including sensor specifications are archived in the PROMICE database and made freely available for display and download at www.promice.dk.

Figure 1. *Location and identification codes of PROMICE automatic weather stations. The ZAK and MAL stations are GEUS stations from other projects. The KAN stations are mosly financed by the Greenland Analogue Project (GAP), a PROMICE collaborator. Dotted lines are elevation contours in m above sea level.*

Table 1. Metadata for the PROMICE automatic weather station network after the 2015 field season.

Station name	Latitude (°N)	Longitude (°W)	Elevation (m asl)	Start date	Last visit	Project
KPC_L	79.9108	24.0832	370	17/07/2008	2012	PROMICE
KPC_U	79.8345	25.1665	870	17/07/2008	2012	PROMICE
SCO_L	72.2240	26.8180	470	21/07/2008	2014	PROMICE
SCO_U	72.3937	27.2383	980	21/07/2008	2014	PROMICE
MIT*	65.6923	37.8277	450	03/05/2009	2015	PROMICE
TAS_L	65.6403	38.8987	260	23/08/2007	2015	PROMICE
TAS_U***	65.6978	38.8668	570	15/08/2007	13/08/2015	PROMICE
TAS_A	65.7797	38.9008	890	28/08/2013	2015	PROMICE/REFREEZE
QAS_L	61.0308	46.8488	280	24/08/2007	2015	PROMICE
QAS_U	61.1758	46.8190	900	07/08/2008	2015	PROMICE
QAS_A***	61.2430	46.7328	1000	20/08/2012	24/08/2015	PROMICE/REFREEZE
NUK_L	64.4822	49.5325	540	20/08/2007	2015	PROMICE/IMGLACO
NUK_U	64.5110	49.2663	1130	20/08/2007	2015	PROMICE/IMGLACO
NUK_K*	64.1623	51.3587	710	28/07/2014	2015	Asiaq/PROMICE
NUK_N***	64.9452	49.8850	920	25/07/2010	25/07/2014	PROMICE/IMGLACO
KAN_B**	67.1252	50.1832	350	13/04/2011	2015	GRASP/PROMICE
KAN_L	67.0957	49.9485	680	01/09/2008	2015	GAP/PROMICE
KAN_M	67.0667	48.8327	1270	02/09/2008	2015	GAP/PROMICE
KAN_U	67.0003	47.0243	1840	04/04/2009	2015	GAP/PROMICE
UPE_L	72.8932	54.2953	220	17/08/2009	2015	PROMICE
UPE_U	72.8883	53.5715	940	17/08/2009	2015	PROMICE
THU_L	76.3998	68.2662	570	09/08/2010	2014	PROMICE
THU_U	76.4197	68.1460	770	09/08/2010	2014	PROMICE

* On independent glacier ** On land *** Discontinued

Servicing the stations in the field

Since PROMICE AWSs are there for an important part to monitor melt and its atmospheric forcings, the stations are often located in high-melt regions where equipment melts out and the uneven terrain can prove harsh on station stability. In addition, the ongoing cycles of freezing and thawing, and the powerful katabatic winds and winter storms can be harmful to instruments. We therefore visit all stations every one to three or four years, balancing cost with necessity and opportunity. In 2015, we serviced PROMICE stations in five regions, namely Tasiilaq (TAS), Qassimiut (QAS), Nuuk (NUK), Kangerlussuaq (KAN), and Upernavik (UPE). The QAS region is regarded as the PROMICE primary site due to its high ablation up to 9 m per year (Fausto et al., 2012), so in 2014 an additional ablation stake line was set up and has been serviced annually since then. Transmissions from the six unvisited stations indicated that they were functional.

Some PROMICE AWSs are partly or entirely financed by other projects, namely the KAN stations (financed by the Greenland Analogue Project) and NUK_K (serviced by PROMICE partner Asiaq).

PROMICE also shares logistics with other projects. For instance, TAS_A is currently accompanied by a snow pack analyzer (SPA) that can provide measurements of changes in the snow pack during melt in Spring. In the SCO, QAS, NUK and UPE region we serviced GPSs and/or time-lapse cameras in addition. At KAN_U we drill firn cores annually, which have been revealing changes in the ice sheet's ability to retain meltwater (Charalampidis et al., 2015; Machguth et al., 2016).

Measurements

The most important PROMICE AWS measurement is that of surface mass balance, which is negative indicating net ablation in the low elevation areas of the Greenland ice sheet. Table 2 lists the annual net ablation values for all PROMICE weather stations for all years. Figure 2 gives an overview of the anomalies in net annual ablation for each year of measurements relative to the period 2011-2015 where all PROMICE stations have been operational. Note that the period 2011-2015 includes extreme years in terms of melt. Thus the figure gives an indication of the relative distribution of melt over the PROMICE period but not the long term evolution. Annual ablation in the southern part of Greenland typically amounts to 3-9 m of ice (at the lower TAS, QAS and NUK stations), while ablation at the more northerly SCO_L and UPE_L stations is 2-3 m. Ablation at the upper stations (>500 m a.s.l.) typically amounts to 0-3 m of ice. Thus ablation is highly dependent on elevation, latitude and local climate. For the year 2015 we find that ablation was average on the southern half of the ice sheet, and even below average in the southwest (Figure 3). During the summer anomalously warm conditions occurred northwest of Greenland, resulting above-average melting on the northern half of the ice sheet (Tedesco et al., 2016), culminating in a 184 ± 43% ablation anomaly at the THU_L station (Van As et al., 2016). Note that these values were adjusted to the commonly used 1961-1990 reference period. Since the start of PROMICE, we obtained ablation totals for all stations and years, adding up to 126 station years. The high success rate can be attributed to our approach of measuring the key observation of ablation with a range of different methods (pressure transducers, sonic rangers and stakes).

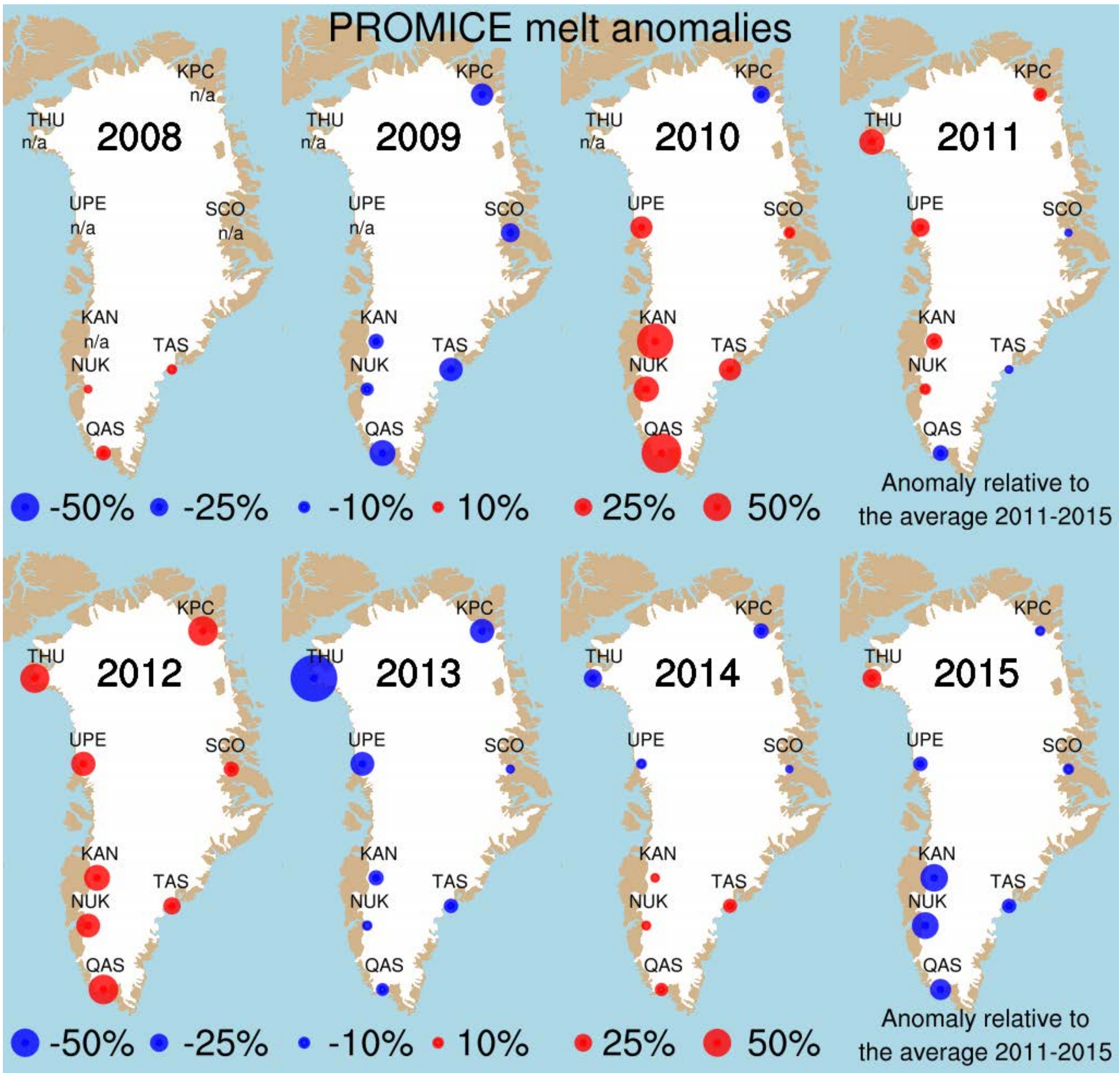

Figure 2. *Annual net ablation anomalies at the PROMICE sites, referenced to the 2011-2015 period. Note that the period 2011-2015 include extreme years in terms of melt.*

Table 2. Annual net ablation (m of ice) at all PROMICE weather stations on the Greenland ice sheet. Negative values indicate net accumulation…

Year	KPC_L	KPC_U	SCO_L	SCO_U	TAS_L	TAS_U	TAS_A	QAS_L	QAS_U	QAS_A	NUK_L	NUK_U	NUK_N	KAN_L	KAN_M	KAN_U	UPE_L	UPE_U	THU_L	THU_U
2008					3.6	3.3		7.3	0.8		5.3	2.2								
2009	1.6	-0.1	2.6	1.4	2.5	1.5		4.1	-0.3		4.8	1.5		3.5	0.3					
2010	1.7	0.1	3.5	2.5	4.9	3.9		9.3	3		7.2	3.3		5.4	2.6		3.2	2.7		
2011	2.5	0.2	3.1	2.3	3.4	2.9		4.7	0.8		5.7	2.3	4.5	4	1.7	-0.2	2.9	2.6	2.4	1.1
2012	3.3	0.3	3.6	2.9	4.3	3.7		8.5	2.1		6.9	3.3	4.7	4.7	2.1	0.7	3.3	2.8	2.5	1.2
2013	1.6	-0.2	3.3	2	2.9	2.5		5.9	0.1	0.1	4.9	1.9	2.5	3	0.8	-0.1	1.6	1	0.3	-0.2
2014	2.1	-0.2	3.4	2	4.3	3.2	1.7	6.1	1.7	1.4	5.7	2		3.5	1.4	-0.3	2.4	1.6	1.6	0.2
2015	2.3	-0.1	3.2	1.8	3.1	2.3	0.3	5.1	-0.5	-0.7	3.8	0.1		2.5	-0.1	-0.4	2.3	1.3	2.4	0.7

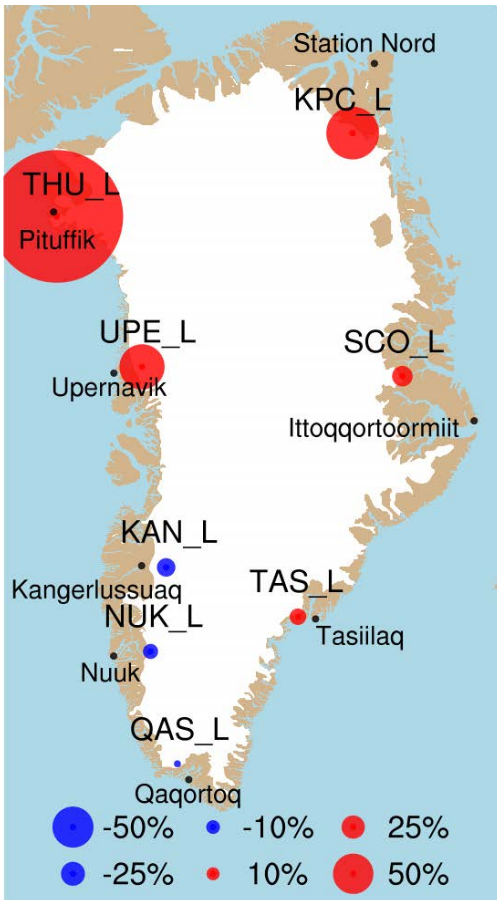

Figure 3. *Annual net ablation anomalies at the lower PROMICE sites for 2015, referenced to the 1961-1990 standard period (Van As et al., 2016; Appendix D).*

Net ablation, air temperature, wind speed, downward solar (shortwave) and terrestrial (longwave) radiation, surface albedo and surface elevation at all AWSs on the ice sheet are plotted in Appendix A. Here we describe the measurements in short.

All PROMICE stations record a distinct annual cycle in air temperature. As is common in the Arctic climate, temporal variability is largest in winter due to a more vigorous atmospheric circulation. The amplitude in the annual air temperature cycle is largest for stations at high latitudes or high elevations since here a melting ice surface capable of local thermo-regulation is least frequent. The more northerly stations also show a larger annual temperature cycle due to the increasing contrast in the lengths of polar day and night with increasing latitude. The smallest amplitude in the annual temperature cycle is seen at QAS_L, the most southerly PROMICE site. 2015 was a cold year according to the PROMICE measurements, especially those taken at the southwesterly NUK and KAN sites. Here, monthly temperatures were below the (relatively warm) PROMICE average throughout the entire year, exceeding one standard deviation below average in January, February, August, November and December. This also occurred at QAS during the entire first half of 2015.In contrast, more than half of all monthly-average temperatures taken in the far north (KPC and THU) were above the PROMICE average. Most notable, and relevant to the above-mentioned ablation anomaly in the north, are the above-average July temperatures, ranging from +0.3 to +1.6 standard deviations at the KPC, SCO, UPE and THU sites. Overall, we have an 88% success rate in collecting monthly average temperatures up to and including the 2015 field season.

The wind regimes over the ice sheet are distinctly different between regions. Winds are stronger at the higher-positioned AWSs. The highest monthly-mean wind speed values were recorded at KAN_M and KAN_U (1270 and 1840 m a.s.l.), and TAS_U and TAS_A (570 and 900 m a.s.l.). The strongest mean wind occurs in winter, causing a pronounced yearly cycle. The exception to the rule is the THU region in northwest Greenland, which does not show a yearly wind speed cycle. These THU AWSs are positioned on a protruding lobe of the ice sheet that does not sufficiently function as a barrier for mesoscale-scale weather systems, resulting in strong winds year-round. Storms are fairly common in the TAS region, as measured by the AWSs. These storm events are known as Piteraqs and build up momentum due to the alignment of katabatic and large-scale synoptic scale weather forcing. These notorious storms have repeatedly caused severe damage to the town of Tasiilaq. The Piteraq on 27 April 2013 as measured at TAS_U was exceptionally strong in reference to the whole PROMICE period, with winds exceeding 42 m/s (150 km/h) at about 3 m above the surface (Van As et al., 2014).

An important instrument on the PROMICE AWS is the radiometer, measuring the up- and downward radiative fluxes, which govern the surface energy budget and thus melt of the ice sheet. Both the short- and longwave components show a large annual cycle, with distinct differences with latitude (see e.g. the length of the polar night from shortwave radiation). In regions with a more frequent cloud cover (e.g. TAS) the radiative fluxes show a larger interannual variability than in regions where clear skies prevail (e.g. KAN).

The surface albedo is generally high in the cold, snow-covered interior of the ice sheet (>0.75), and lower along the ice sheet margin where melting occurs in summer. In wintertime, the ice sheet is fully snow covered except where wind erosion dominates. Depending on the location of each AWS in the ablation area, snow melt starts in April or May as seen from air temperatures and decreasing albedo. Thereafter, albedo drops throughout the melt season until snowfall occurs in autumn, yielding a distinct annual cycle which is largest at the high-melt sites. Surface melt chiefly causes this annual darkening of the ice sheet surface as snow undergoes heat-driven metamorphosis, or completely melts to expose darker bare ice. The ice sheet surface may also darken as impurities collect on the ice surface or supraglacial meltwater-filled features become more abundant. We find that surface albedo on average drops below fresh snow values as monthly-mean temperatures exceed –2°C due to an increase in surface melt. Although absorbed solar radiation is the primary source of melt energy, the melt-albedo feedback is initiated by the energy fluxes that respond to changes in temperature, such as downward longwave radiation and the turbulent heat fluxes. Since both atmospheric warming and ice sheet darkening increase surface melt intensity and melt area, the anticipated future warming will result in a self-reinforcing ice sheet mass loss contribution from the melt-albedo feedback. At the PROMICE sites, where ice surfaces after the winter snow cover has melted, the length of the bare ice season is most important for annual ablation as the interannual variability in albedo minimum is small. With the exception of the northerly sites, we find that 2015 summer albedo was either average or above-average (see e.g. KAN_M in Appendix A). In very few sites we may detect a darkening trend in summer albedo, e.g. at QAS_L. PROMICE keeps a close eye on the darkening of the ice sheet due to its importance to the ice sheet surface mass balance (Van As et al., 2013). In general the PROMICE albedo measurement receives proper attention due to its relevance to satellite validation, and for instance the MODIS satellite sensor degradation.

The bottom right plots in the AWS data figures (Appendix A) illustrate GPS-derived elevation. All stations display a lowering over the years which is mostly due to it moving downslope, with the flowing ice. These GPS show a remarkable amount of detail and information that is yet fairly unexplored in PROMICE. The small but distinct annual cycles in elevation at e.g. KPC_U, QAS_L and the UPE sites may suggest an intimate interplay between surface melt in summer and dynamic thickening in winter. Also, the lowering illustrates that once every few years the AWSs need to be relocated to a higher position to safeguard that data series are from the same climate zone / elevation. To date, this was done for QAS_L and the two NUK stations, as also revealed from Appendix A.

Ice velocity mapping

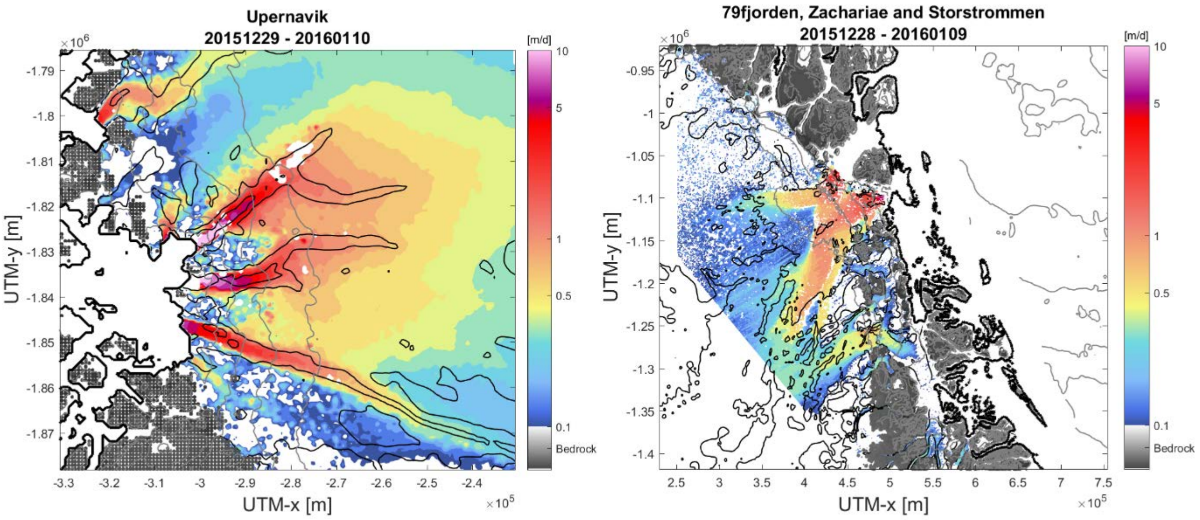

Figure 4. *Maps of surface velocity for Upernavik Isstrøm (left) and Nioghalvfjerdsfjorden Glacier, Zachariae Isstrøm and Storstrømmen Glacier (located top to bottom) (right). The velocities are derived from Sentinel-1 data covering a 12-day period at the beginning of January 2016 using the IPP software.*

Ice sheet velocities based on synthetic aperture radar (SAR) satellite data are derived at GEUS using software developed by DTU Space. Recently a new processing chain developed at DTU-spaced named IPP was implemented at GEUS. This has made it possible to process data from the new Sentinel-1 satellites. Figure 4 shows examples of ice velocity maps for Upernavik Isstrøm in West Greenland and Nioghalvfjerdsfjorden, Zachariae Isstrøm and Storstrømmen Glacier in Northeast Greenland based on data from the Sentinal-1a satellite having a 12-day repeat cycle.

The purpose is to use ice sheet velocities at regular intervals in order to assess changes in ice flow dynamics and quantify the impact of the changes on the mass loss of the Greenland ice sheet. Combining the velocity maps with ice thickness observations across a flux perimeter around the ice sheet as measured by the PROMICE airborne campaigns (described in the next chapter) allows quantification of the dynamic mass loss from glacier discharge. This was done for 2007 and 2011 in Andersen et al. (2015). With 2015 data from Sentinel-1a covering almost the entire Greenland ice sheet available and the ice thickness observations from the 2015 PROMICE airborne campaign processed shortly we will be in a position where we can calculate the 2015 dynamic mass loss.

Producing velocity maps over a region as large as the Greenland ice sheet is a major undertaking, relying on the availability and processing of large amounts of radar remote sensing data. Presently, GEUS is involved in the ESA Climate Change Initiative Ice Sheets Project lead by DTU Space, where one of the major products to be provided is ice velocity maps from ESA's SAR missions. PROMICE and the ESC_CCI Ice Sheets project benefit mutually by the sharing of data and processing tools.

Airborne LiDAR campaign 2015

Figure 5. *Twin Otter and crew from the airborne campaign.*

Introduction

In 2015, the National Space Institute (DTU Space) coordinated an airborne campaign in the periods August 21 – September 4 and September 29 – October 5 as part of PROMICE.

For the airborne campaign, a Twin Otter (TF-POF) was chartered from Norlandair, Iceland. The aircraft was equipped with a laser scanner to map the topography of the margins of the Greenland ice sheet as well as a selection of the major outlet glaciers. Similar PROMICE airborne campaigns were carried out in 2007 and 2011.

Summary of operation

Figure 6 shows an overview of the flight tracks from the PROMICE 2015 airborne campaign, shown with red lines and the date of flight and airport codes (see table below) indicated by blue. The PROMICE 2015 airborne campaign was split into two parts because of poor weather conditions in September.

Table 3.

Airports	
AEY	Akureyri
CNP	Constable Point
BGDB	Daneborg
DMH	Danmarkshavn
NRD	Station Nord
TAB	Thule Airbase
JQA	Qaarsut
SFJ	Kangerlussuaq
KUS	Kulusuk
UAK	Narsarsuaq
GOH	Nuuk

The first part took place in the period August 22 to September 6, 2015, and covered the stretch CNP-BGDB-BMH-NRD-TAB-JQA-SFJ while the second part took place in the period September 29 to October 4, 2015, and covered the stretch CNP-KUS-UAK-GOH-SFJ. For both parts the instruments were installed in the airplane in AEY.

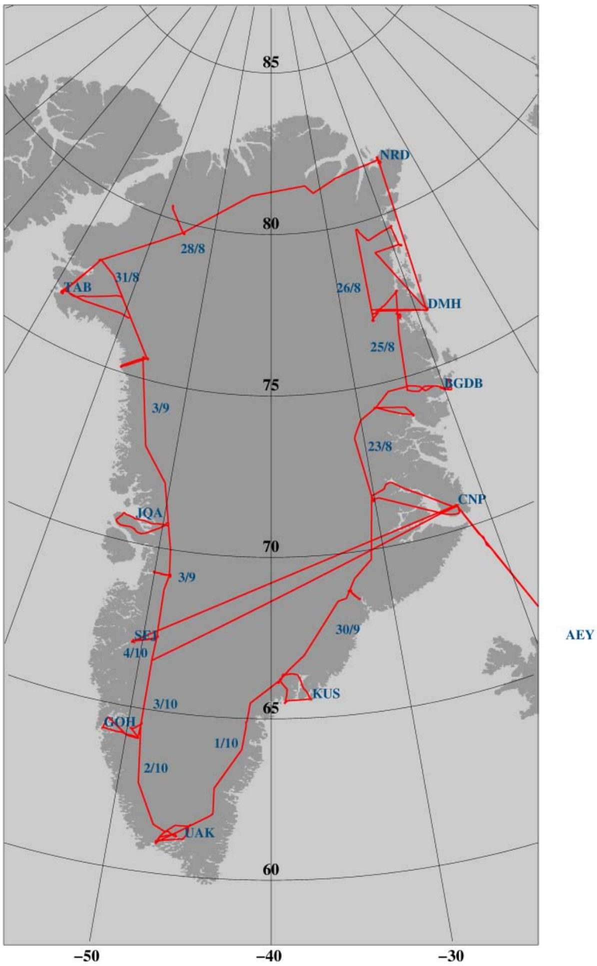

Figure 6. *Overview of the flight tracks from the PROMICE 2015 airborne campaign. Dates of the respective flights are marked next to the flight lines.*

The purpose of the PROMICE airborne campaigns is to measure the ice thickness (the flux gate) all around the Greenland ice sheet margin and along some of the major outlet glaciers. Since both the surface and bottom topography were measured along these flight lines in 2007 and 2011, and the bottom topography can be assumed constant, only the surface elevations were measured during the 2015 campaign. This was mapped by LiDAR measurements.

Status of data processing

All LiDAR data have now been processed, and the result is shown in Figure 8. This figure shows nadir elevations above the ellipsoid in the flight track.

The data still contains some outliers due to e.g. cloud cover and these still have to be filtered out (two examples are indicated by circles in Figure 7), and the data will then be packed in the right format and delivered together with a detailed data collection and processing report.

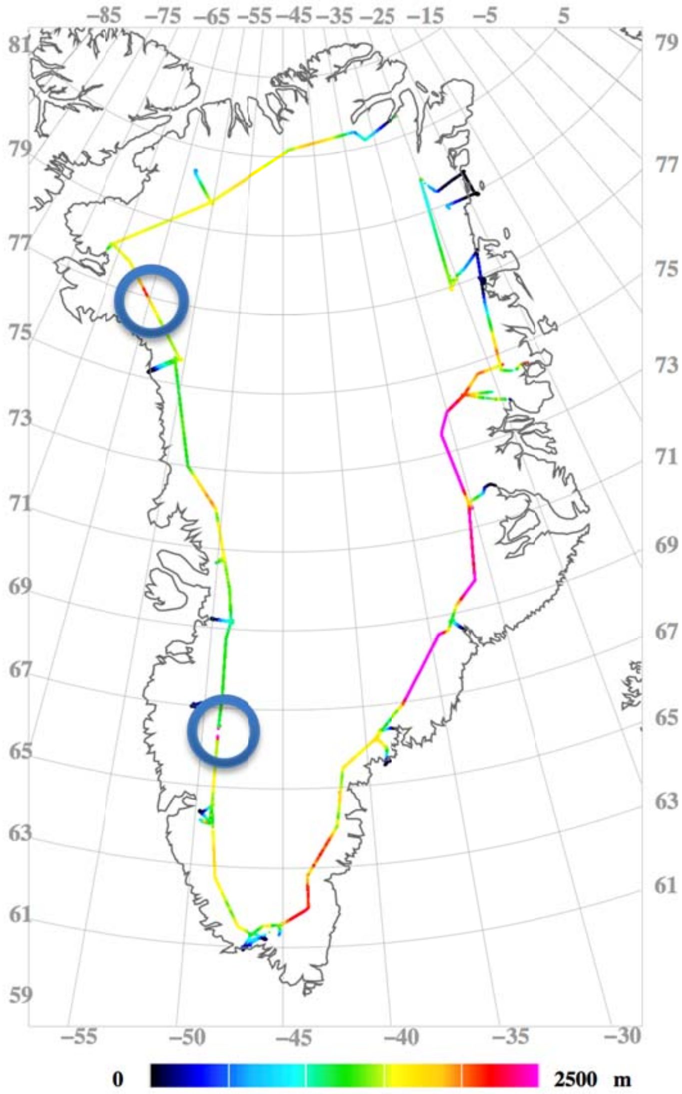

Figure 7. *Ice sheet elevations derived from the PROMICE 2015 airborne campaign. Circles indicate areas where outliers caused by clouds are evident.*

Airborne survey camera and spectrometer

A set of optical sensors were included in the 2015 PROMICE Twin Otter Survey around Greenland. These produce high spatial and spectral resolution imagery useful in studying factors (lakes, streams, dust, and microbial growth) contributing to reduction of surface albedo.

By combining a 20 band 'hyperspectral' (OCI) imager and 4 band 'multispectral' camera with incident light sensor, we build capacity to accomplish a new set of science goals. The 'multispectral' camera gives 1) snow/ice discrimination and 2) matches spectral regions from two satellite missions: a) NASA's Moderate Resolution Imaging Spectroradiometer (MODIS) on Terra and Aqua satellites and b) the recently launched European Space Agency (ESA) Sentinel-3 Ocean Land Colour Instrument (OLCI)/Sea and Land Surface Temperature Radiometer (SLSTR) combination.

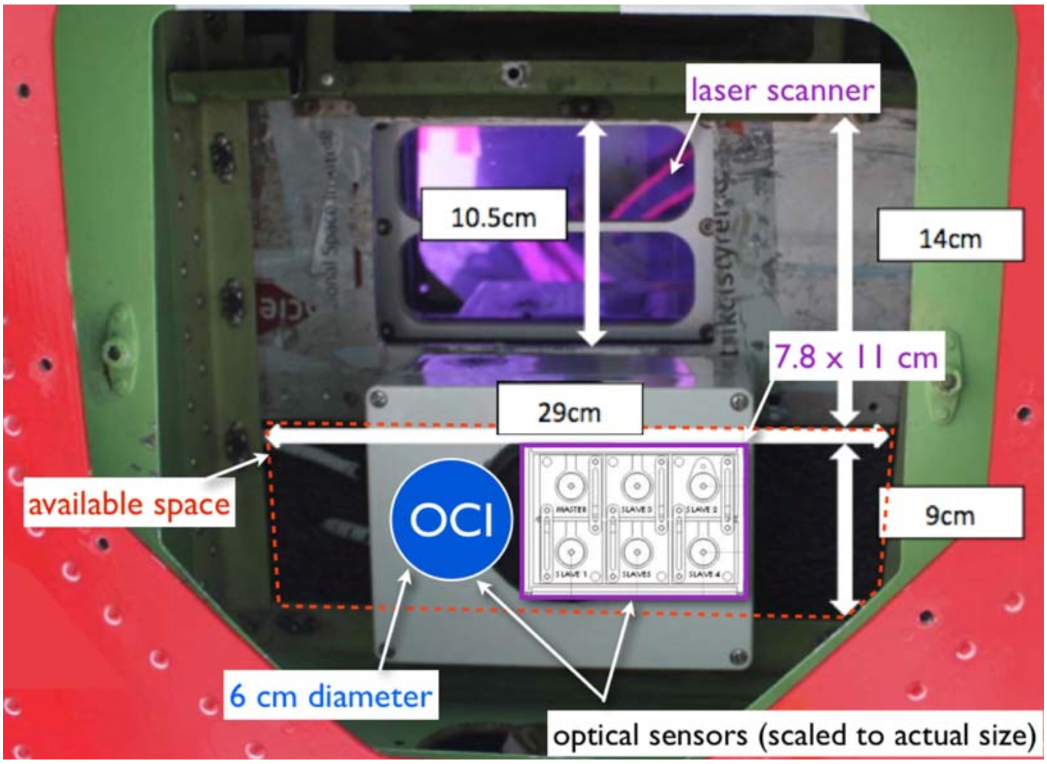

Figure 8. *Twin Otter belly port, photographed from below, showing the locations of OCI hyperspectral and MCA multispectral cameras complimenting the laser altimetry measurements.*

Each MCA scan produces 4 images corresponding to new ESA satellite Sentinel-3 with camera filters selected to match Sentinel-3 bands. The survey collected many thousands of images from the Multi Camera Array (MCA). Below is an example from photos captured over a snow surface.

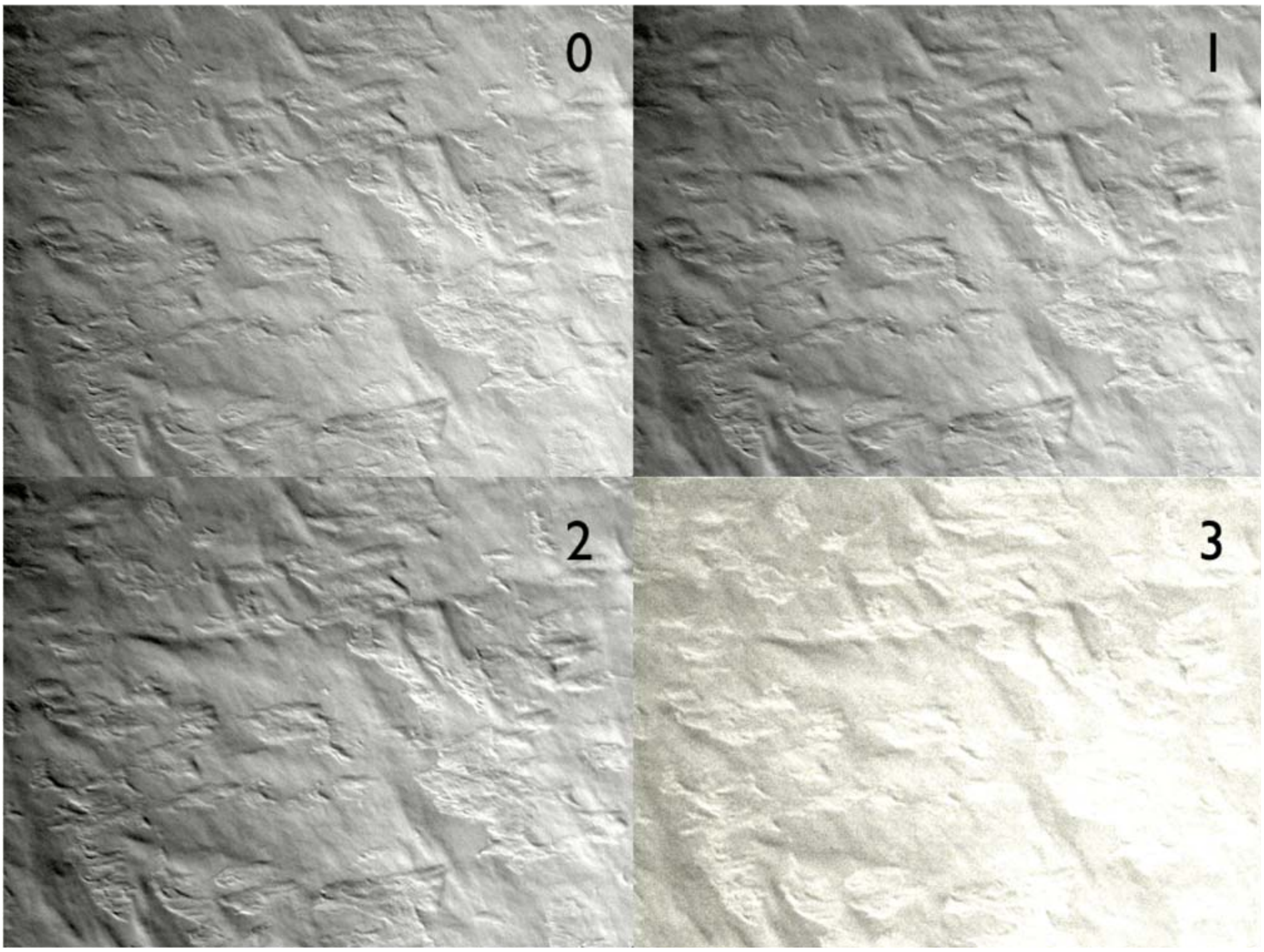

Figure 9. *Example of Multi Camera Array images acquired over the Greenland ice sheet by PROMICE airborne survey. Image 0 using a 490+/-5 nm filter represents OLCI band 4 and has 80% overlap with MODIS band 10; Image 1 using a 560+/-5 nm filter represents OLCI band 6 and has 75% overlap with MODIS band 4; Image 2 using a 680+/-5 nm filter represents OLCI band 8 and has 80% overlap with MODIS band 13; Image 3 using a 1000+/-10 nm filter represents OLCI band 21 does not overlap with a MODIS band.*

We hope to engage a PhD student through a 18 March, 2016 submitted ESA funding application to use this high spatial resolution PROMICE airborne data to partition the albedo signal in NASA MODIS and Sentinel-3 imagery among different surface classes: bare ice; snow; surface water; impurity rich ice. The OCI hyperspectral data are to be used to create synthetic spectral bands to more precisely match data coincident with MODIS.

Glacier Mapping

Several complete glacier maps covering all Greenland are currently available: the Rastner et al. (2012) Inventory and the Howat et al. (2014) GIMP land classification, both of which represent the state of glaciers around year 2000 as obtained from satellite remote sensing, and the PROMICE glaciers map of Citterio & Ahlstrøm (2013) which is based on from approximately the mid-1980's and older aerophotogrammetric maps. Only two (GIMP and PROMICE) include the margin of the Geenland Ice Sheet. One reason for the lack of more recent maps is the hardware failure occurred in 2003within the ETM+ instrument of Landsat 7, which resulted in severe striping of the images acquired ever since, rendering them difficult to use for automatic or semi-automatic image classification and segmentation. The successful launch of Landsat 8 in 2013 and Sentinel-2 in 2015 make it possible to produce up to date glacier maps and to assess any change occurred during the last 10-15 years. PROMICE is actively working toward producing a glacier covering the margin of the Greenland Ice Sheet and all local glaciers, ice caps in a format suitable for comparison with the existing maps.

The 2014 PROMICE report described a promising algorithm able to create an update glacier mask with very little manual tuning and editing. In 2015 the goal was to implement the new algorithm operationally and begin producing the updated map. This however was not possible because an unanticipated problem was found with the orthorectification and geolocation of Landsat imagery. The most apparent evidence is the poor co-registration of Landsat scenes acquired in different WRS2 paths and rows (World Reference System), corresponding to different view geometry from the sensor to the ground. It is well known that scenes from different acquisition rows and paths should not be mixed when the highest consistency is required, as for instance in feature tracking applications. However, the magnitude of the errors observed in some regions can exceed 250 m and reach an order of magnitude higher than specified by the Landsat 8 requirements and documented by the specific scene's processing metadata. The impact of these errors is two-fold:

- the automatic glacier mapping algorithm developed in 2014 becomes unstable in the presence of large geolocation errors because extraneous ice or land can contaminate pixels assumed known by the algorithm as belonging with high probability to the opposite land cover type;
- any new map inheriting these geolocation errors would be rather pointless, as the uncertainty of comparing it against older maps to detect glacier change will be of the same magnitude of the expected change signal. In facts, Fig. 10 suggests the possibility that most differences visible between these glacier margins in 1980's and 2000's are in reality geolocation artefacts of the Landsat L1T scene underlying the Rastner et al. (2012) inventory. It is interesting in this respect to note that the lower panel in Fig. 10, showing an L8 path 230, row 9 scene, fits best with the Rastner et al. (2012) outlines, which are also documented to be from L7 path 230, row 9.

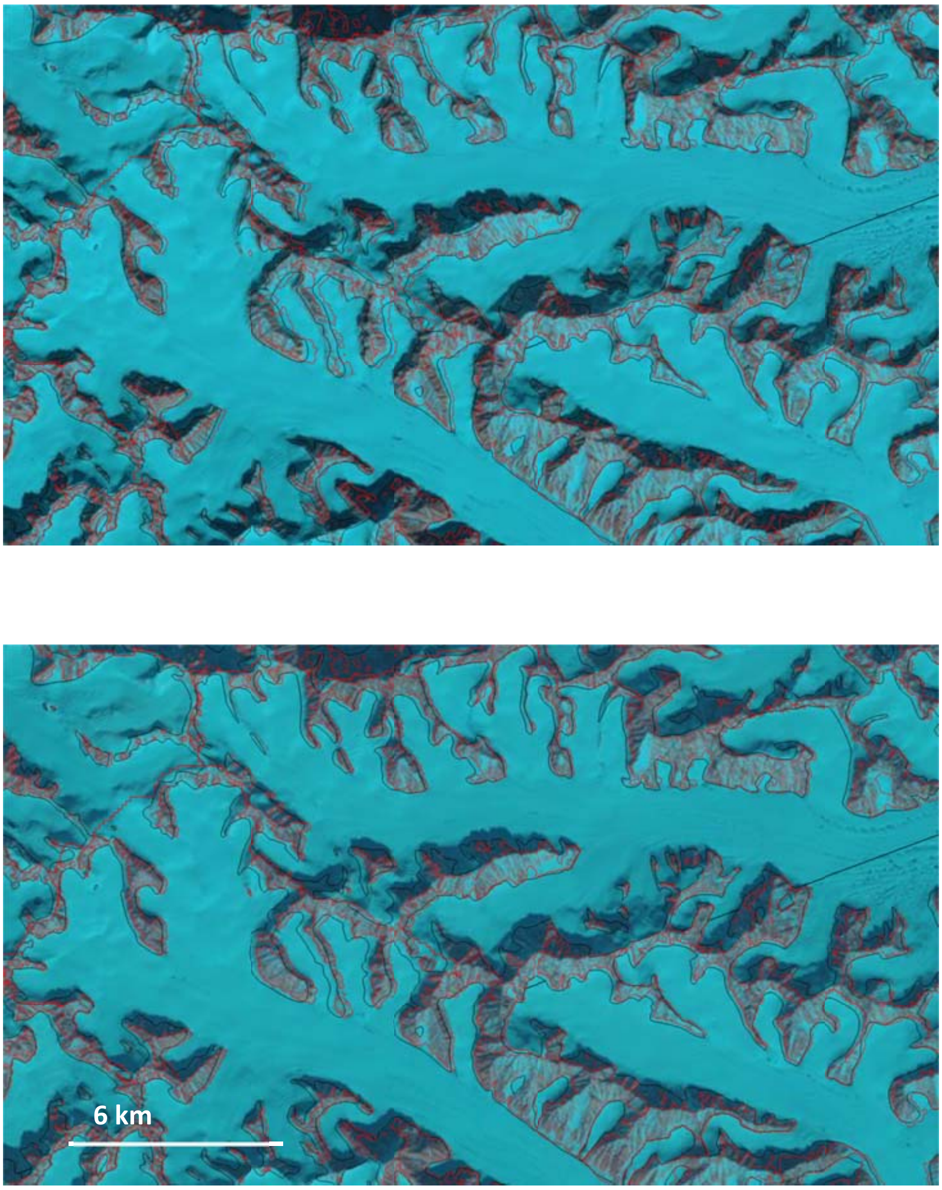

Figure 10. *Landsat 8 L1T details over the upper basins of Schuchert Glacier and Storgletscher (Stauning Alps), showing E-W error at places exceeding 200 m. Top image: path 227, row 9, year 2015, DOY 178; bottom image: path 230, row 9 year 2015, DOY 185. Red and black lines respectively from the glacier inventory of Rastner et al, 2012 and the PROMICE glacier map of Citterio & Ahlstrøm, 2013.*

In 2015 work has therefore been redirected to investigating and if possible correcting the Landsat L1T geolocation errors.

Virtually all scenes made available by the USGS are processed to the L1T Terrain Corrected level, and the accompanying metadata document the rms geolocation uncertainty as estimated by the L1T processor. The geolocation uncertainty arises from imperfect matching of the image to a set of ground control points (GCP) due to clouds and terrain conditions, from limitations dictated by the image resolution, from the uncertainty of the GCP coordinates, and from the orbit and pointing uncertainty of the Landsat platform.

Over the decades of the Landsat project the USGS significantly improved the geolocation accuracy of their Landsat products. The global geolocation accuracy of Landsat-8 has been estimated as 18.1 m (Storey et al., 2014), which improves to ca. 12 m at 90% circular error (CE90) after application of the GCP. Unfortunately, the L1T relies uniquely on the GLS (Global Land Survey) dataset both for the location of GCP's and as a source of surface elevation for the orthorectification step, and GLS has much coarser (Fig. 2) and occasionally distorted and biased elevations at latitudes higher than the 60N reach of the 2000 SRTM (Shuttle Radar Topography Mission). A 3-phases programme of GCP refinement is ongoing and some parts of Greenland are included in phase 2 and especially phase 3 (Storey at al., 2014), but it is not clear whether this improvement will also include a complete update of the GLS DEM over Greenland.

As apparent from Fig. 11, which is representative of all Greenland, the GLS DEM (Fig. 11a) is coarse enough for large valleys and mountain ridges to become blurred or even disappear, while they are clearly visible in the more recent 30 m resolution GIMP DEM by Howat et al., 2014 (in Fig. 2b, reduced from ellipsoidal to orthometric heights using an EGM2008 geoid model). Elevation errors reach ±1000 m and the error patterns indicates that the two DEMs also differ by some horizontal distortion, especially in the western half of the scene (Fig.12). The errors in the GSC DEM used for orthorectification in the L1T processing are capable of producing the observed co-registration errors.

We do not know to what extent the limited accuracy of the GCP's also contribute to the observed distortions, but it seems possible to at least remove the distortion due to the incomplete or erroneous orthorectification by calculating and removing the erroneous correction due to the GSC DEM and then applying a new and accurate correction based on a more reliable and detailed DEM such as the GIMP DEM. In doing this operation, knowledge of the precise orbit of the satellite is required as it determines the instantaneous field of view. For Landsat 5 and7, the USGS distribute precise ephemeris. However, this product has been discontinued in the current L8 processor (USGS EROS pers. comm., 2015) and only the NORAD Space Track orbital data is available, which has an unspecified accuracy in the order of a few km. A simplified approach based on the metadata accompanying each Landsat scene can be used, where the orthorectification correction is calculated from the accurate elevation, the coarse elevation, the satellite orbit altitude, the Earth radius and the across-track distance from the ground track of the satellite assumed as coincident with the centreline of the scene after correction for satellite roll angle from metadata (Fig. 12).

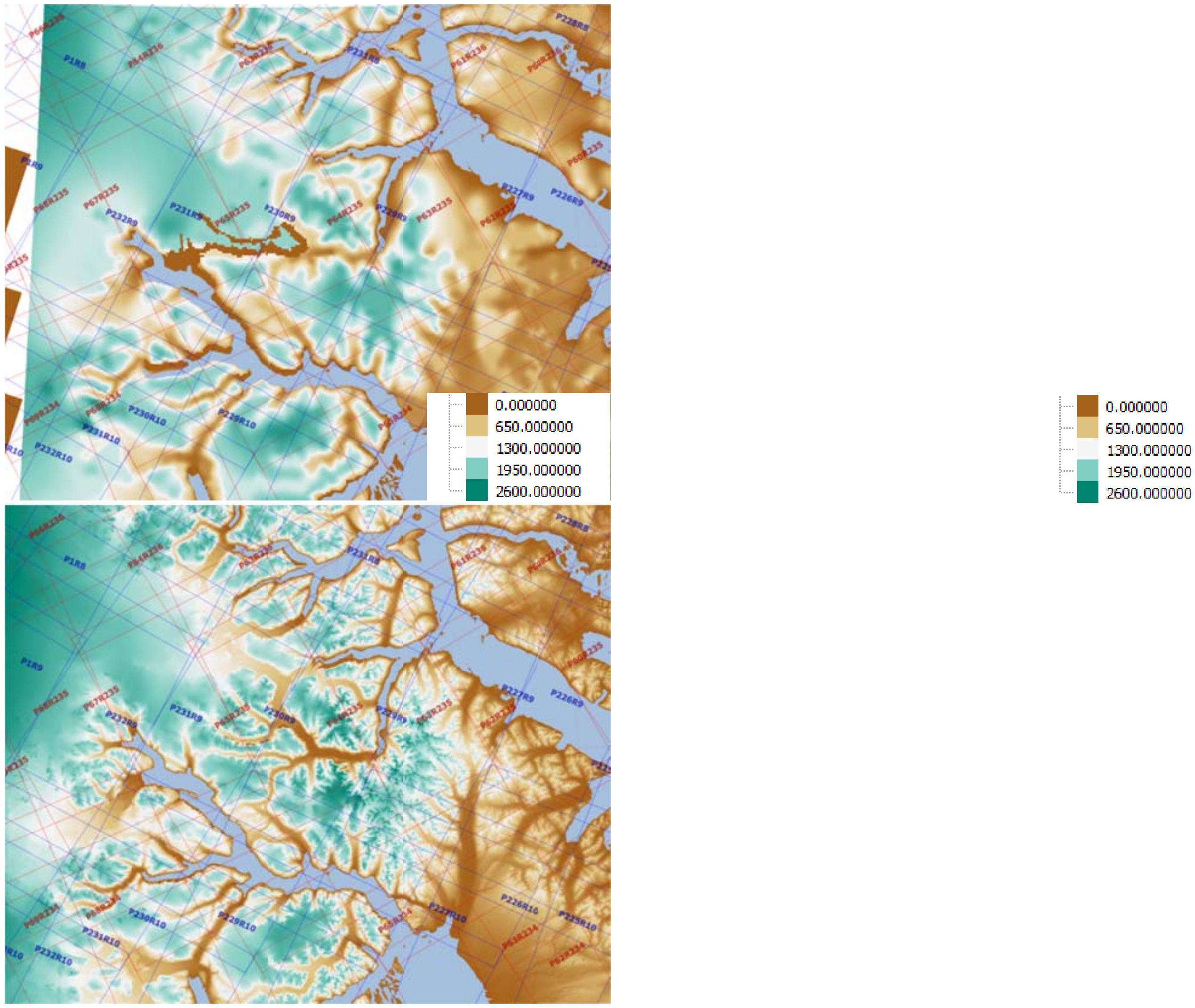

Figure 11. *a: coarse surface elevation according to the GLS DEM; b detailed surface elevations from the GIMP DEM. Red and blue lines and labels indicate ascending and descending orbits respectively and WRS2 path and row numbers*

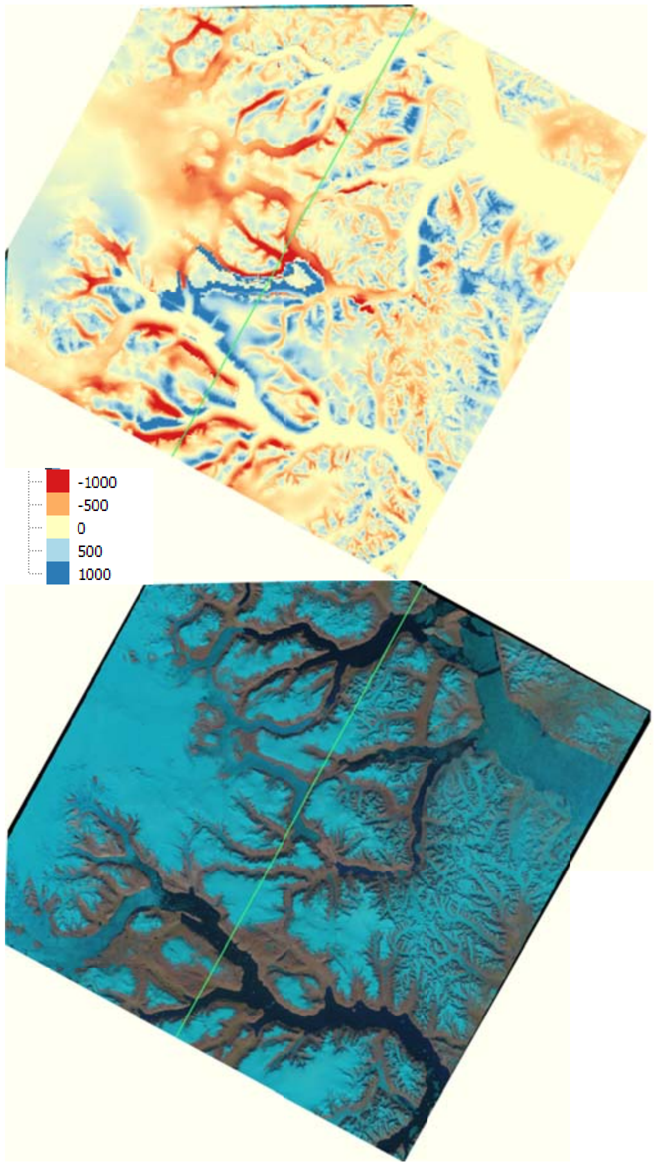

Figure 12. *a: elevation difference between GSL DEM and GIMP DEM; b: Landsat 8 false color composite overview of the region in central east Greenland used as an example throughout this section. The scene has sides of ca. 190 km.*

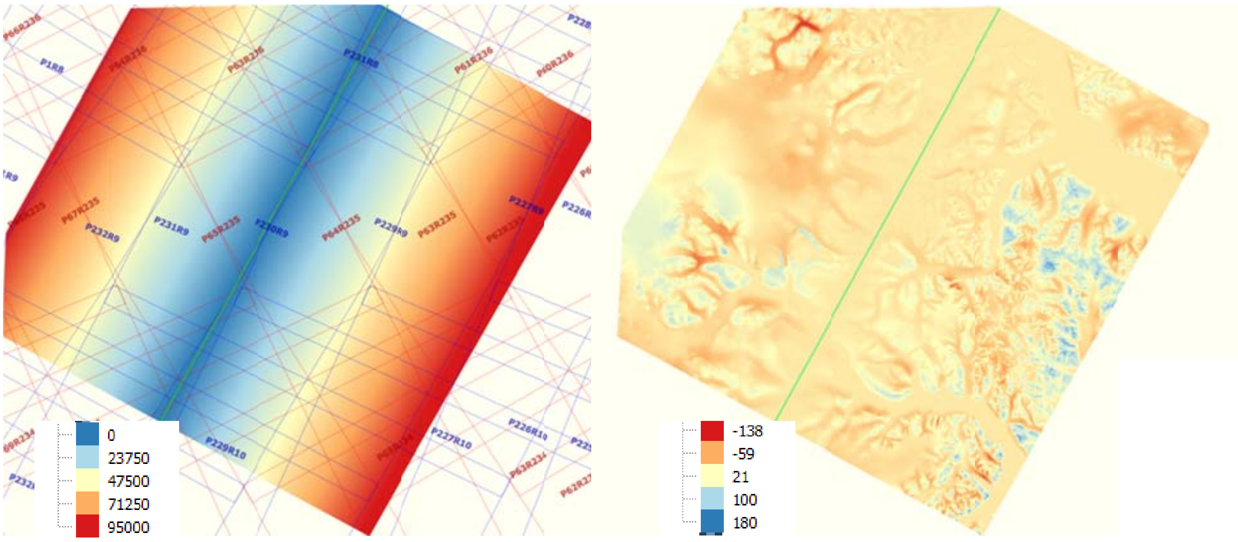

Figure 13. *a: across-track distance in metres from the satellite ground track (marked by the green line); b: calculated total horizontal error in metres in the across-track direction for WRS2 path 230, row 9 due to the inaccurate DEM. The scene has sides of ca. 190 km.*

The error we are attempting to remove is systematic and stable over time but strongly spatially variable, and it needs to be recalculated for each WRS2 row and path, and preferably for each individual scene as there are minor variations in the repeat cycle. Fig. 13 provides an enlarged detail showing that serious mis-registration (note the narrow glacier tongues in the north-eastern sector of the ice mass) can result even quite close to the satellite ground track and with immediately adjacent paths (here, 230 and 231), the DEM elevation error and the calculated correction are also shown.

In 2015 a simple implementation of the correction procedure has been written that does not yet account for the satellite roll angle (which is however most often documented in the metadata as nominally 0 degrees) and it will be further developed and tested in 2016. In particular the possibility of obtaining precise ephemeris for L8 through other channels will be investigated, as an alternative to the use of the poorly documented NORAD Space Track orbital data. Once finalized, the procedure can be fully automated and applied operationally to new and archived acquisitions. Based on current information on the Sentinel -2 processing levels, the procedure should be easily adapted to also support terrain correction of Sentinel -2 imagery.

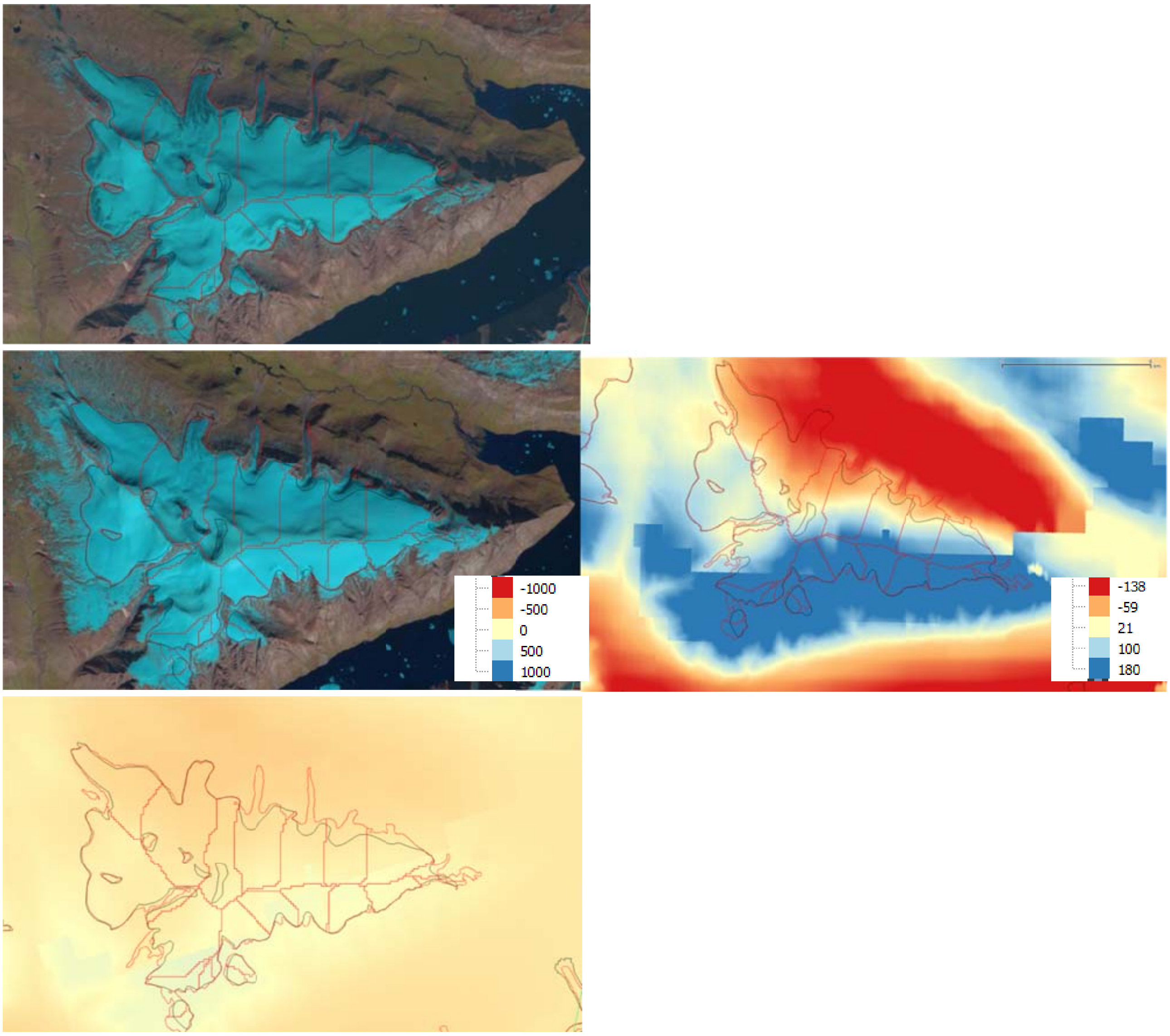

Figure 14. *Enlarged example of large DEM error introducing co-registration errors between two scenes from path 230, row 9, year 2015, DOY 183; bottom image: path 231, row 9 year 2015, DOY 174.*

Observations of runoff from the Greenland ice sheet

Regional climate models (RCMs) are often employed to quantify the surface mass balance of the Greenland ice sheet, yet attempts to validate the model output against observations has been limited to short periods of time at selected locations. An efficient method to validate the important runoff component of the RCM's is to compare to time series of discharge from rivers draining large catchments on the ice sheet (Van As et al., 2014; Langen et al., 2015). PROMICE is involved in two such efforts, one at the Tasersiaq catchment south of Kangerlussuaq and one at the Watson River, Kangerlussuaq.

PROMICE has supported the post-processing of the discharge observations from Tasersiaq, whereas the monitoring program is run by Asiaq and financed by the Government of Greenland. Tasersiaq is one of the largest known hydrological catchments in Greenland in terms of hydropower potential (see location in Figure 15). This time series of discharge is currently being prepared for scientific publication, implying that we cannot show the results yet as this precludes publication in most journals. What is presented in the following is thus the background information for the generation of the discharge time series, in order to provide an overview of the activity.

The GEUS glaciology group has been responsible for the gauging of the discharge at Watson River since 2014, but observations were initiated in 2006 as further described in a following section.

Tasersiaq

The Tasersiaq catchment has the largest known hydropower potential in Greenland. Consequently, the Greenland Government funds a monitoring programme to gauge the discharge as well as a number of related climatic variables. Tasersiaq is a >60 km long narrow lake with a surface area of c. 92.5 km2 situated at 700 m a.s.l. in Southwest Greenland at 66.5°N (Figure 15). The catchment lies north of the Greenland ice sheet outlier Tasersiaq Sermia and several local ice caps including the Sukkertoppen ice cap. These ice caps rise above 2000 m a.s.l. and extend all the way to the coast. Air masses moving over this topographic barrier are depleted in moisture due to orographic forcing, making the region north of it extremely dry. The catchment discharge therefore mostly consists of meltwater from the ice sheet, making it a promising time series for RCM validation and historical runoff analysis.

Delineation of the catchment was carried out using the hydrological software Rivertools 3.0 and based on the surface elevation model GIMP (Howat et al., 2014) in a slightly downscaled version with 150 m grid posting from Morlighem et al., 2014. The resulting catchment is shown in Figure 15, specifying which part of the catchment is glaciated and which is ice free. A sub-catchment related to a small lake adjoining the ice sheet outlier has been subtracted from the catchment as it is the source of glacial lake outburst floods that have been removed from the discharge time series.

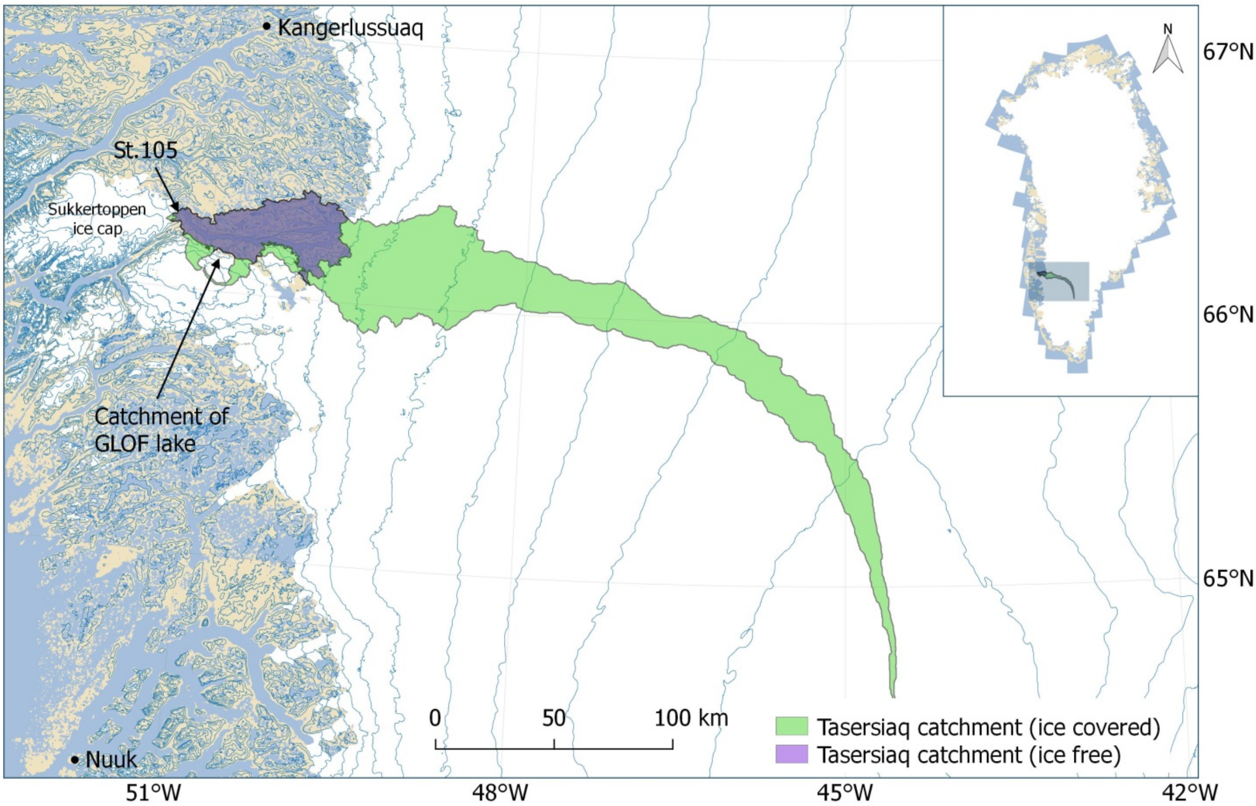

Figure 15. *The Tasersiaq catchment, showing both the ice-covered and ice-free part and the position of the hydrometric station 105. The high elevation part of the catchment delineation on the ice sheet is less reliable. Note that the sub-catchment delivering glacial lake outburst floods (GLOF's) has been subtracted as the discharge released through these events have been removed from the time series.*

The overall characteristics of the discharge time series reflects that Tasersiaq is a large, high altitude, arctic lake with the major part of its water resource originating from melt water from the Greenland ice sheet and local ice caps. Thus the discharge is very low during winter, the season with high flow rates normally lasts from June to October and the highest discharge is normally seen when the air temperature and thereby the glacial melt is at its maximum in late July - early August, Figure 16. The large size of the lake dampens out small variations in the inflow of water like any diurnal variation in melt, which is thus not resolved in the discharge time series.

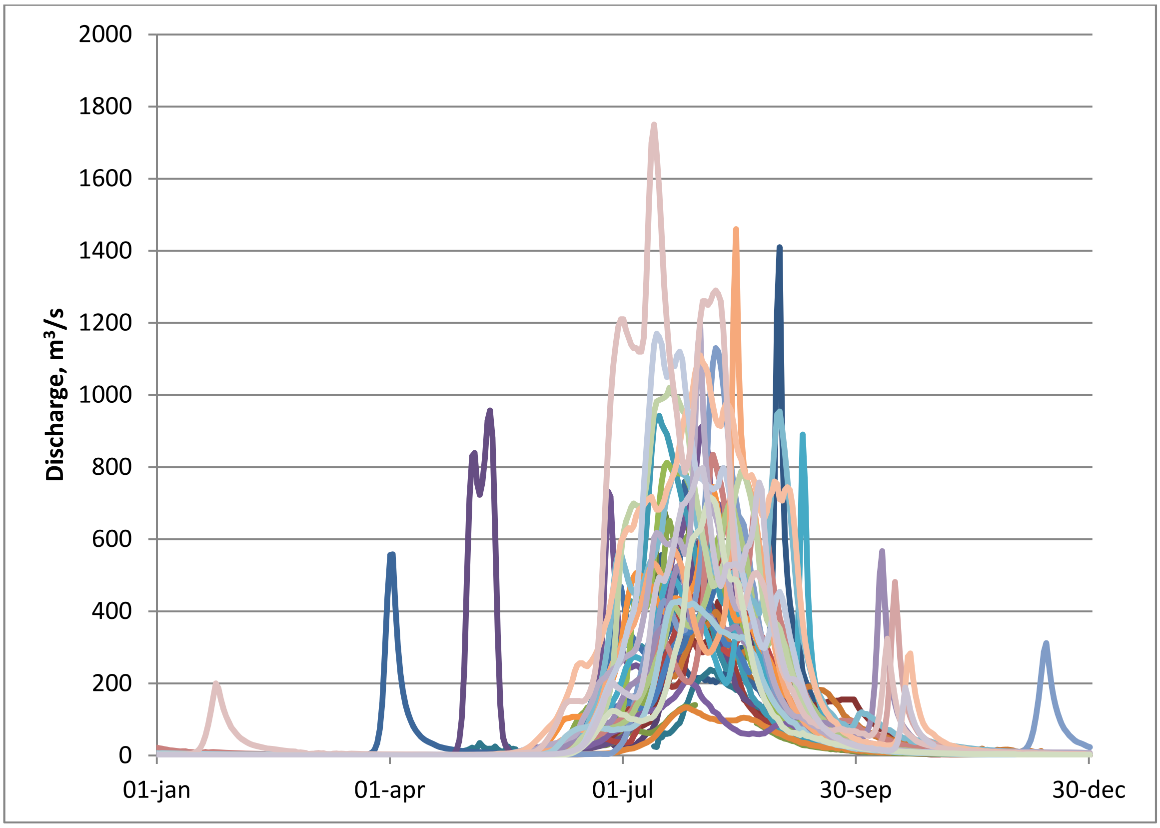

Figure 16. *Distribution of discharge from lake Taserisaq over the year. Plots from the period 1975-2014. Note the odd peaks at various times of the year, indicating periodical glacial lake outburst floods from an ice-dammed lake.*

Beside the yearly melt peak the discharge time series show occasional short-term peaks that can occur on all times of year, but are most common in the autumn. These peaks are characterized by a fast increase in discharge from lake Tasersiaq followed immediately by a decrease of similar or slightly lower rate. The short-term peaks thus have a recognizable signature in the time series of rate of change in discharge even when they occur within the melt season. The period with increased water level lasts 4-17 days with a median length of 6 days.

The characteristics of the short-term peaks show that the peaks reflect a sudden inflow of a large amount of water and that this inflow of water stops abruptly after a short time, typically a few days (see Figure 17). The source is glacial lake outburst floods (GLOFs) from an upstream ice dammed lake found at position N66°09', W050°54' (see Figure 15 and Figure 18). The time series of Landsat imageries (USGS Landsatlook Viewer) show that the water level in the ice dammed lake builds up over a period of typically two years, where after the lake empties abruptly. Especially in the period from 1999 to 2014 Landsat images are so frequent that all outburst floods happening in this period from this ice-dammed lake can be identified (nine in all). In three cases even a precise timing can be found as an image of the lake in the process of emptying exist, in which case a pronounced increased size/width of the river carrying water from the ice dammed lake to Tasersiaq can be seen. All eight outbursts from the ice-dammed lake coincide with short-term peaks in the Tasersiaq discharge time series. Furthermore there are no short-term peaks in this period in the

Tasersiaq discharge time series not accounted for. We conclude that this ice-dammed lake is the only source for the short-term peaks.

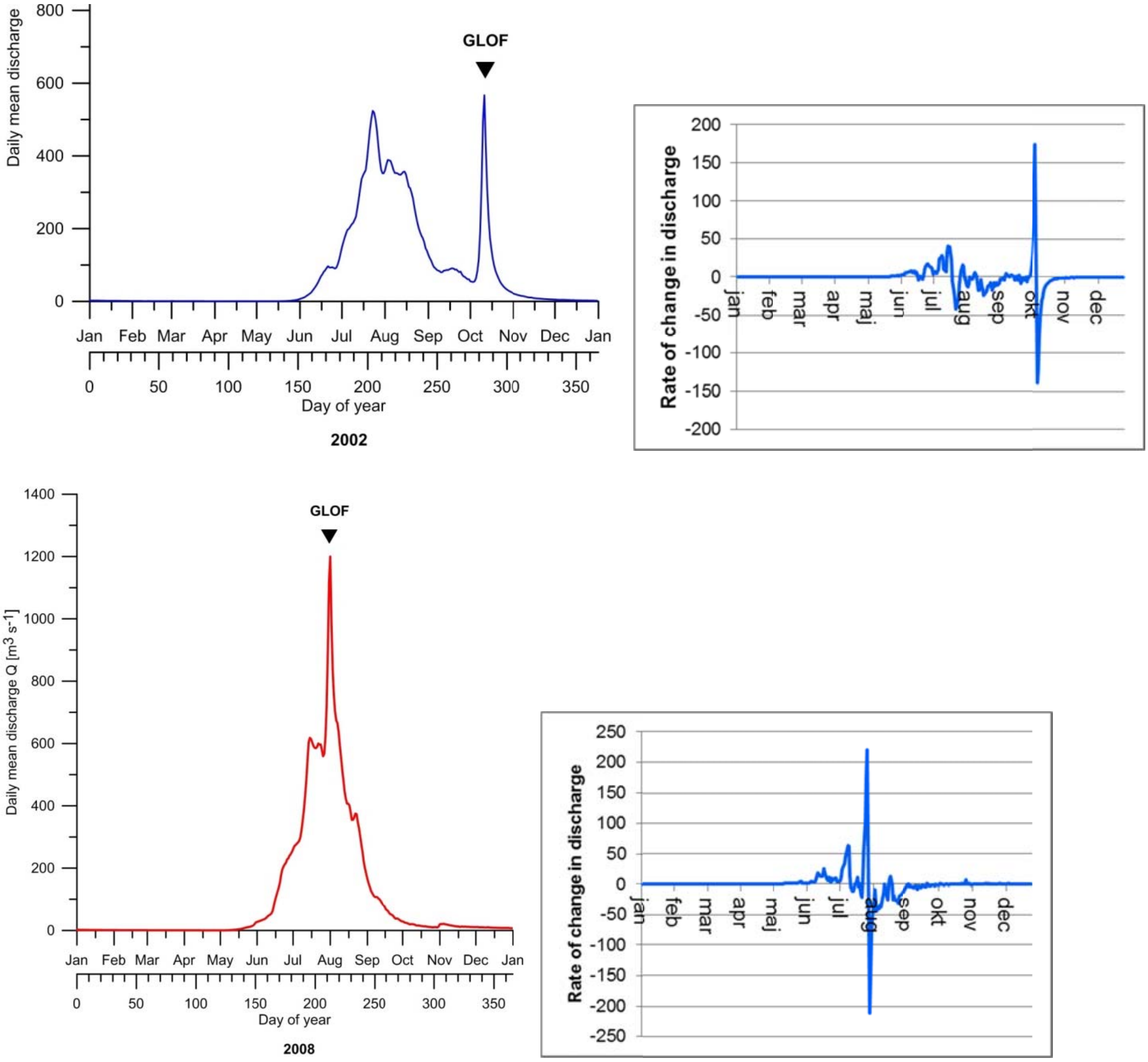

Figure 17. *Annual discharge curves showing sudden peaks related to glacial lake outburst floods. Note how the rate curve (inserted graphs) has a clear signature, revealing the GLOF even when it occurs in the middle of the peak discharge of the main catchment.*

By utilizing the relation between GLOF volume and the sum of positive degree-days (PDDs) between events, and supportive evidence from Landsat imagery, it has been possible to clarify that three GLOF events have taken place which are not documented in the Tasersiaq discharge time series due to data gaps. For the period 1975-2014 a total of 17 jökulhlaups have been identified.

The GLOF peaks in the Tasersiaq discharge time series represent melt water released after a considerably delay in the ice dammed lake. In the further analyses of the Tasersiaq discharge time series we would like to compare the discharge with runoff calculated by the RCMs over the glaciated parts of the catchment and here the GLOF peaks would create temporal inconsistency in the analysis. Therefore the GLOF events will be removed from the discharge time series, effectively subtracting the water originating from the sub-catchment of the ice dammed lake (as seen in Figure 15).

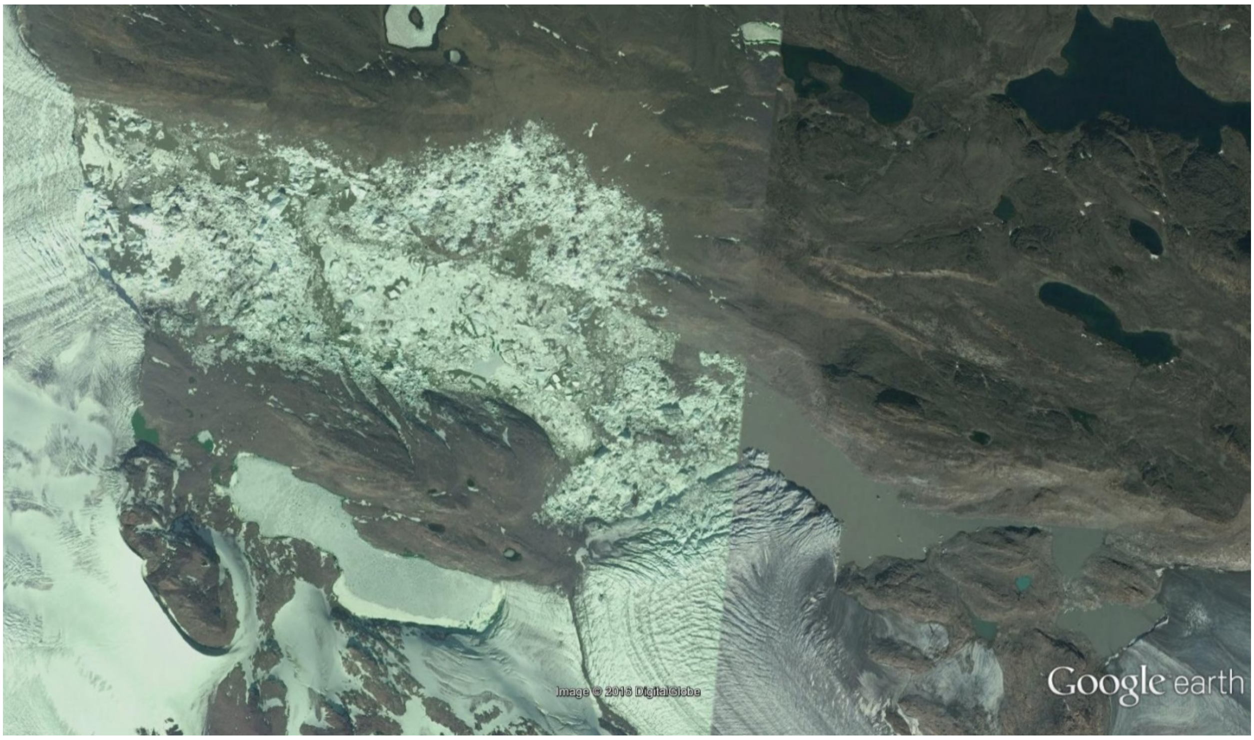

Figure 18. *Two high resolution images from Google Earth merged right through the identified source lake of the GLOF's in the discharge time series. Note how the calved pieces of ice are left partly on the bottom of the drained lake in the left hand side of the merged image, while the lake is full of water on the right hand side.*

A climatological analysis of the unique 40-year discharge time series from Tasersiaq, relating the ice sheet runoff to climate variability is underway with further use in subsequent publications on validation of RCM runoff output. In this way PROMICE provides a opportunity to evaluate and improve model performance against observations over more than the 30-year time period defined as being necessary to assess the climatological state of the ice sheet.

Watson River

Continuous monitoring of Watson River water and sediment discharge started in 2006. Until 2013 the monitoring was performed by Copenhagen University, Department of Geosciences and Natural Resource Management (IGN). Due to budget issues and personnel changes, in 2014 GEUS took over the infrastructure and responsibility to keep the monitoring program running. Since then the monitoring has been primarily funded by the Greenland Analogue Project, which also funds the "KAN" weather stations that deliver data to PROMICE (Figure 20). The motivation to continue the monitoring of Watson River is that it is becoming increasingly relevant for studies of climate variability and ice sheet processes with its time series spanning a decade. This is testified by the increasing amount of researchers using these data for their research, which benefits GEUS' level of international collaboration and publication record.

The measurement site is located at the bridge in the settlement of Kangerlussuaq (Figures 1 and 19). Water level is monitored by means of two divers, a sonic ranger and a radar recording water stage. Two turbidity sensors and a CTD diver provide the means to determine sediment content in the water, which is unique to Greenland. Yet here we focus on water discharge due to its relevance to PROMICE.

Similar to the Tasersiaq approach described above, we translate river stage into water discharge by applying a stage-discharge relation. Two such relations have been developed by IGN over the past years, but with new ADCP data becoming available to GEUS, we will develop a further improved equation. In Figure 20 preliminary results for the 2006-2015 discharge are plotted. We highlighted the year 2010, which was a high melt year with a long melt season. 2012 experienced the largest-yet discharge, resulting in the partial destruction of the bridge over the Watson River during the peak melt event in mid-July. In comparison, 2015 proved to be a year with more average melt conditions, representative of 1961-1990 conditions (see Appendix D), but with low discharge values with regard to the 2006-2015 period. Finally, note that Watson River discharge values are generally similar to or larger than those of Tasersiaq, which is indicative of its large ice sheet catchment (>10.000 km^2) and thus highly convenient setting for such measurements.

Figure 19. *The location of the Watson river monitoring site in relation to PROMICE weather stations within the hydrological catchment.*

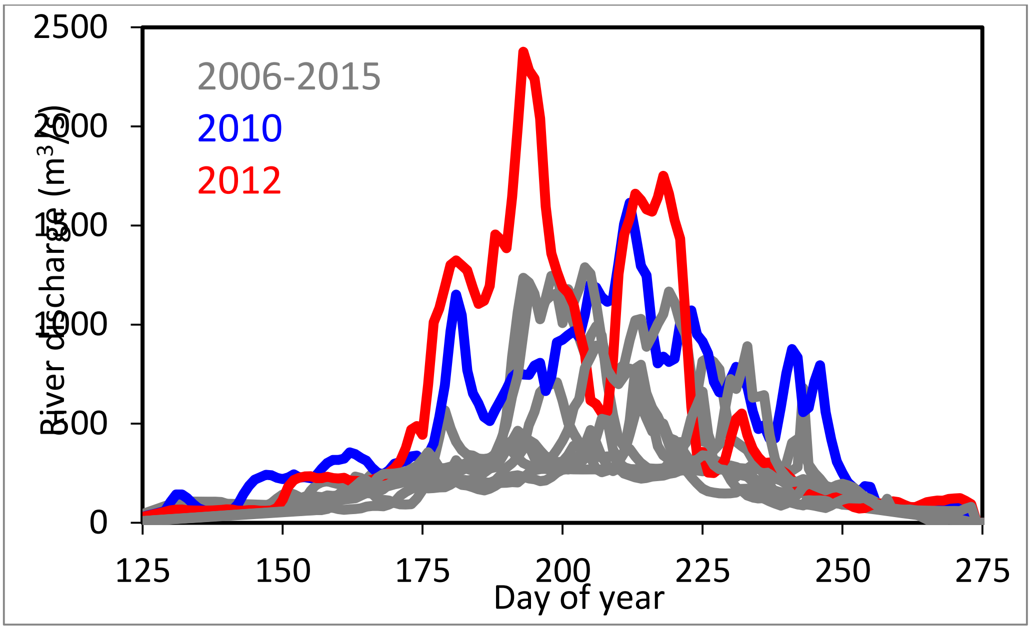

Figure 20. *Preliminary results for the recalculated daily-mean discharge estimates from Watson River.*

Collaboration with DMI on model development

The PROMICE data provides possibilities for developing physical parameterizations that may be utilized in models. GEUS is engaged in establishing a new water percolation and retention parameterization for snow and firn on the ice sheet; work using PROMICE observations and which is currently funded by FNU. Water percolation and retention in snow and firn on the ice sheet is a process that is currently inadequately modelled. Understanding and representing this process in a model will reduce the uncertainties on determining the future contribution to sea level rise from the Greenland ice sheet.

Regional climate model HIRHAM5 subsurface scheme

Collaboration with DMI is ongoing and in addition to advances in the treatment of refreezing and densification processes obtained in recent years, we aim for advances in the treatment of water percolation and retention of the HIRHAM5 Regional Climate Model (RCM) subsurface model that calculates daily surface mass balance (SMB). The HIRHAM5 subsurface model now accounts for density varying processes that give a more physical representation of meltwater storage in the snow and firn and meltwater runoff. As a consequence of the added densification processes last year, the representation of the mass and energy exchange through the subsurface layers had to be changed. Our aim is to make the HIRHAM5 subsurface scheme more physical in how it handles the percolation and retention of liquid water and water flow through the subsurface.

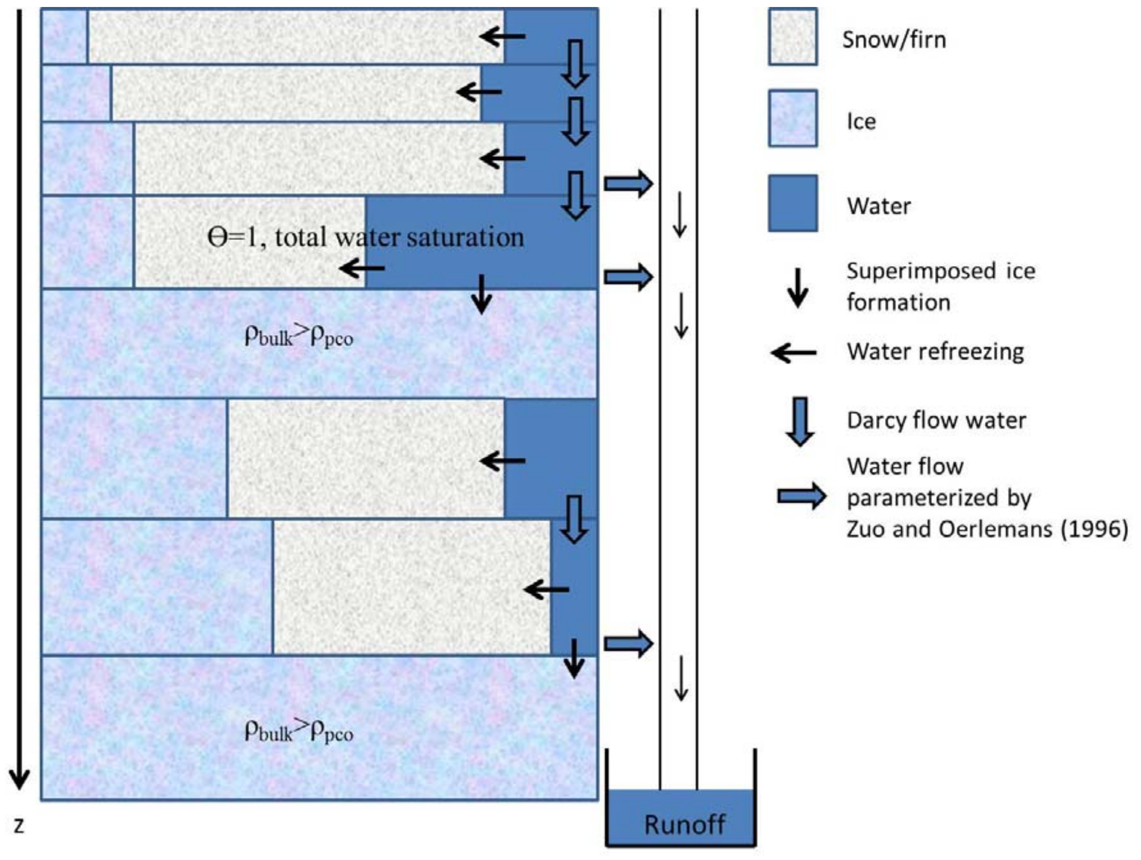

Figure 21. *Schematics of idealized water percolation and retention in HIRHAM5 subsurface scheme.*

Figure 21 illustrates the proposed handling of subsurface water percolation and retention. First, it updates the liquid water content of the surface snow layer by including all water contributions at the surface. Then, it estimates the amount of energy available for liquid water freezing based on the temperature of each snow layer. If freezing occurs in a given layer, its liquid water content is decreased and its temperature is increased accordingly. The water flow through the snow layers is then simulated. The liquid water content of the snowpack is modeled as a series of reservoirs, one for each model layer. Water flow occurs when the liquid water content exceeds the maximum liquid water holding capacity (Wliq max in kg m^{-2}) set to 5%. Due to snow being a porous medium, the vertical water movement through the snow and firn will be estimated using the Darcy flow law with an associated hydraulic conductivity (K) and pressure head (h, suction). When water meets an impermeable ice layer, defined as the snow density $\rho_{bulk} > \rho_{pco} = 830$ kg m^{-3}, water is allowed to pond until the layer is totally saturated. Total saturation is reached when the effective water saturation Θ equals 1 (Figure 21). Water in a layer above an impermeable layer may runoff into the ocean as parameterized by Zuo and Oerlemans (1996), but may also refreeze on top of the ice layer as superimposed ice. Overall, the water percolation and retention model will be able to simulate hydraulic conductivity, water flux/percolation, pressure heads/suction, and distributed water content for all layers in the subsurface scheme, based on initial values of surface water supply from SMB and rain, snow grain size, and the density of snow and firn.

Checking High Resolution Climate Models

PROMICE data are also extremely valuable for validation purposes. Showcasing GEUS-DMI collaboration, the checking of a high resolution DMI climate model using PROMICE data is making its way into publications in high-impact journals: Langen et al. (2015) and Van as et al. (2014).

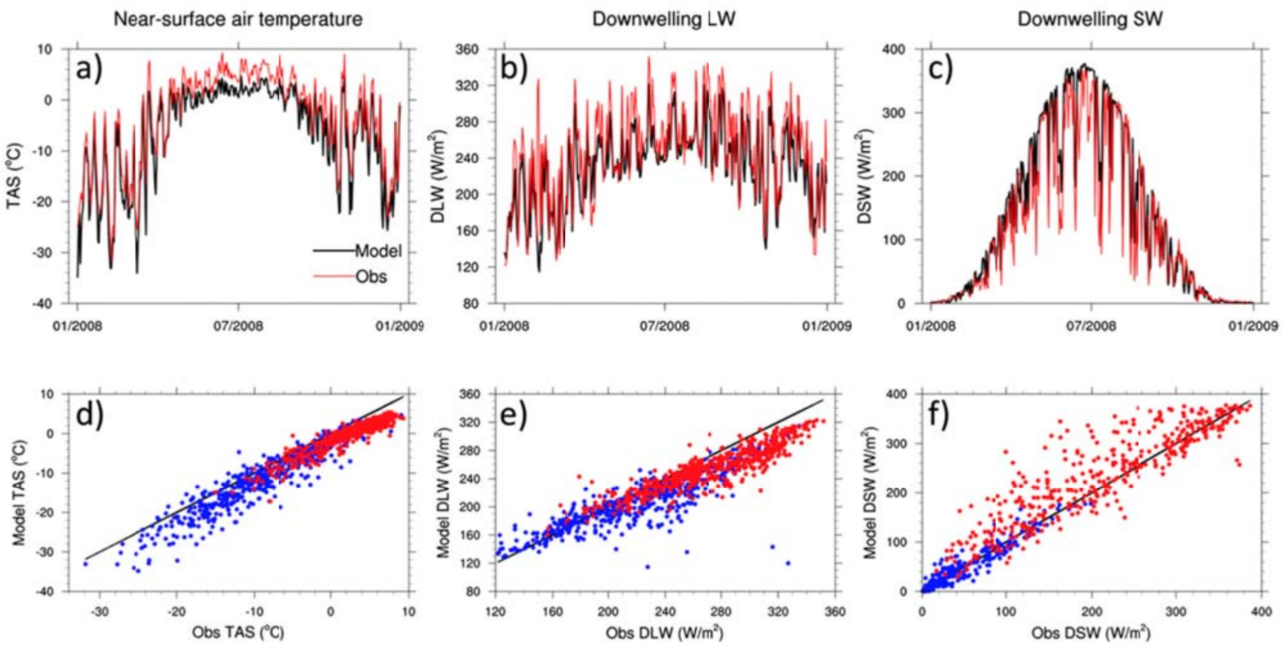

Figure 22. *Published in Langen et al. (2015) in collaboration between GEUS and DMI, daily averaged PROMICE NUK_L observations and DMI HIRHAM model output. Shown are subsets of the full series showing (a) near- surface air temperature and downwelling (b) LW and (c) SW radiation. (d)–(f) Scatterplots for 3 yr of data (20 Aug 2007–19 Aug 2010) of (a)–(c). Blue dots are winter half-year [October–March (ONDJFM)], red dots are summer (AMJJAS) and black lines denote a 1:1 relationship.*

Outreach

The PROMICE website (www.promice.org) provides information on the project as well as the possibility to browse and download data. It includes real time and quality checked AWS data from all PROMICE stations as well as download possibilities for three other products: the PROMICE map of margins of all ice masses in Greenland (Citterio and Ahlstrøm, 2013), the ice thickness from the Airborne surveys carried out in August 2007 and 2011 and the PROMICE historical surface mass balance data from the ablation zone of the ice sheet and the local glaciers of Greenland. Shortly glacier area changes will also be included. The data are available for everyone and at no charge by filling in a short form.

PROMICE is present on Twitter and Facebook and new product releases are also announced on Cryolist.

As of the end of 2015, 274 data users registered on the PROMICE website. Of these, 86 users are from the US, 148 are from EU, 64 users are from Denmark and six are from Greenland. As the data records grow in length and more people are aware of the PROMICE data products, the PROMICE website is visited more frequently and data downloads occur more often. The purpose of data download as stated by the users differs highly, ranging from scientific to educational and private. Below follows a few selected user-written purposes of download from 2015:

- Characterizing differences between ECMWF and in situ pressure measurements to obtain pressure errors in GRACE gravity data over Greenland
- Examination of a basic climatology for planning for 2015 field season
- I plan to use this data to validate the SMB of my regional climate MAR model over the Greenland ice sheet. Thanks for providing this kind of very useful data set
- To study the vegetation phenology in Greenland. This part includes investigating the potential relationship between vegetation phenology and proximity to the ice sheet
- Study the 2015 melting season for studying melting anomaly in a long-term context as part of the Arctic report card. In particular, we are interested in the surface temperature and albedo over the locations where the stations are collecting data
- Relationship between air temperature at different sites and flow velocity and calving front retreat of adjacent glaciers

A number of products related to PROMICE are displayed on the Polar Portal a website where Danish research institutions display the results of their monitoring of the Greenland ice sheet and Arctic sea ice to the general public.

A e-learning website Isskolen for children aged 12 to 14, giving a basic introduction to ice and climate change was developed in 2014 in all Nordic languages and English. Versions in Greenlandic, German and French were implemented in 2015. The webpage is published by the Nordic centre of excellence SVALI in collaboration with PROMICE and maintained at GEUS. www.isskolen.dk.

Two PROMICE newsletters were published in 2015: ‘Survey of Greenland Glacier area changes’ and ‘How meltwater can create an ice lid in the snow blanket over the Greenland ice sheet’ (Appendix D). The ‘Survey of Greenland Glacier area changes’ newsletter is cited in the high impact factor Bulletin of the American Meteorological Society's State of the Climate report to be published July 2016.

The number of scientific publications resulting from the PROMICE observations is increasing steadily. Year 2015 reached a new high in productivity for peer reviewed ISI tracked publications from the PROMICE team that incorporate PROMICE observations as may be seen in figure 23. In addition publications are appearing which make use of PROMICE data without having coauthors from the PROMICE team (Wake et al., 2015, Van Tricht et al., 2016).

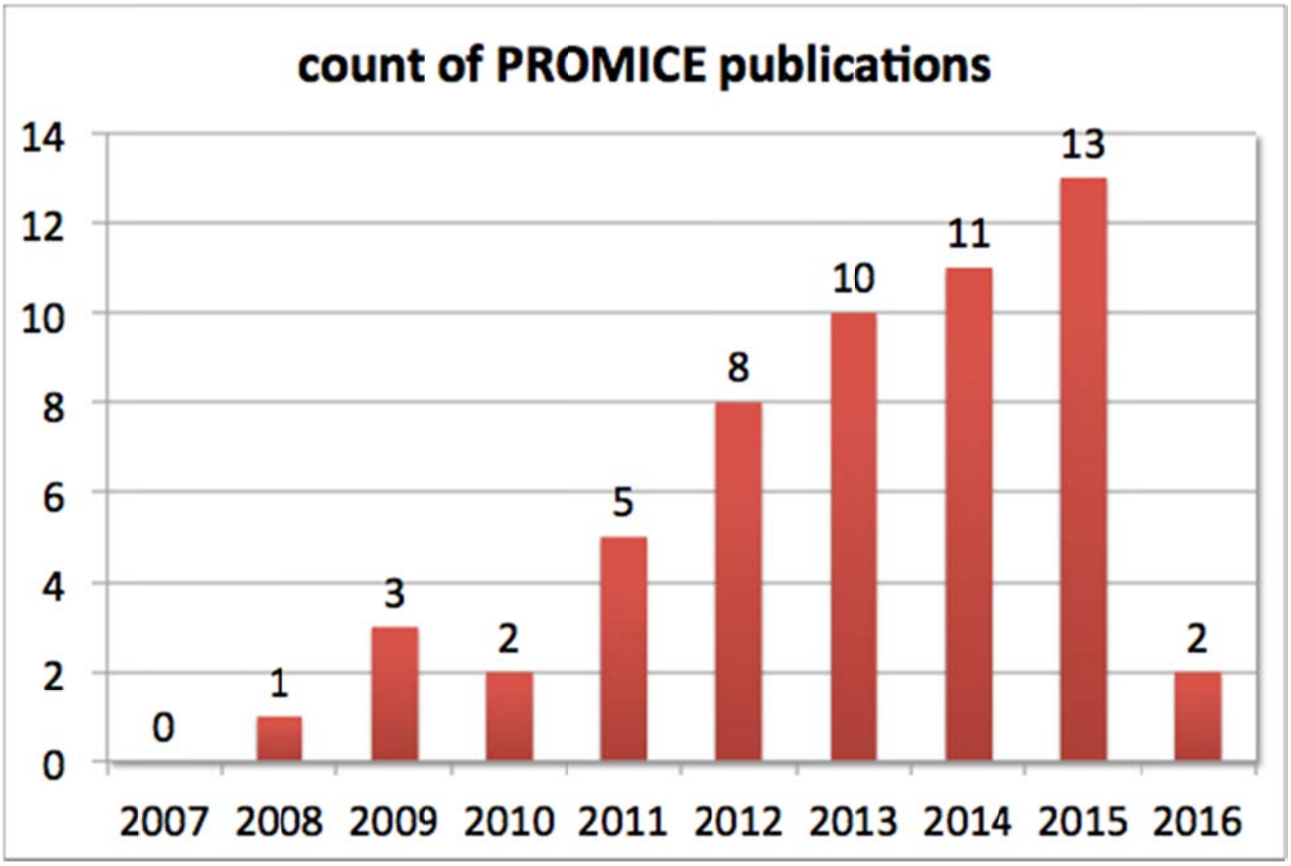

Figure 23. *Annual count of peer reviewed ISI tracked publications from GEUS incorporating PROMICE data. Year 2016 is incomplete given that the compilation is as of 22 March, 2016.*

July 2015, film star and UN Peace Ambassador Leonardo DiCaprio joined Jason Box on a PROMICE maintenance visit. DiCaprio and Box filmed for an upcoming documentary that includes the two discussing the climate station and using the pressure transducer host to physically illustrate how much melting the stations are recording.

SWIPA input

The Arctic Monitoring and Assessment Program (AMAP) Snow Water Ice Permafrost in the Arctic (SWIPA) Update (in preparation) captures new and significant knowledge on Arctic glaciology, coincides with the inception of continuous PROMICE data in 2007. The survey of scientific literature with direct support from PROMICE consists of 21 publications. PROMICE brings an invaluable observational perspective to a model dominated field. What we have learned thanks to PROMICE data grounding us in nature is summarised in the following.

Understanding Melt

Charalampidis et al. (2015) make direct measurements of albedo feedback using KAN_U PROMICE station data while constraining a calculation that suggests reduced meltwater buffering capacity. The recent strong increase in surface melting has produced negative surface mass balance along south western ice sheet (Van As et al. 2014). Van Tricht et al. (2016) isolated the effect of clouds that on average enhance meltwater runoff by about one-third relative to clear skies by surface heating that limits meltwater refreeze. Fausto et al. (2016) find that the extreme melt episodes July and August 2012 were dominated at the lowest 1/3 of the ice sheet elevation profile by heat advection, not absorbed sunlight despite the dark surface of the lower ablation area because of the cloudy conditions that dominate advective cases. This study also isolates the potential heat delivery impact from rainfall.

Rain speeds the ice sheet

Rainfall is further brought into focus with its role in amplified melt and flow of the Greenland ice sheet (Doyle et al. 2015). In a warming climate, the rain season expands. This study documents cases when late summer rain events speed the ice sheet importantly at a time of year seasonal acceleration was thought to be self-limiting.

Reduced meltwater retention in successive high melt years

PROMICE (formerly Greenland Analogue Project, GAP) climate station data have driven a runoff calculation for the Kangerlussuaq region by Van As et al. (2012). These data were used extensively by KU PhD student; Andreas Mikkelsen, supervised by Dirk van As, in a study: Mikkelsen et al. (2015) who compare meteorological, melt, firn-stratigraphy and discharge data from the extreme 2010 and 2012 summers to determine the relationship between atmospheric forcing and melt runoff at the land-terminating, Kangerlussuaq sector of the Greenland ice sheet which drains into Watson River. The 6.8 km^3 bulk discharge in 2012 exceeded that in 2010 by 28%, despite only a 3% difference in net melt energy between the two years. This large disparity can be explained by a 10% contribution of runoff originating from above the long-term equilibrium line (up to 1850 m a.s.l.) in 2012 caused by diminished firn retention. The 2012 discharge response was amplified by catchment hypsometry - the disproportionate increase in the area contributing to runoff as the melt-level rose into the accumulation area.
Satellite imagery and oblique aerial photographs of an active network of supraglacial rivers extending 140 km from the ice margin confirm meltwater runoff originating well above the equilibrium line. This runoff culminated in three days of record discharge of 3,100 $m^3 s^{-1}$ (0.27 Gt d^{-1}) that peaked on 11 July and washed-out the Watson River bridge. The findings corroborate meltwater infiltration across the percolation zone though the resulting patterns of refreezing are complex and can lead to spatially extensive, perched superimposed layers within the firn. In 2012, such layers extended to an elevation of at

least 1840 m, providing a semi-impermeable barrier to further meltwater storage and promoting enhanced runoff that contributed directly to global sea-level rise.
In an independent study enabled by the repeat visits to the KAN_U site for PROMICE station maintenance, successive firn cores were obtained, leading to a high impact confirmation of the Mikkelsen et al. (2015) result. Machguth et al. (2015) find using ice cores and a simple runoff model the development of thick ice layers after successive high melt years (2010 and 2012 in particular) promoted reduced melt water retention through increased runoff. The effect of expected future increases in melting on reduced meltwater retention is anticipated to continue as pore space fills, producing an increasing ice sheet sea level response.

Understanding meltwater at the bed of the ice sheet

Data from the three PROMICE (formerly Greenland Analogue Project, GAP) automatic weather stations were used for meltwater runoff calculations (Van As et al., 2012) in a study which documents the ice sheet bed in unprecedented detail, finding it is now more conceivable that lake drainage events may occur more commonly as future surface melting increases. Lindbäck et al. (2015) present a high (150 m) resolution sub-glacial map covering a 12,000 km^2 sector of southwestern ice sheet indicating probable existence of small subglacial lakes undetectable by surface elevation change or airborne radar. Their analysis suggests switching of drainage between subglacial competing catchments driven by seasonal changes in the basal water pressure.

Mapping bare ice and melt areas

Using NASA MODIS optical satellite data, Fausto et al. (2015) produce daily automated classifications of the Greenland ice sheet into bare ice melting and dry snow areas. The surface classes, useful as ice-sheet climate indicators, are complementary to existing thermal infrared and passive microwave products.

Checking satellite derived albedo

Because Mittivakkat Gletscher, southeast Greenland, is well instrumented and host to the longest surface mass balance record of any Greenland glacier isolated from the ice sheet, it provides an important test bed for satellite observations and models. Mernild et al. (2015) use PROMICE AWS data from Mittivakkat Gletscher to check NASA Moderate Resolution Imaging Spectroradiometer (MODIS) albedo data, finding 0.05 RMSE which is less than the -0.10 MODIS albedo trend evident for this glacier.

Ice sheet surface meltwater lakes are sensitive climate indicators

PROMICE climate station data constrain melt calculations by Fitzpatrick et al. (2014) who find that the inland expansion of lakes is strongly correlated with air temperature. During the record melt years of 2010 and 2012, lakes formed and drained earlier, attaining their maximum volume 38 and 20 days earlier than the 11 year average, as well as occupying a greater area and forming at higher elevations (> 1800 m) than previously. Despite occupying under 2 % of the study area, lakes delay the transmission of up to 7–13 % of the bulk meltwater discharged. Roughly one third of the lakes drain rapidly (< 4 days). Clustering of such events in space and time suggests a trigger mechanism.

Greenland local glaciers present and future

PROMICE support of the time of H. Machguth is attributed in two important studies. For the 2009-2013 period, Bolch et al. (2013) who find Greenland peripheral glaciers, covering 5% of the island's total ice area are responsible for 14-20% of the whole island mass loss. Machguth et al. (2013) use DMI and other regional climate model output to represent the sea level contribution of Greenland local glaciers to sea level through year 2100, finding they contribute between 5.8 ± 0.4 and 11.2 ± 0.3 mm sea level equivalence in future scenario A1B.

Importance of Land/Ice/Ocean Mask product from PROMICE

A high resolution land/ice/ocean map (Citterio and Ahlstrøm, 2013) has been published through PROMICE, which better constrains ice sheet area change studies (Kargel et al. 2012). Because it is near the ice/land or ice/ocean boundaries where surface mass fluxes are largest, a comparison of surface mass balance models reached the conclusion that common land/sea/ice masks are prerequisite to reconciling differences among various estimates. The same data set is fed into Leclercq et al. (2012) who document use terminus positions from 18 south and west Greenland land-terminating glaciers since the 19th century, finding average of 1.2 ± 0.2 km retreat over the 20th century characterised by overall warming.

Dynamic mass losses

For 2007 – 2011, the total mass balance was -262 ± 21 Gt/year, of which 61% was due to negative surface mass balance (Andersen et al., 2014).

Inland ice sheet acceleration

Initially Greenland Analogue Project (GAP) data, but beyond year 2012 PROMICE climate station data, support a study documenting inland ice sheet acceleration above the lower ablation area (Doyle et al. 2014). An increasingly wet bed exhibits increasing velocities over time. This result is countering the self-regulation hypothesis that seasonal flow acceleration has been shown to occur further inland than earlier studies have shown.

Glacier area changes

Marine terminating outlets from the Greenland ice sheet have been retreating with few exceptions. Box and Hansen (2015) surveyed 45 glaciers that collectively lost an area of -1799 km^2. In August 2010, the longest ice shelf connected to the Greenland ice sheet calved 245 km^2 from the Petermann Glacier (Jensen et al. 2015). The Arctic's largest ice shelf was reduced in area by half when the 2010 Petermann ice shelf calving combined with a 140 km^2 calving in 2012 (Jensen et al. 2015). Now, the largest Greenland and Arctic ice shelf is at the front of the Northeast Greenland Ice Stream.
For summer air temperature records at all 11 DMI stations around Greenland, the correlation with glacier front area change is consistent with hypothesis: in warm summers, more ice area is lost. At 4 of the 11 sites, the confidence in that correlation is above 95%. At 7 of the 11 sites, the confidence in that correlation is above 80% (Box and Hansen, 2015).

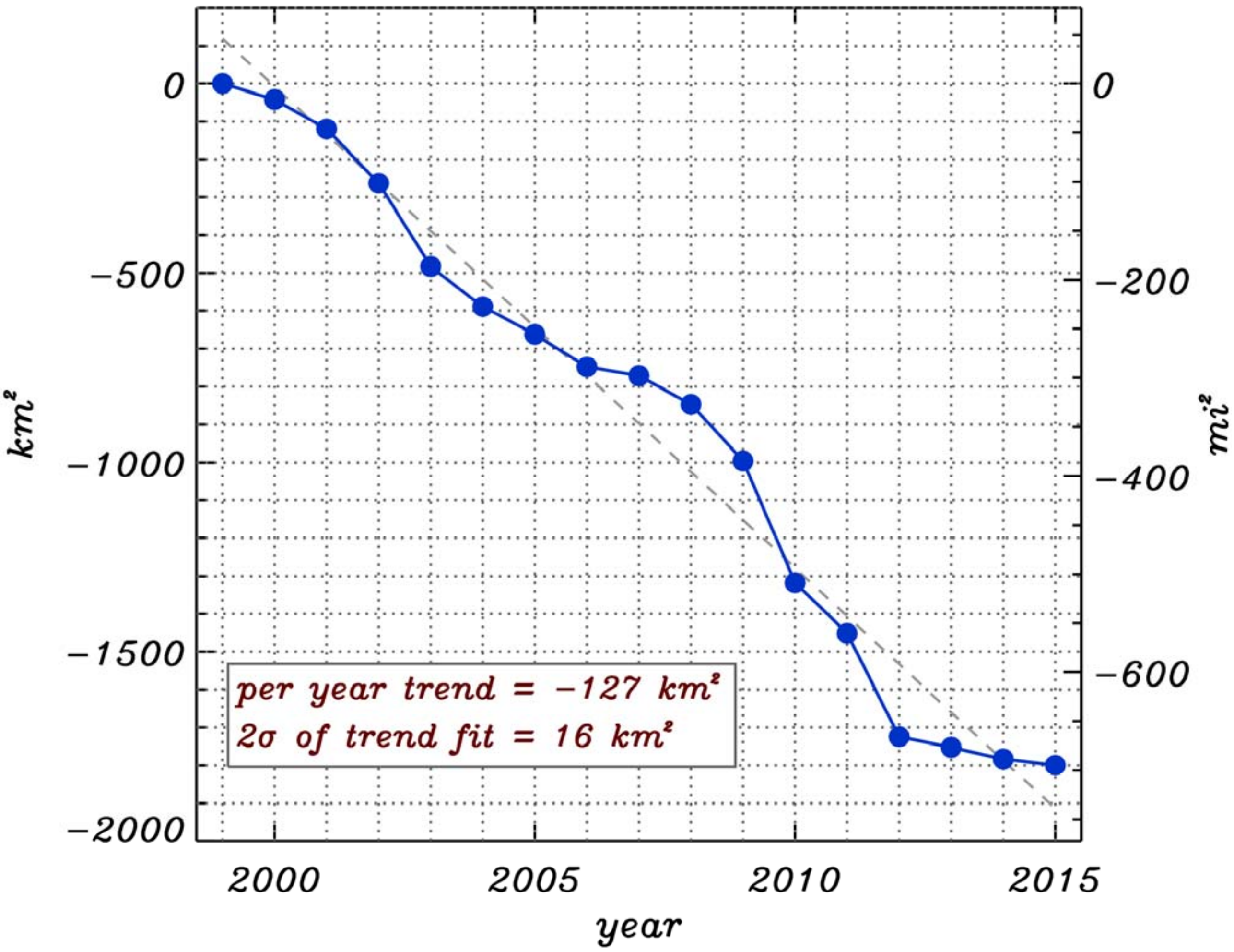

Figure 24. *GL_AREA_CHANGE Cumulative area change of 45 of the widest Greenland tidewater glaciers after Jensen et al. (2016) and Box and Hansen (2015).*

Microbial Abundance in Glacier Ice

Measuring microbial abundance in glacier ice and identifying its controls is essential for a better understanding and quantification of biogeochemical processes in glacial ecosystems. Sharing PROMICE logistics, Stibal et al. (2015) publish the first survey of ice microbial cells abundance from geographically widespread sites on the Greenland ice sheet. The study reviewed published data on microbial abundance in glacier ice and tested the three methods on artificial ice samples of realistic cell (102–107 cells ml−1) and mineral particle (0.1–100 mg ml−1) concentrations, simulating a range of glacial ice types, from clean subsurface ice to surface ice to sediment-laden basal ice. The study then used multivariate statistical analysis to identify factors responsible for the variation in microbial abundance on the ice sheet. The lowest abundances were found in ice sampled from the accumulation area of the ice sheet and in samples affected by fresh snow; these samples may be considered as a reference point of the cell abundance of precipitants that are deposited on the ice sheet surface. Dust content was the most significant variable to explain the variation in the abundance data, which suggests a direct association between deposited dust particles and cells and/or by their provision of limited nutrients to microbial communities on the ice sheet.

Related projects

PROMICE demonstrates the Danish responsibility to monitor the Greenland ice sheet. The PROMICE AWS network presently includes 22 stations on the ice sheet. Only 14 of these have been funded by PROMICE. The rest have been funded by the ongoing Greenland Analogue Project (GAP) and a number of previous projects including SEDIMICE, REFREEZE and Imglaco. In addition, GEUS also maintains three stations on the A. P. Olsen ice cap in the GlacioBasis project within the Greenland Ecosystem Monitoring framework.

In this way, the monitoring effort is enhanced and PROMICE is provided with additional field instrumentation, logistics sharing and instrument knowhow, making it more cost effective. Also, the fieldwork of the smaller research projects benefit strongly from PROMICE and would in many cases not have been feasible without the PROMICE platform as a basis.

PROMICE team members were in 2015 involved in a number of national and international research projects including the European Space Agency (ESA) funded Climate Change Initiative Ice Sheets (CCI_Ice Sheets) and CryoClim and the Nordic Top Research Initiative Center of Excellence 'Stability and Variations of Arctic Land Ice' (SVALI), RETAIN funded by The Danish Council for Independent Research, the Geocenter project 'Multi-millennial ice volume changes of the Greenland ice sheet' and Dark Snow Project. All of these projects make use of PROMICE data and provides PROMICE with additional scientific insights and data.

Four PhD projects are currently performed at GEUS in connection with PROMICE. They are entitled respectively: 'Modelling the Upernavik Glacier Complex', 'Multi-millennial ice volume changes of the Greenland ice sheet', 'Improving Greenland ice sheet surface mass budget models of the accumulation zone' and 'How multi-year snow (firn) affects the mass balance of the Greenlandic inland ice'.

PROMICE is taking part in a number of international cryosphere monitoring and assessment activities including WMO CryoNet, the AMAP SWIPA report, GLIMPSE and IASC.

The long term consistent knowledge and data which PROMICE can provide to the projects is extremely important and makes the PROMICE project team members attractive as project partners. E.g. Danish institutions have a strong involvement in the ESA CCI_Ice_sheets project and it is led by DTU Space. A large component of the project is concerned with ice velocity mapping. This is partly based on the ice velocity mapping knowhow maintained in Denmark due to the ice velocity mapping tools developed within PROMICE. Also, data from PROMICE are valuable for validation of the satellite-derived products in the ESA CCI_Ice_Sheets project.

PROMICE team members have also engaged in applied glaciology by performing commercial evaluations of future hydropower potential in Greenland and AWS of the type developed within PROMICE have been sold for commercial and research purposes.

In this respect, PROMICE provides knowledge and data of use directly for society and also for international projects enhancing the possibility of Danish involvement. At the same time, PROMICE serves as a way to utilize and sustain the scientific insights, instruments and data obtained in the related research projects.

WMO CryoNet

In 2015, the activities of WMO GCW CryoNet have started focusing increasingly on the implementation of the network. GEUS hosted the GCW Joint Meeting of CryoNet Team and Portal & Website Team and the GCW Steering Group Meeting, both in Copenhagen (19-23 January 2015). Plans were finalized to prepare the relevant documents and information for the quadrennial WMO Congress. The 17th WMO Congress (25 May – 12 June 2015, Geneva, Switzerland) voted and approved GCW as a core WMO activity. This has made continued and increased WMO funding available to establish a stronger Secretariat in support of the GCW Working Groups activities. The WMO Congress also approved the list of pilot and candidate GCW and CryoNet sites. The PROMICE and GEM ZERO sites are pilot CryoNet sites (Figure 25).

Figure 25. *Map of the pilot CryoNet sites. PROMICE and GEM ZERO are indicated by number 2 and 28, respectively.*

The experience of collecting information from a growing number of candidate and pilot sites has led to a simplification and clarification of the overall structure of CryoNet. The new structure makes it easier to highlight the peculiarities of each station, their suitability for in situ process studies, long time series, suitability for cal/val of remote sensing and model products, training facilities and so on (Figure 26). Work has started to review and define recommended best practices for in situ observations. This work will develop over the coming years.

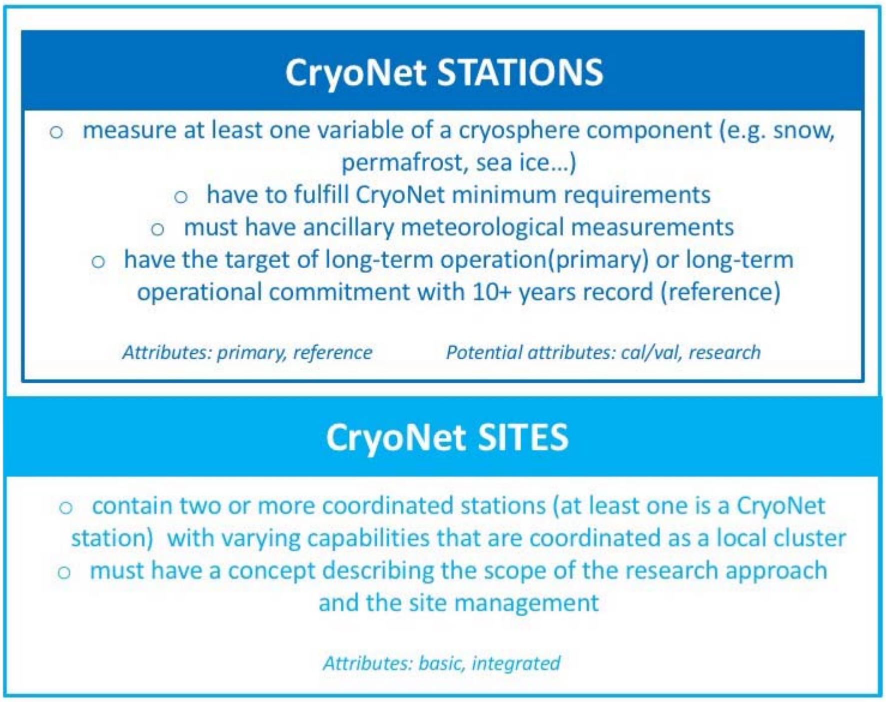

Figure 26. *Design of the WMO GCW CryoNet network, composed of Baseline, Reference and Integrated Sites. The major requirements for joining CryoNet are listed.*

PROMICE and GEUS contributed to this ongoing organization effort through a member in the GCW Steering Group and in the CryoNet Team (Michele Citterio) and by hosting the January 2015 meetings.

References

Andersen, M., L. Stenseng, H. Skourup, W. Colgan, S. Khan, S. Kristensen, S. Andersen, J. Box, A. Ahlstrøm, X, Fettweis and R. Forsberg. 2015. Basin-scale partitioning of Greenland ice sheet mass balance components (2007–2011). Earth and Planetary Science Letters. 409: 89-95. doi:10.1016/j.epsl.2014.10.015

Andersen, S.B., Ahlstrøm, A.P., Andersen, M.L., Box, J.E., Citterio, M., Fausto, R., Machguth, H., van As, D., Edelvang, K., Forsberg, R., Skourup, H., Sørensen, L.S., Kristensen, S.S., Dall, J., Boncori, J.P.M. & Petersen, D. 2013: PROMICE 2011-12. Danmarks og Grønlands Geologiske Undersøgelse Rapport 2013/54, 82 pp.

Andersen, S.B., Ahlstrøm, A.P., Andersen, M.L., Box, J.E., Citterio, M., Colgan, W.T., Fausto, R., van As,D., Forsberg, R., Skourup, H., Sørensen, L.S., Kristensen, S.S., Dall, J., Kusk, A. & Petersen, D. 2014: PROMICE 2013. Report from the 2013 operational phase of the Programme for Monitoring of the Greenland Ice Sheet. Danmarks og Grønlands Geologiske Undersøgelse Rapport. 2014/57. GEUS, 72 pp.

Bolch, T., Sandberg Sørensen, L., Simonsen, S. B., Mölg, N., Machguth, H., Rastner, P., & Paul, F. (2013). Mass loss of Greenland's glaciers and ice caps 2003–2008 revealed from ICESat laser altimetry data. Geophysical Research Letters, 40(5), 875-881.

Box, J.E., and K. Hansen, 2015, Program for the Monitoring of Greenland Ice Sheet (PROMICE) Newsletter 8, December, 2015, http://promice.org/Newsletter.html

Charalampidis, C., van As, D., Box, J. E., van den Broeke, M. R., Colgan, W. T., Doyle, S. H., Hubbard, A. L., MacFerrin, M., Machguth, H., and Smeets, C. J. P. P.: Changing surface–atmosphere energy exchange and refreezing capacity of the lower accumulation area, West Greenland, The Cryosphere, 9, 2163-2181, doi:10.5194/tc-9-2163-2015, 2015.

Citterio M and Ahlstrøm AP (2013) Brief communication "The aerophotogrammetric map of Greenland ice masses". Cryosph., 7, 445-449 (doi: 10.5194/tc-7-445-2013)

Doyle SH, Hubbard A, Fitzpatrick AAW, Van As D, Mikkelsen AB, Pettersson R and Hubbard B (2014) Persistent flow acceleration within the interior of the Greenland Ice Sheet. Geophys. Res. Let., 41 (3), 899-905 (doi:10.1002/2013GL058933)

Doyle, S.H., A. Hubbard, R.S.W. van de Wal, J.E. Box, D. van As, K. Scharrer, T.W. Meierbachtol, P.C. J. P. Smeets, J.T. Harper, E. Johansson, R.H. Mottram, A.B. Mikkelsen, F. Wilhelms, H. Patton, P. Christoffersen, Bryn Hubbard, Amplified melt and flow of the Greenland ice sheet driven by late-summer cyclonic rainfall, Nature Geoscience, 8, pages 647-653, doi:10.1038/ngeo2482.

Fausto, R.S., Van As, D., Ahlstrøm, A.P., Andersen, S.B., Andersen, M.L. Citterio, M., Edelvang, K., Machguth, H., Nielsen, S. & Weidick, A. (2012) Ablation observations for 2008–2011 from the Programme for Monitoring of the Greenland Ice Sheet (PROMICE). Geological Survey of Denmark and Greenland Bulletin 26, 25–28.

Fausto, R.S., Van As, D., Antoft, J.A., Box, J.E., Colgan, W. and PROMICE project team (2015) Greenland ice sheet melt area from MODIS (2000-2014). Geol. Surv. Denmark Greenland Bull., 33, 57-60

Fausto, R. S., D. van As, J. E. Box, W. Colgan, P. L. Langen, and R. H. Mottram (2016) The implication of nonradiative energy fluxes dominating Greenland ice sheet exceptional ablation area surface melt in 2012,Geophys. Res. Lett., 43, doi:10.1002/2016GL067720.

Fitzpatrick AAW, Hubbard A, Joughin I, Quincey DJ, Van As D, Mikkelsen APB, Doyle SH, Hasholt B and Jones GA (2013) Ice flow dynamics and surface meltwater flux at a land-terminating sector of the Greenland Ice Sheet. J. Glac., 59 (216), 687-696 (doi: 10.3189/2013JoG12J143)

Fitzpatrick AAW, Hubbard AL, Box JE, Quincey DJ, van As D, Mikkelsen APB, Doyle SH, Dow CF, Hasholt B and Jones GA (2014) A decade (2002–2012) of supraglacial lake volume estimates across Russell Glacier, West Greenland. The Cryosphere, 8, 107-121 (doi: 10.5194/tc-8-107-2014)

Howat, I. M., A. Negrete, and B. E. Smith. 'The Greenland Ice Mapping Project (GIMP) Land Classification and Surface Elevation Data Sets'. The Cryosphere 8, no. 4 (2014): 1509–18.

Jensen, T., J.E. Box, and C.S. Hvidberg, A sensitivity study of yearly Greenland ice sheet marine terminating outlet glacier changes: 1999-2013, J. Glaciol., 15J085, accepted Dec. 2015

Kargel JS, Ahlstrøm AP, Alley RB, Bamber JL, Benham TJ, Box JE, Chen C, Christoffersen P, Citterio M, Cogley JG, Jiskoot H, Leonard GJ, Morin P, Scambos T, Sheldon T and Willis I (2012) Brief communication: Greenland's shrinking ice cover: "fast times" but not that fast. Cryosph., 6, 533-537 (doi: 10.5194/tc-6-533-2012)

Langen, P.L., R.H. Mottram, J.H. Christensen, F. Boberg, C.B. Rodehacke, M. Stendel, D. van As, A.P. Ahlstrøm, J. Mortensen, S. Rysgaard, D. Petersen, K.H. Svendsen, G. Aðalgeirsdóttir, and J. Cappelen (2015) Quantifying Energy and Mass Fluxes Controlling Godthåbsfjord Freshwater Input in a 5-km Simulation (1991Ð2012), J. Climate, 28, 3694Ð3713. doi: http://dx.doi.org/10.1175/JCLI-D-14-00271.1.

Leclercq, P. W., Weidick, A., Paul, F., Bolch, T., Citterio, M., and Oerlemans, J.: Brief communication "Historical glacier length changes in West Greenland", The Cryosphere, 6, 1339-1343, doi:10.5194/tc-6-1339-2012, 2012.

Machguth H, Rastner P, Bolch T, Mölg N, Sandberg Sørensen L, Aðalgeirsdottir G, Van Angelen JH, Van den Broeke MR and Fettweis X (2013) The future sea-level rise contribution of Greenland's glaciers and ice caps. Environ. Res. Lett., 8, 025005, doi: 10.1088/1748-9326/8/2/025005

Machguth, H., M. MacFerrin, D. van As, J.E. Box, C. Charalampidis, W. Colgan, R.S. Fausto, H.A. J. Meijer, E. Mosley-Thompson & R.S. W. van de Wal, Greenland meltwater storage in firn limited by near-surface ice formation, Nature Climate Change, doi:10.1038/nclimate2899

Mernild SH, Malmros JK, Yde JC, Wilson R, Knudsen NT, Hanna E, Fausto RS and Van As D (2015) Albedo decline on Greenlands Mittivakkat Gletscher in a warming climate. Int. J. Climatol., 35, 2294-2307 (doi:10.1002/joc.4128)Fausto RS, Van As D, Antoft JA, Box JE, Colgan W and PROMICE project team (2015) Greenland ice sheet melt area from MODIS (2000-2014). Geol. Surv. Denmark Greenland Bull., 33, 57-60

Mikkelsen, A. B., Hubbard, A., MacFerrin, M., Box, J., Doyle, S., Fitzpatrick, A., Hasholt, B., and Bailey, H.: Extraordinary runoff from the Greenland Ice Sheet in 2012 amplified by hypsometry and depleted firn-retention, The Cryosphere Discuss., 9, 4625-4660, doi:10.5194/tcd-9-4625-2015, 2015.

Morlighem, M., E. Rignot, J. Mouginot, H. Seroussi and E. Larour. 2014. Deeply incised submarine glacial valleys beneath the Greenland Ice Sheet, Nature Geoscience, 7:418–422. doi:10.1038/ngeo2167.

Rastner, P., T. Bolch, N. Mölg, H. Machguth, and F. Paul. 'The First Complete Glacier Inventory for the Whole of Greenland'. The Cryosphere Discussions 6, no. 4 (16 July 2012): 2399–2436. doi:10.5194/tcd-6-2399-2012.

Stibal M, Gözdereliler E, Cameron KA, Box JE, Stevens IT, Gokul JK, Schostag M, Zarsky JD, Edwards A, Irvine-Fynn TD and Jacobsen CS (2015). Microbial abundance in surface ice on the Greenland Ice Sheet. Front. Microbiol. 6:225. doi: 10.3389/fmicb.2015.00225

Storey, James, Michael Choate, and Kenton Lee. 'Landsat 8 Operational Land Imager On-Orbit Geometric Calibration and Performance'. Remote Sensing 6, no. 11 (11 November 2014): 11127–52. doi:10.3390/rs61111127.

Van As D, Hubbard AL, Hasholt B, Mikkelsen AB, Van den Broeke MR and Fausto RS (2012) Large surface meltwater discharge from the Kangerlussuaq sector of the Greenland ice sheet during the record-warm year 2010 explained by detailed energy budget observations. The Cryosphhere, 6, 199-209 (doi: 10.5194/tc-6-199-2012)

Van As D, Andersen ML, Petersen D, Fettweis X, Van Angelen JH, Lenaerts JTM, Van den Broeke MR, Lea JM, Bøggild CE, Ahlstrøm AP and Steffen K (2014) Increasing meltwater discharge from the Nuuk region of the Greenland ice sheet and implications for mass balance (1960-2012). J. Glac., 60 (220), 314-322 (doi: 10.3189/2014JoG13J065)

Van Tricht, K., S. Lhermitte, J.T.M. Lenaerts, I.V. Gorodetskaya, T.S. L'Ecuyer, B. Noël, M.R. van den Broeke, D.D. Turner & N.P.M. van Lipzig, 2016. Clouds enhance Greenland ice sheet meltwater runoff, Nature Communications, DOI: 10.1038/ncomms10266

Wake, L.M. and S.J. Marshall, 2015, Assessment of current methods of positive degree-day calculation using in situ observations from glaciated regions, Journal of Glaciology, Vol. 61, No. 226, 2015 doi: 10.3189/2015JoG14J116

Zuo, Z., and J. Oerlemans, 1996. Modelling albedo and specific balance of the Greenland ice sheet: Calculations for the Søndre Strømfjord transect. J. Glaciol., 42, 305– 317.

Appendix A: Data

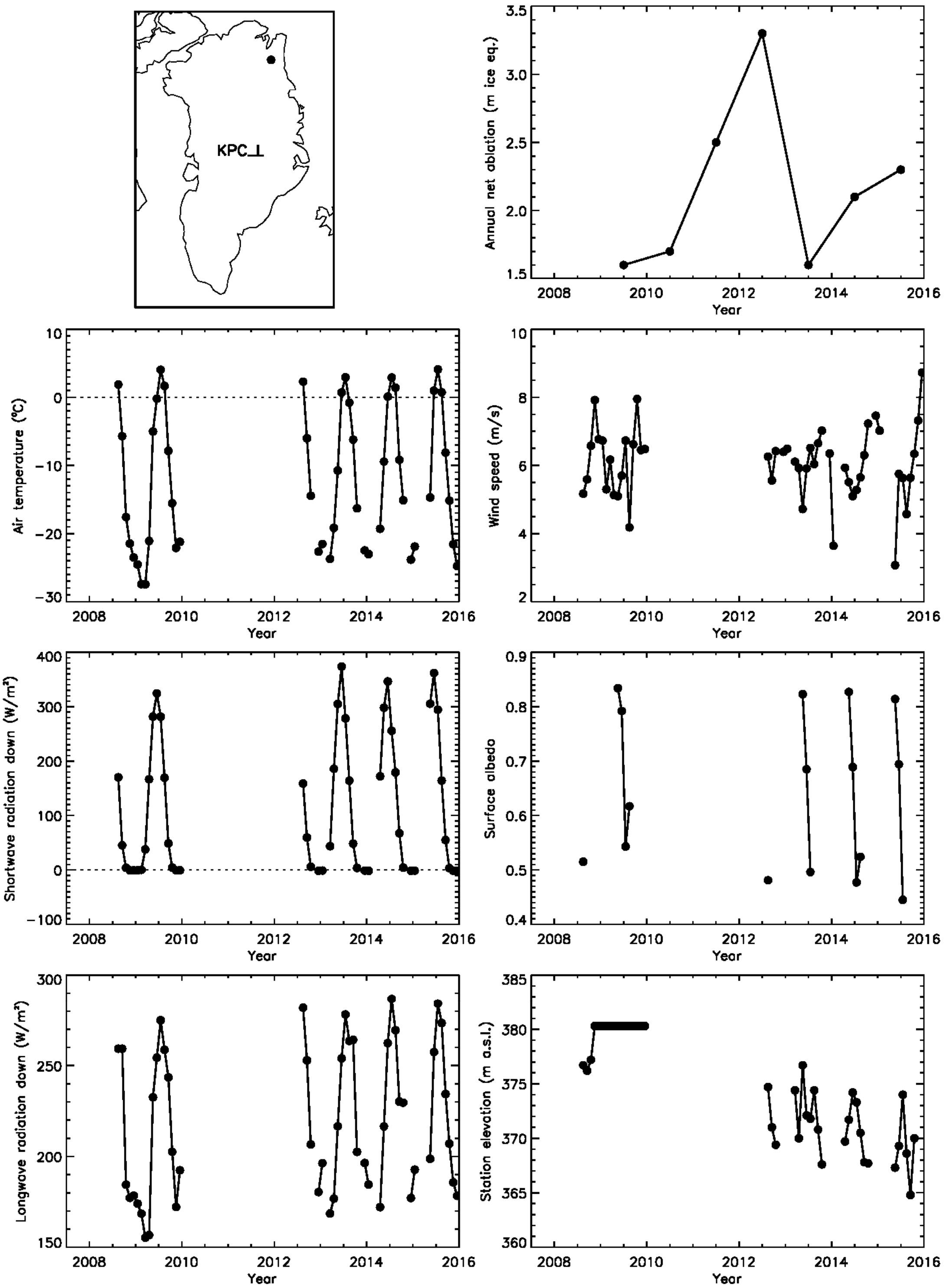

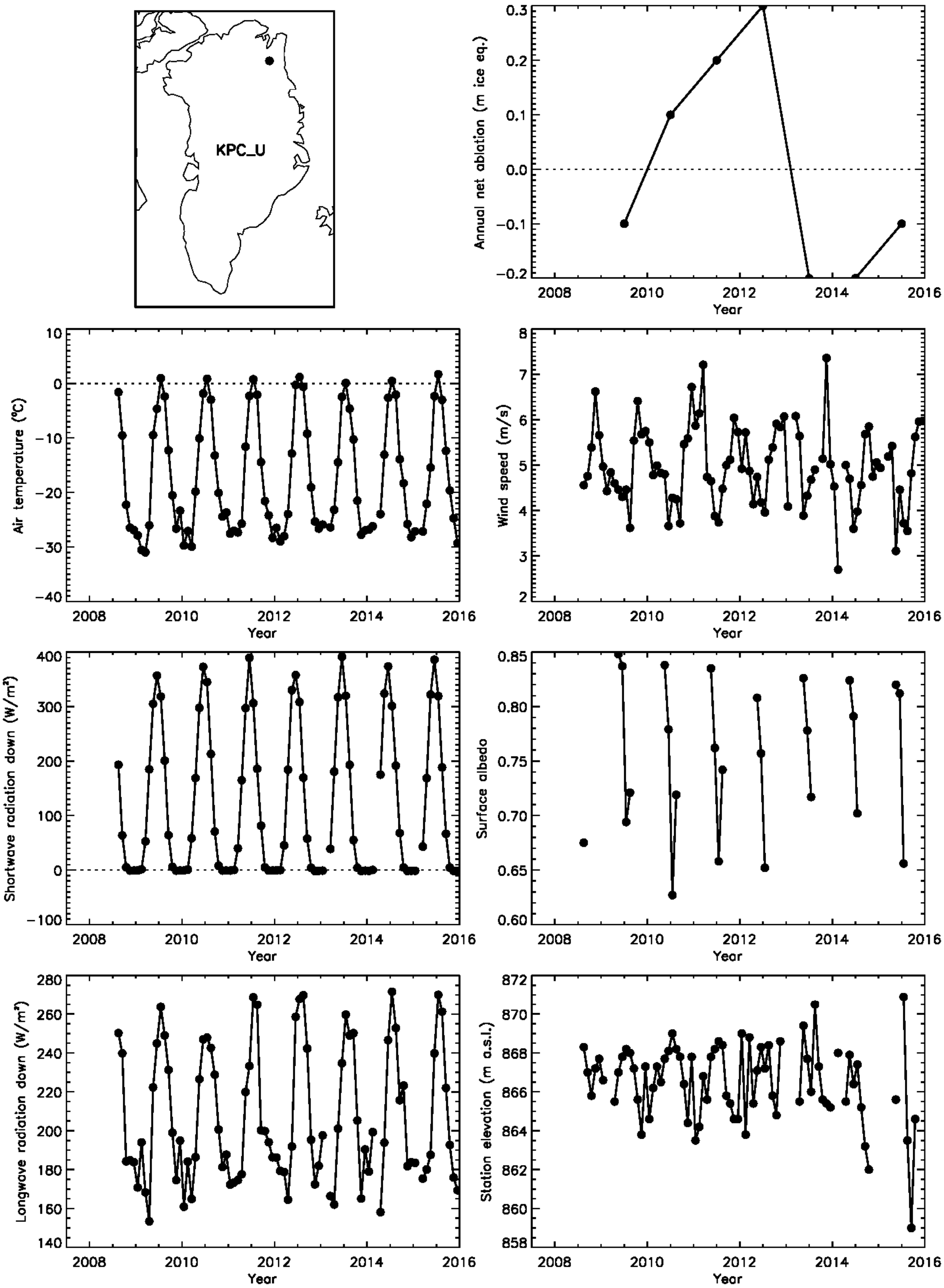

KPC_U
Annual net ablation (m ice eq.)
Air temperature (°C)
Wind speed (m/s)
Shortwave radiation down (W/m²)
Surface albedo
Longwave radiation down (W/m²)
Station elevation (m a.s.l.)
Year

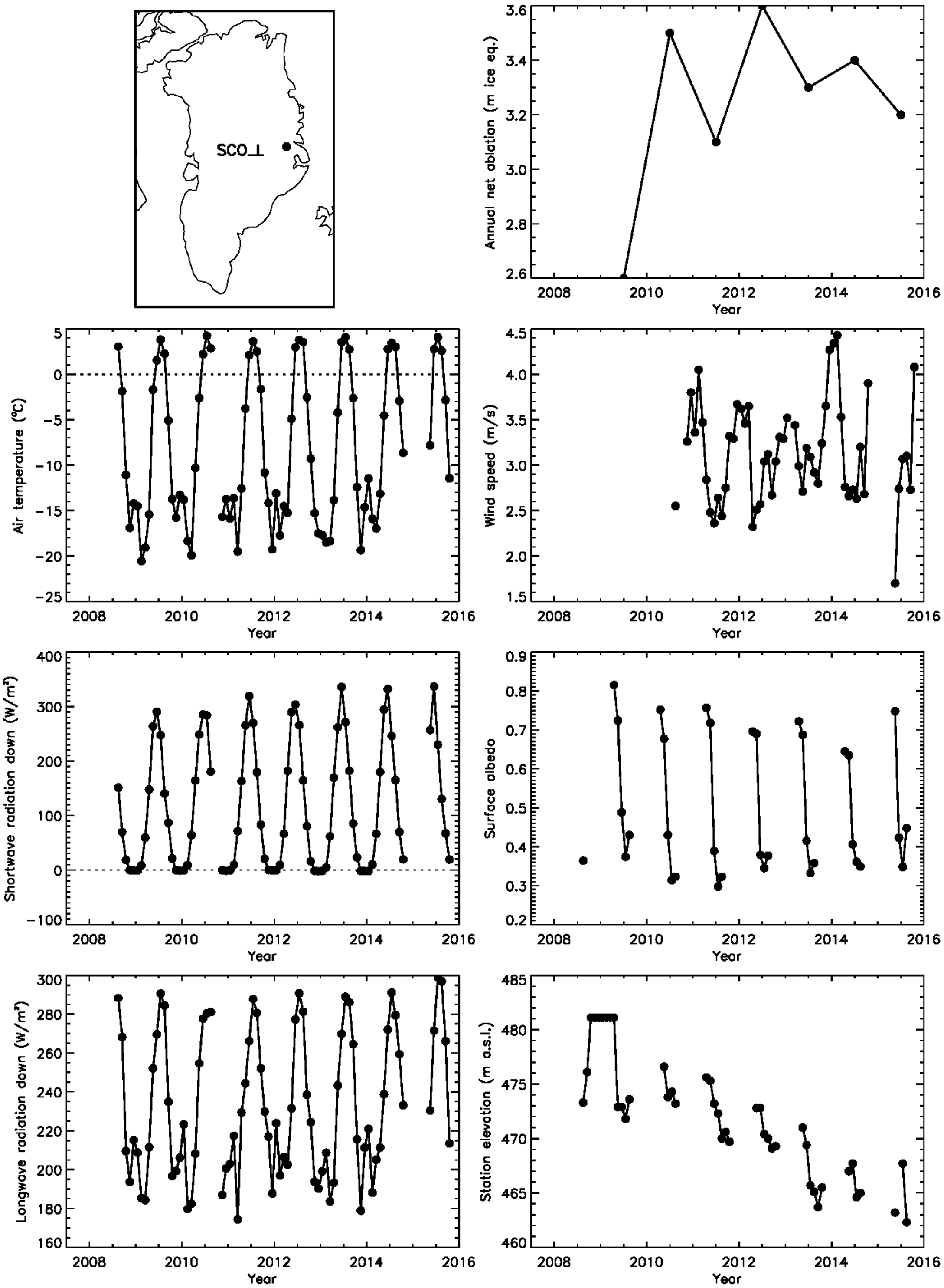
Annual net ablation (m ice eq.)
Air temperature (°C)
Wind speed (m/s)
Shortwave radiation down (W/m²)
Surface albedo
Longwave radiation down (W/m²)
Station elevation (m a.s.l.)
Year

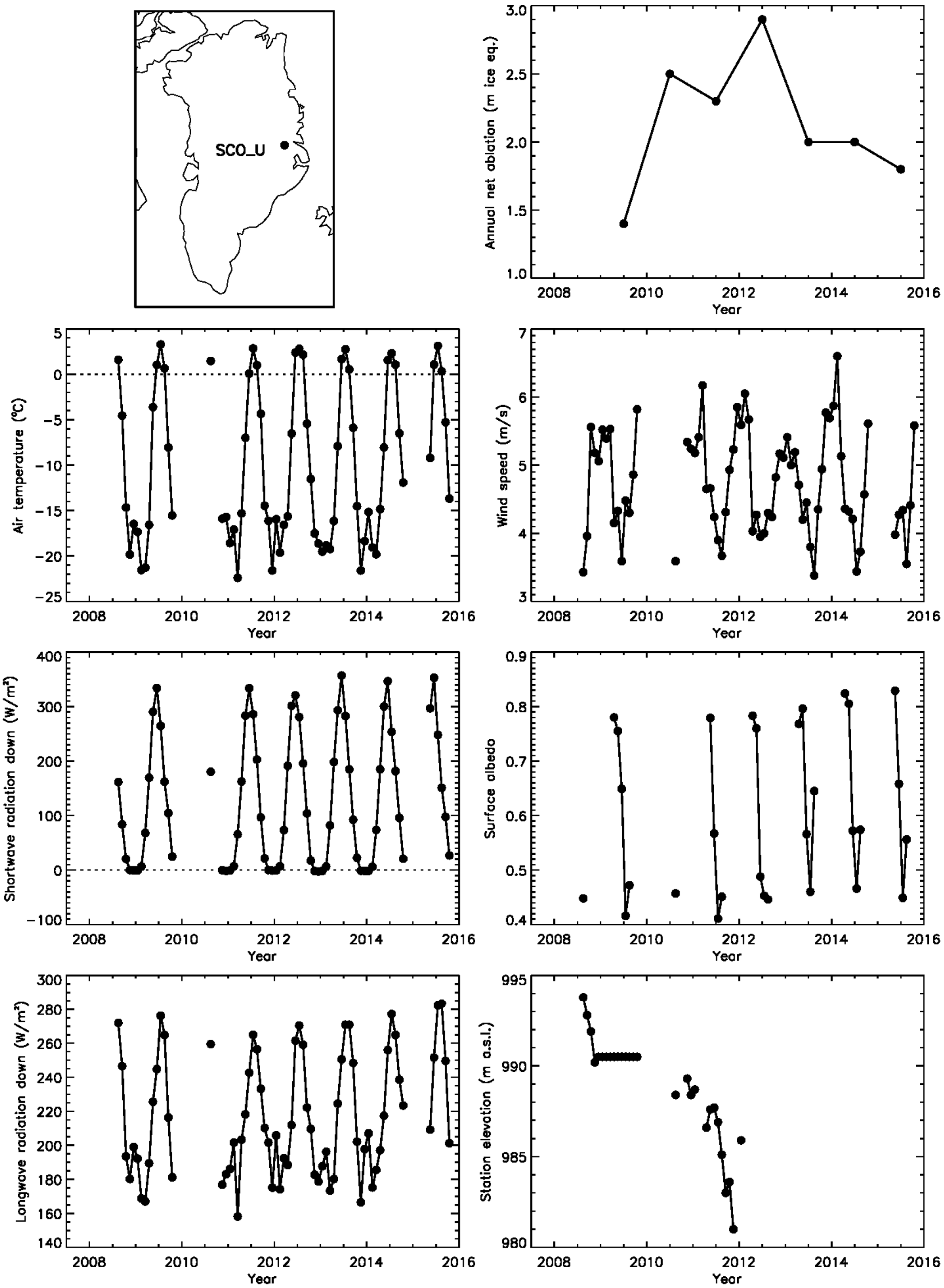
SCO_U
Annual net ablation (m ice eq.)
Air temperature (°C)
Wind speed (m/s)
Shortwave radiation down (W/m²)
Surface albedo
Longwave radiation down (W/m²)
Station elevation (m a.s.l.)
Year

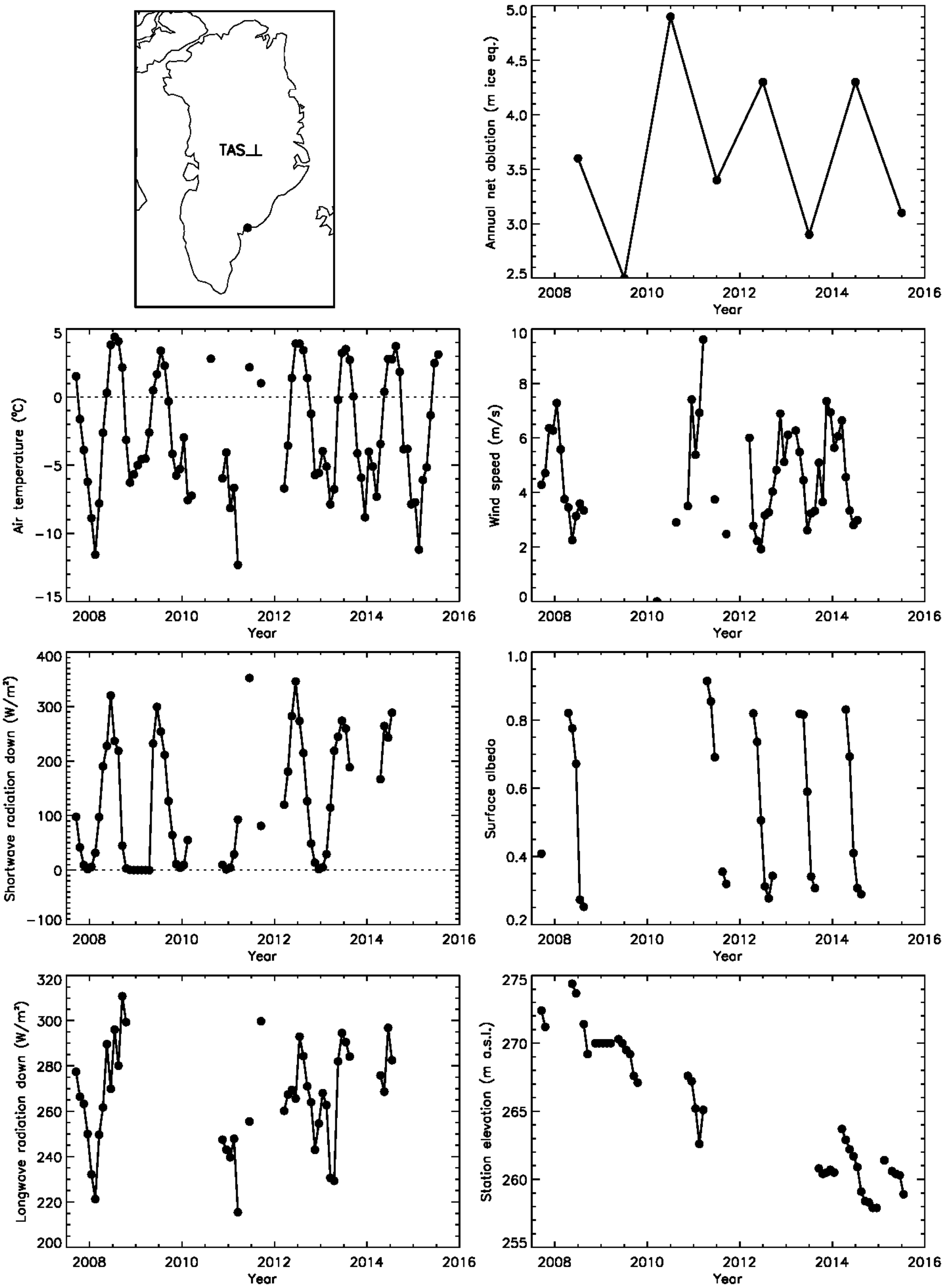
TAS_L
Annual net ablation (m ice eq.)
Air temperature (°C)
Wind speed (m/s)
Shortwave radiation down (W/m²)
Surface albedo
Longwave radiation down (W/m²)
Station elevation (m a.s.l.)
Year

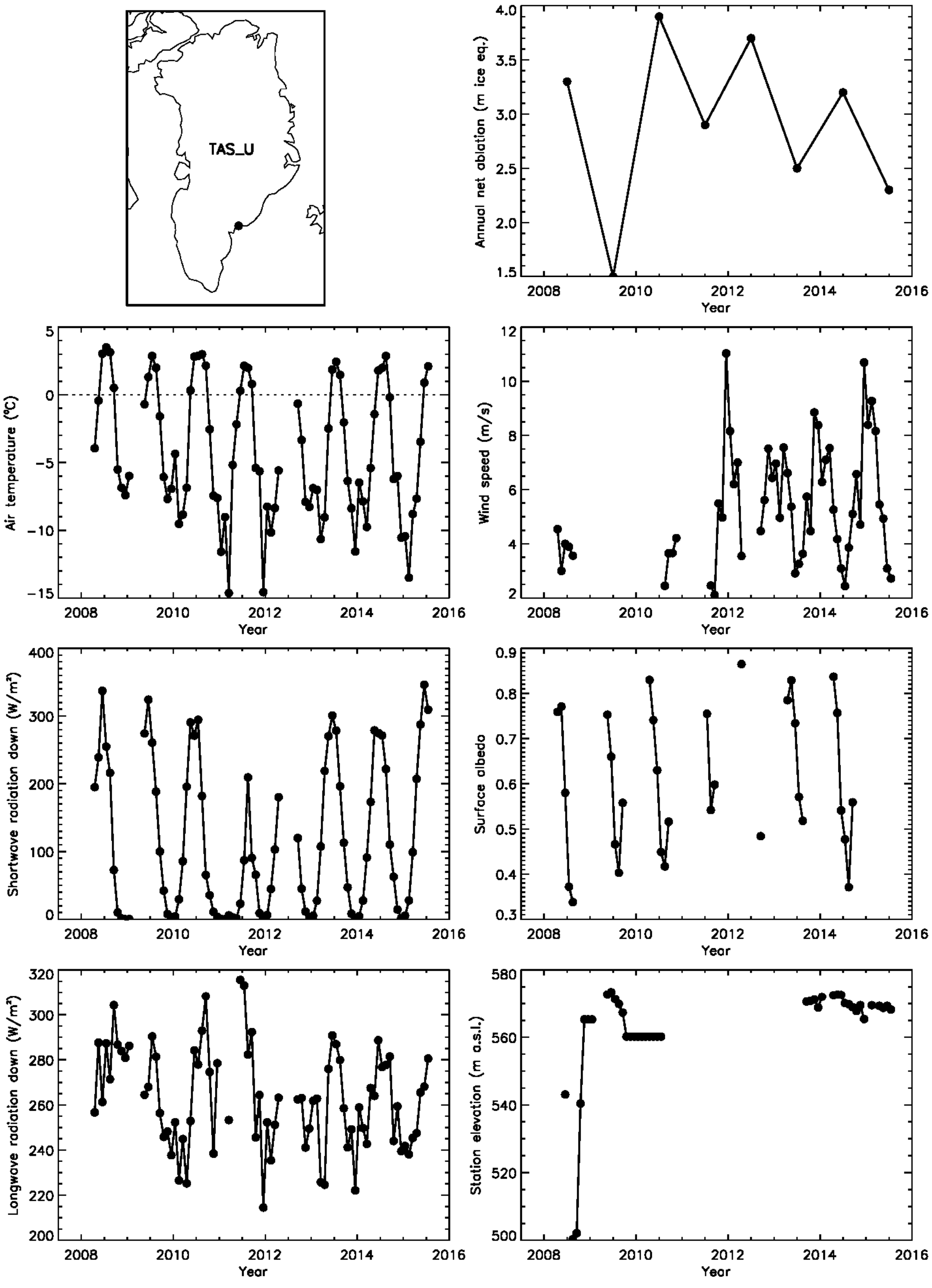
TAS_U
Annual net ablation (m ice eq.)
Air temperature (°C)
Wind speed (m/s)
Shortwave radiation down (W/m²)
Surface albedo
Longwave radiation down (W/m²)
Station elevation (m a.s.l.)
Year

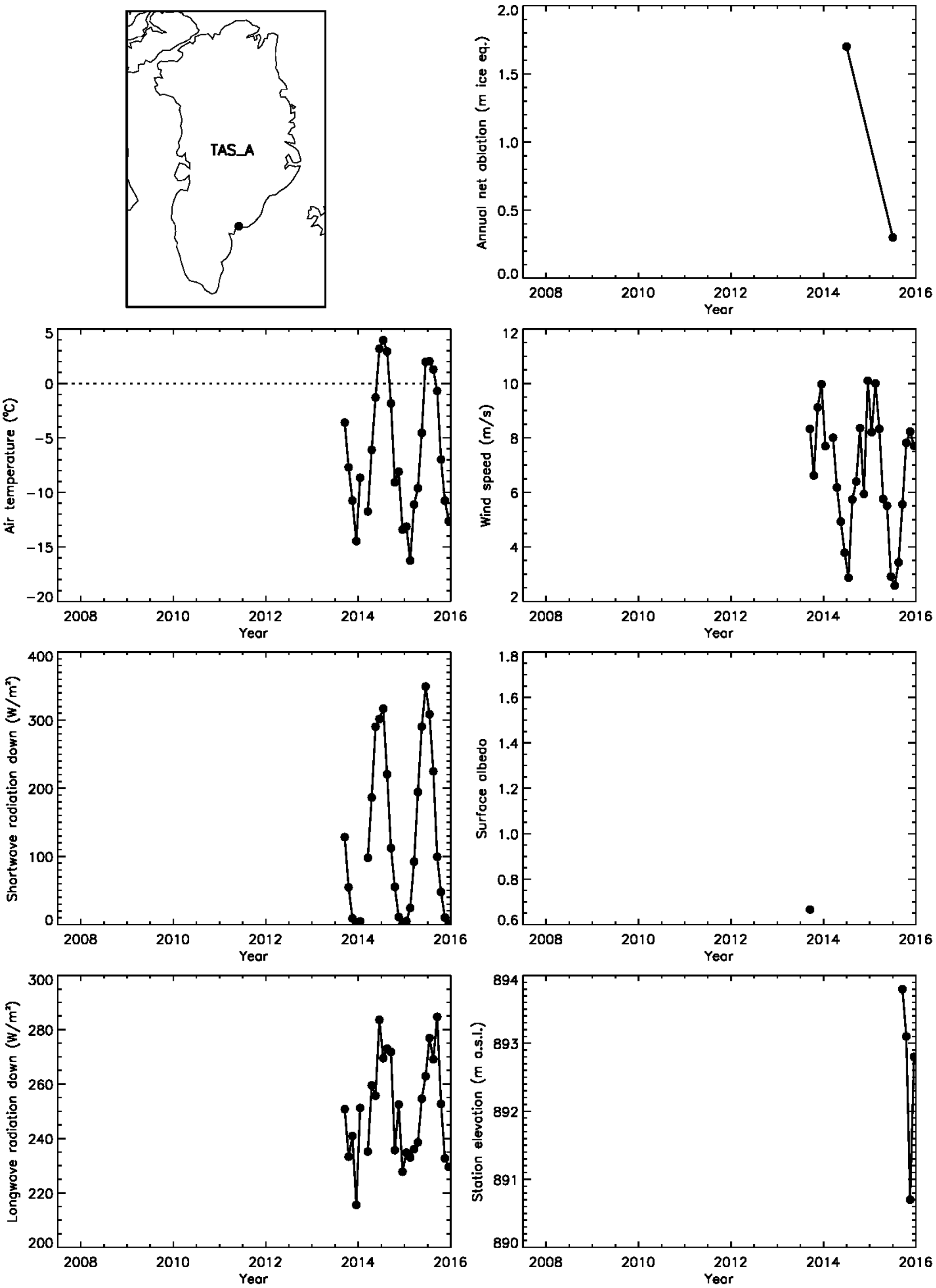
TAS_A
Annual net ablation (m ice eq.)
2.0
1.5
1.0
0.5
0.0
2008
2010
2012
2014
2016
Year
Air temperature (°C)
5
0
−5
−10
−15
−20
Wind speed (m/s)
12
10
8
6
4
2
Shortwave radiation down (W/m²)
400
300
200
100
0
Surface albedo
1.8
1.6
1.4
1.2
1.0
0.8
0.6
Longwave radiation down (W/m²)
300
280
260
240
220
200
Station elevation (m a.s.l.)
894
893
892
891
890

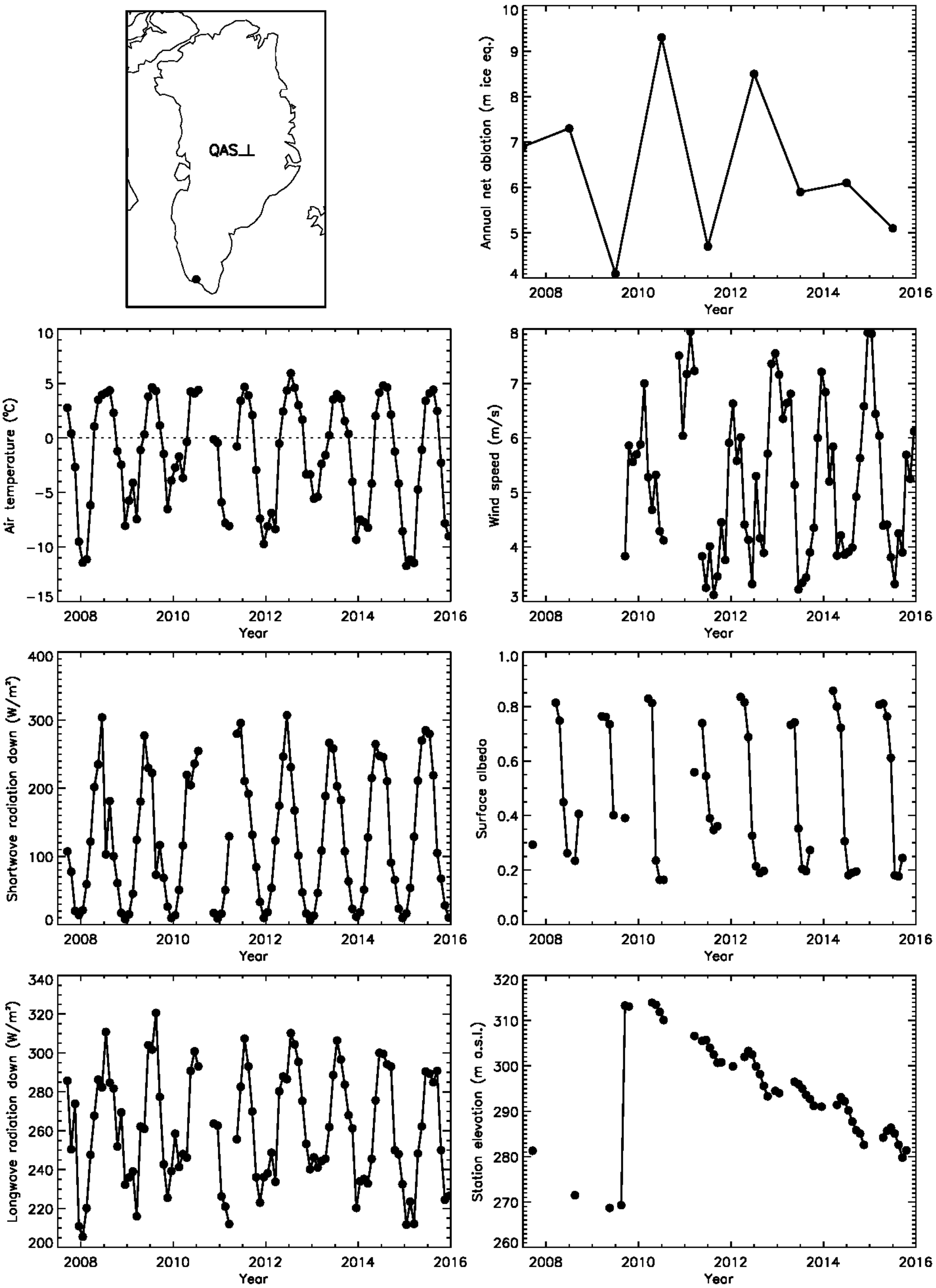
QAS_L
Annual net ablation (m ice eq.)
Air temperature (°C)
Wind speed (m/s)
Shortwave radiation down (W/m²)
Surface albedo
Longwave radiation down (W/m²)
Station elevation (m a.s.l.)
Year

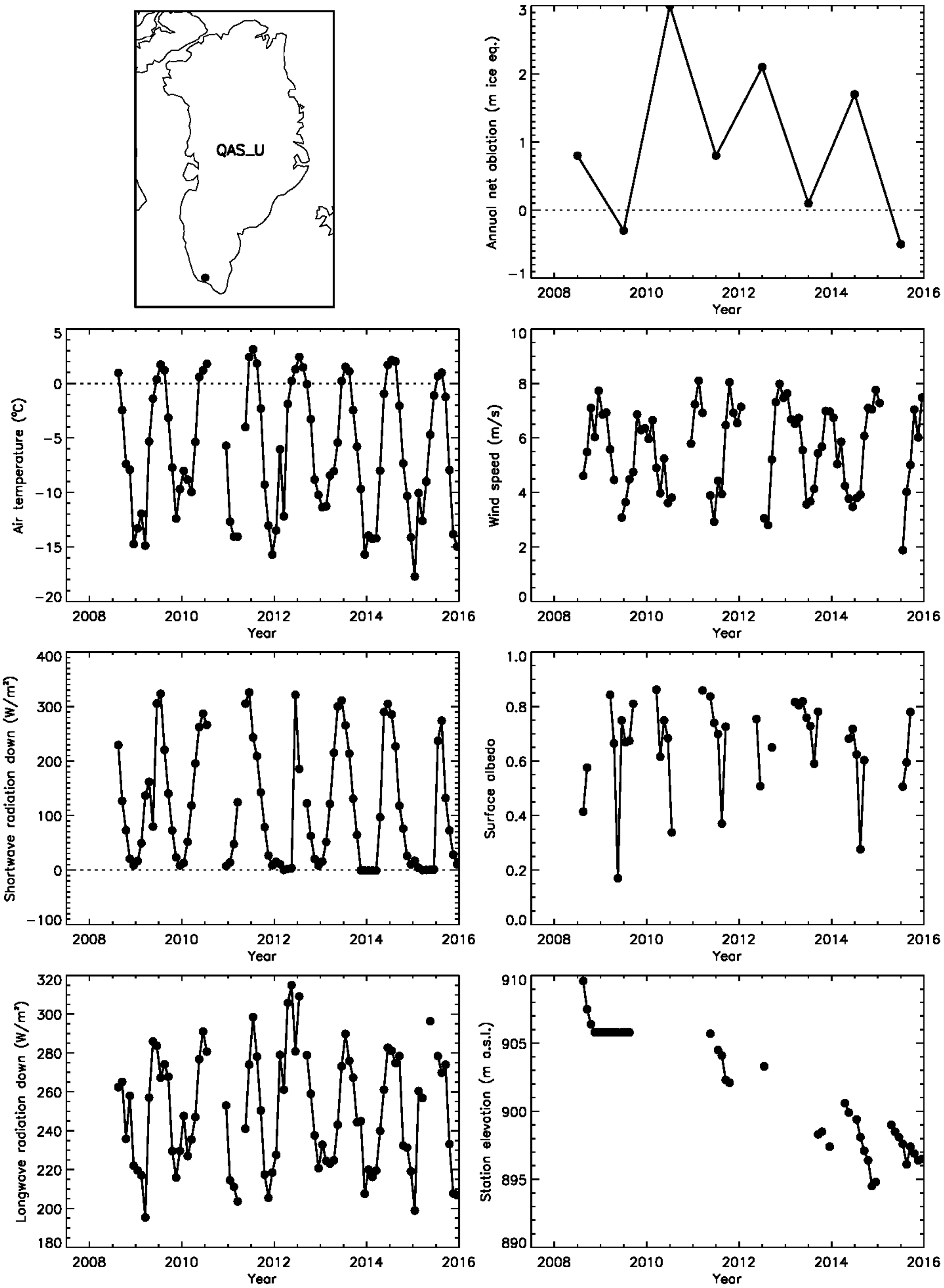
QAS_U
Annual net ablation (m ice eq.)
Air temperature (°C)
Wind speed (m/s)
Shortwave radiation down (W/m²)
Surface albedo
Longwave radiation down (W/m²)
Station elevation (m a.s.l.)
Year

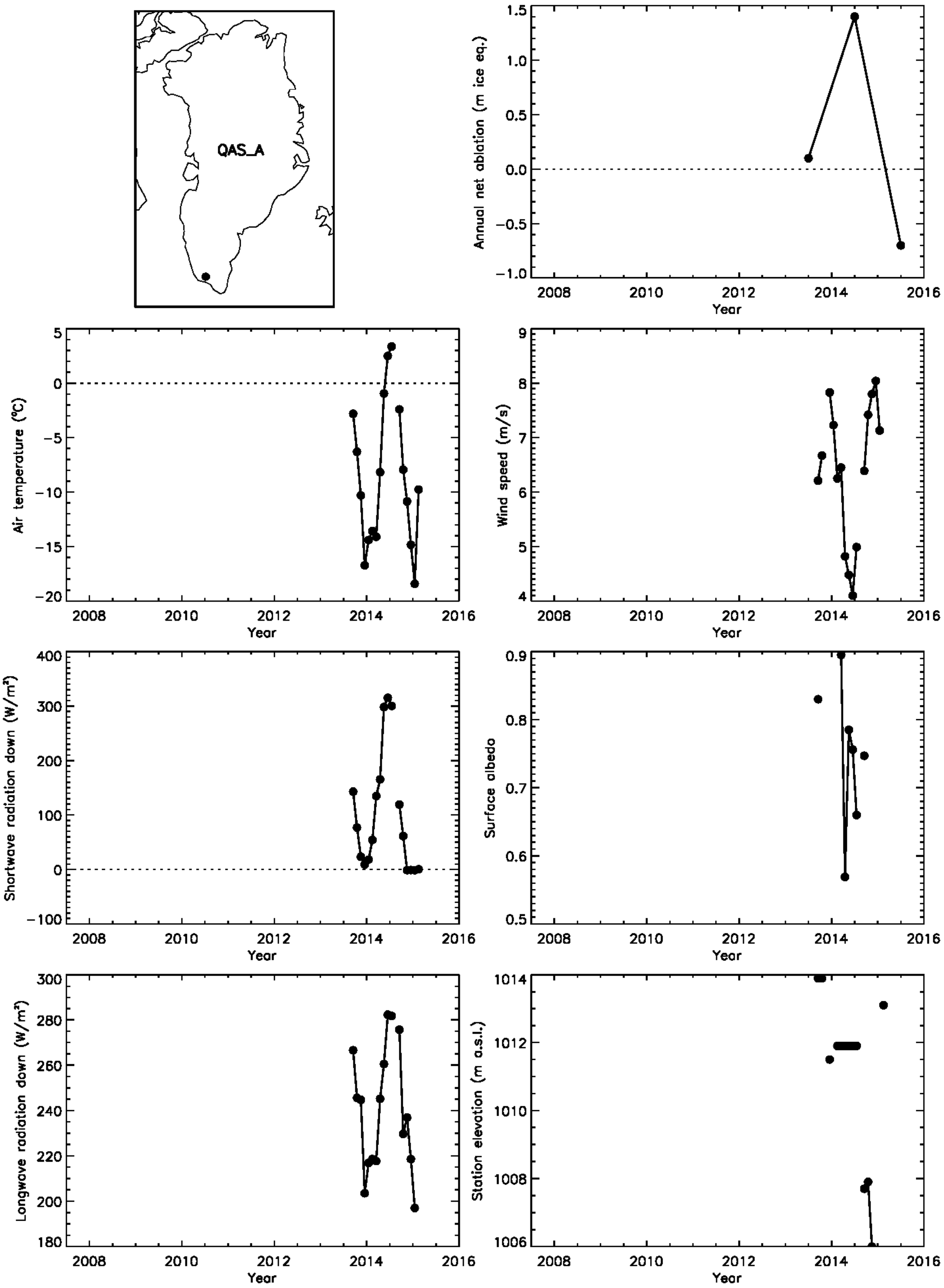
QAS_A
Annual net ablation (m ice eq.)
Air temperature (°C)
Wind speed (m/s)
Shortwave radiation down (W/m²)
Surface albedo
Longwave radiation down (W/m²)
Station elevation (m a.s.l.)
Year

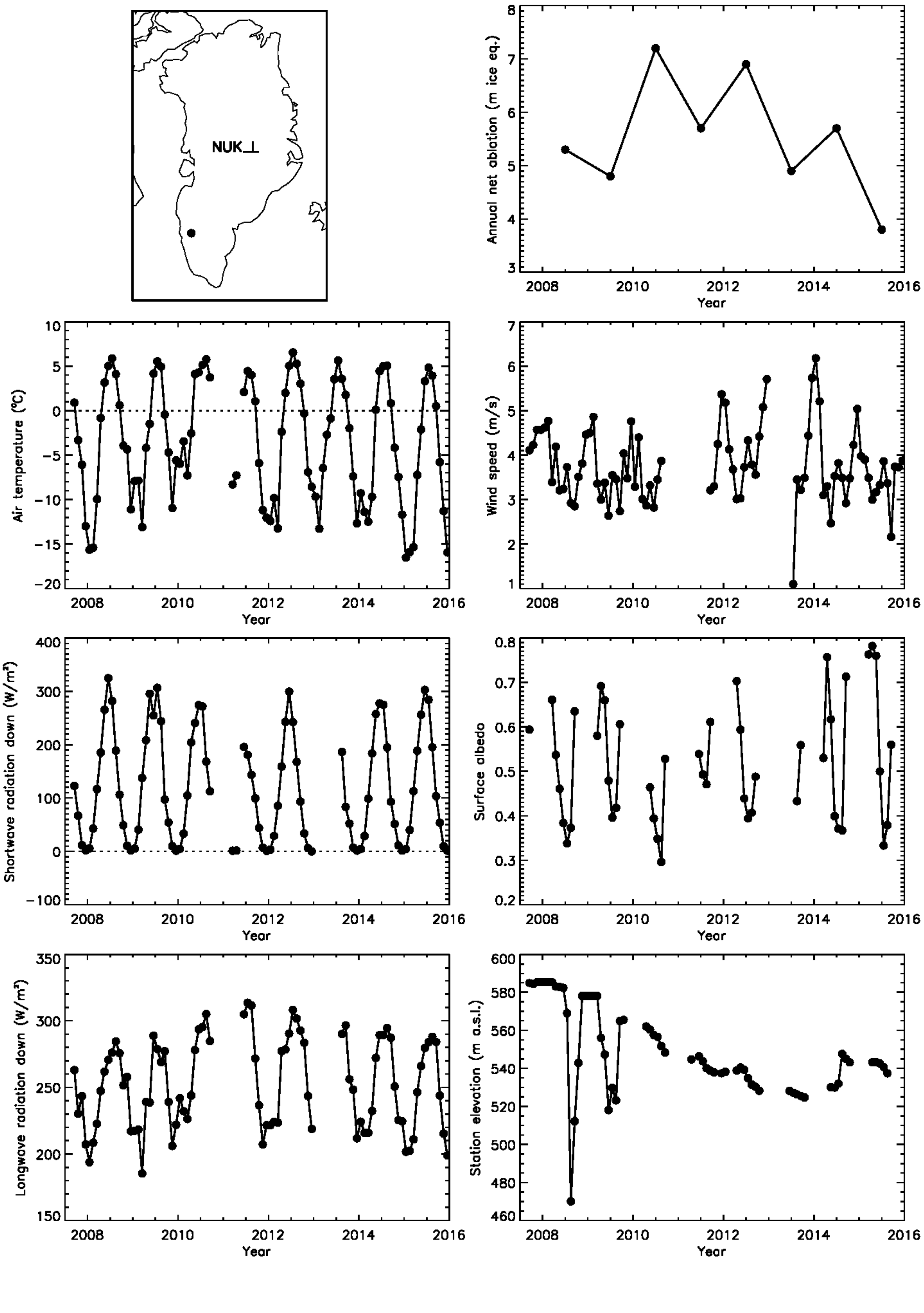
NUK_L
Annual net ablation (m ice eq.)
Air temperature (°C)
Wind speed (m/s)
Shortwave radiation down (W/m²)
Surface albedo
Longwave radiation down (W/m²)
Station elevation (m a.s.l.)
Year

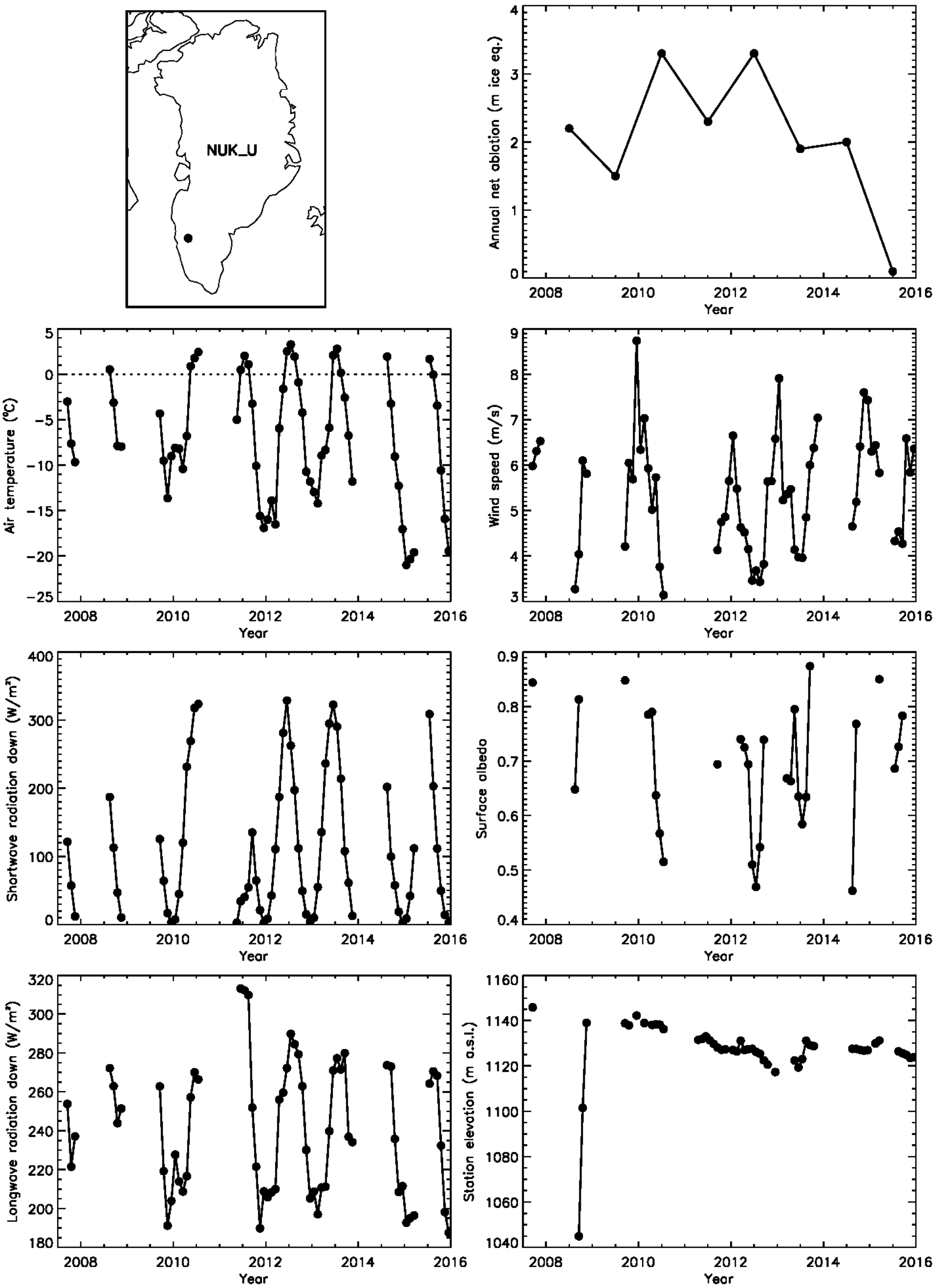

NUK_U
Annual net ablation (m ice eq.)
Air temperature (°C)
Wind speed (m/s)
Shortwave radiation down (W/m²)
Surface albedo
Longwave radiation down (W/m²)
Station elevation (m a.s.l.)
Year
2008
2010
2012
2014
2016

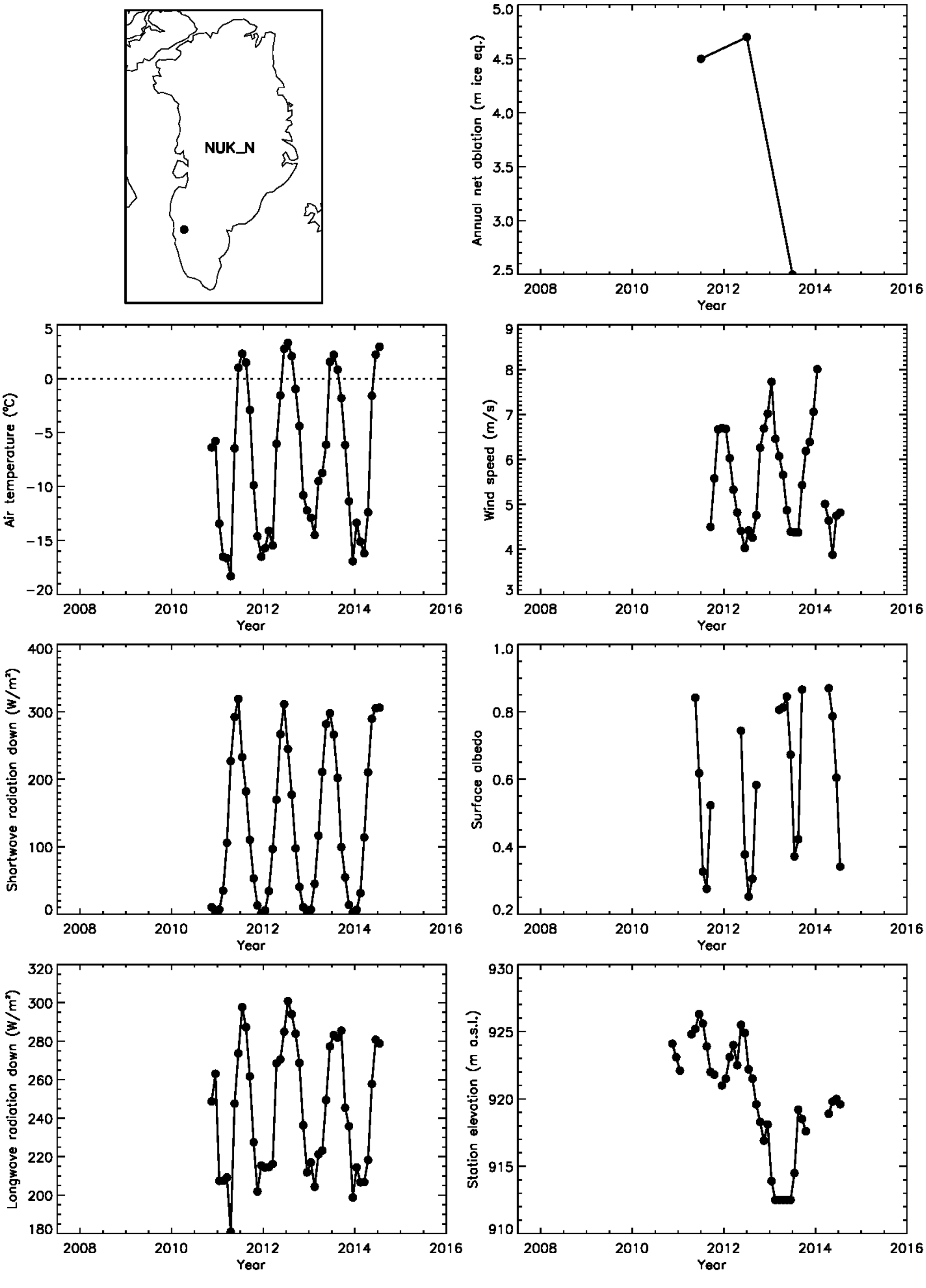
NUK_N
Annual net ablation (m ice eq.)
Year
Air temperature (°C)
Wind speed (m/s)
Shortwave radiation down (W/m²)
Surface albedo
Longwave radiation down (W/m²)
Station elevation (m a.s.l.)

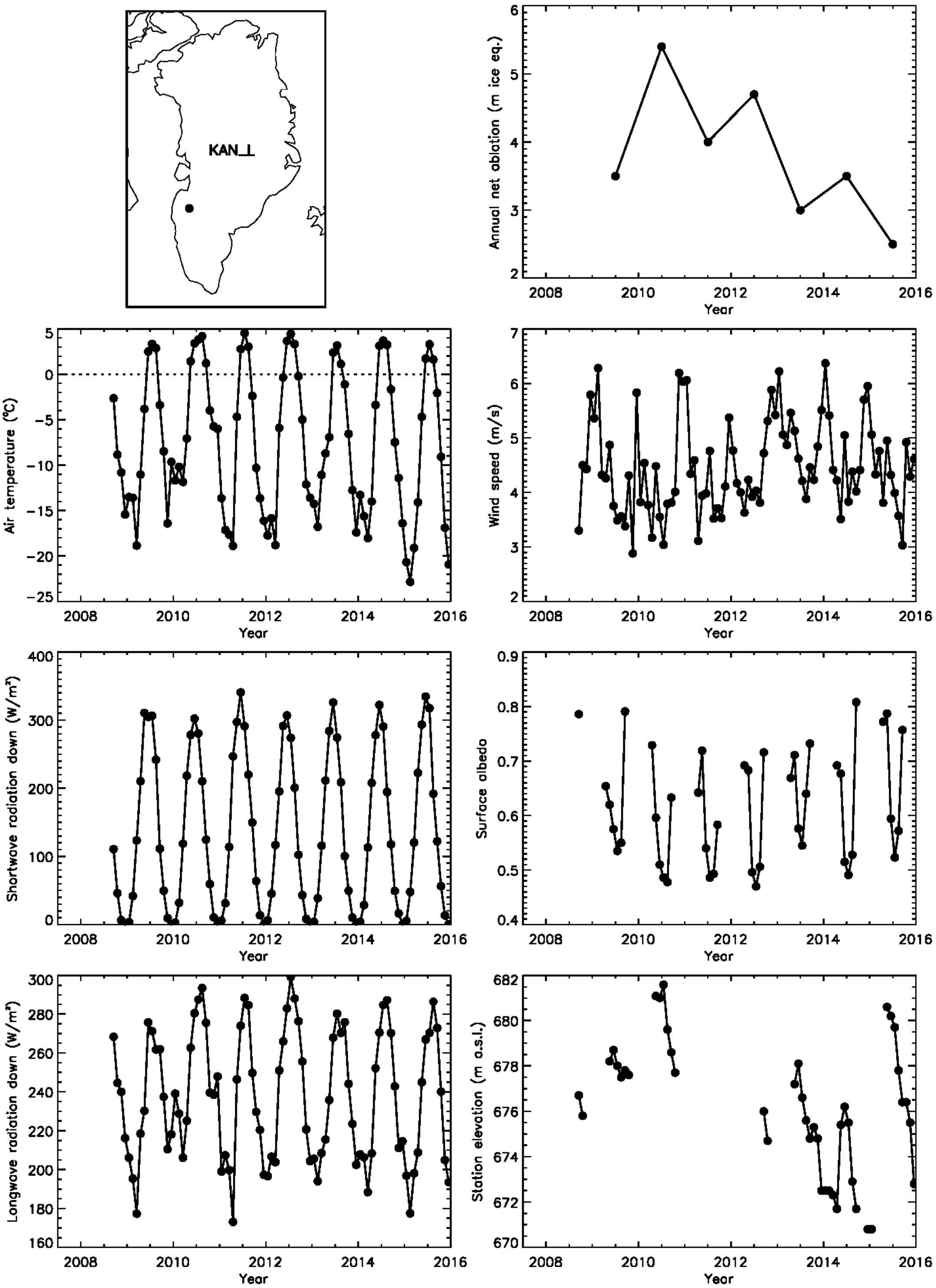
KAN_L
Annual net ablation (m ice eq.)
Air temperature (°C)
Wind speed (m/s)
Shortwave radiation down (W/m²)
Surface albedo
Longwave radiation down (W/m²)
Station elevation (m a.s.l.)
Year

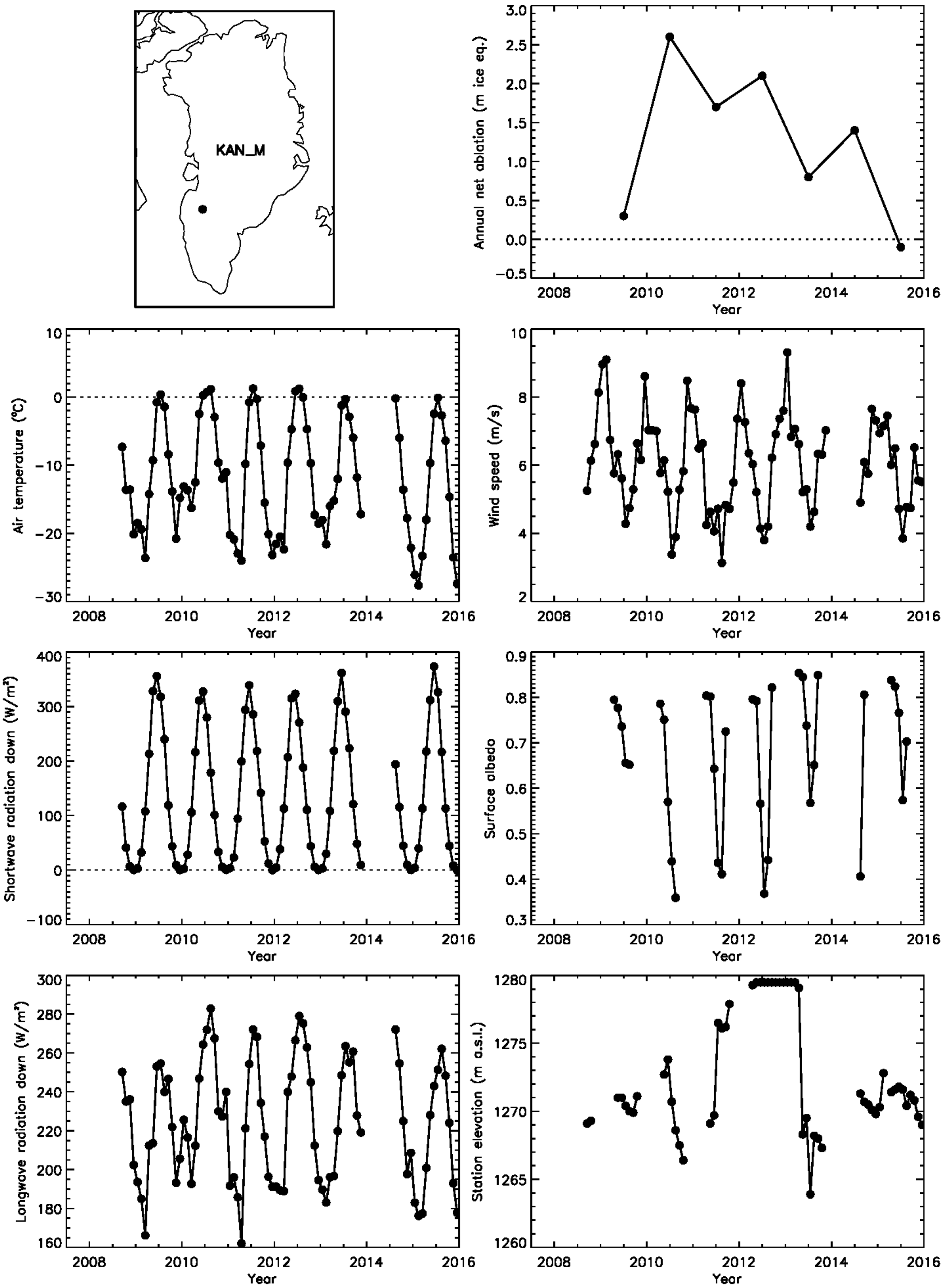
KAN_M
Annual net ablation (m ice eq.)
Year
Air temperature (°C)
Wind speed (m/s)
Shortwave radiation down (W/m²)
Surface albedo
Longwave radiation down (W/m²)
Station elevation (m a.s.l.)

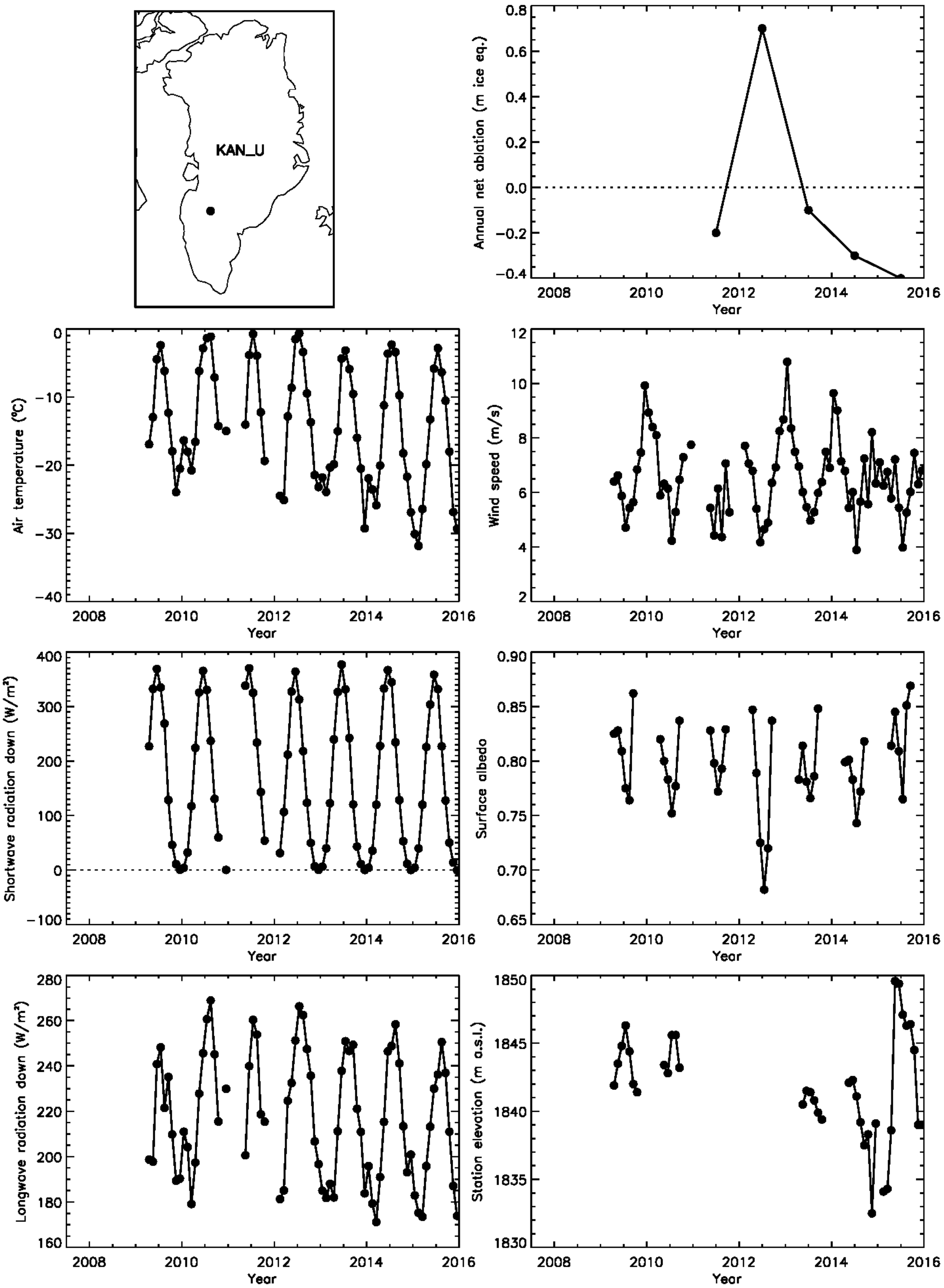
KAN_U
Annual net ablation (m ice eq.)
Air temperature (°C)
Wind speed (m/s)
Shortwave radiation down (W/m²)
Surface albedo
Longwave radiation down (W/m²)
Station elevation (m a.s.l.)
Year

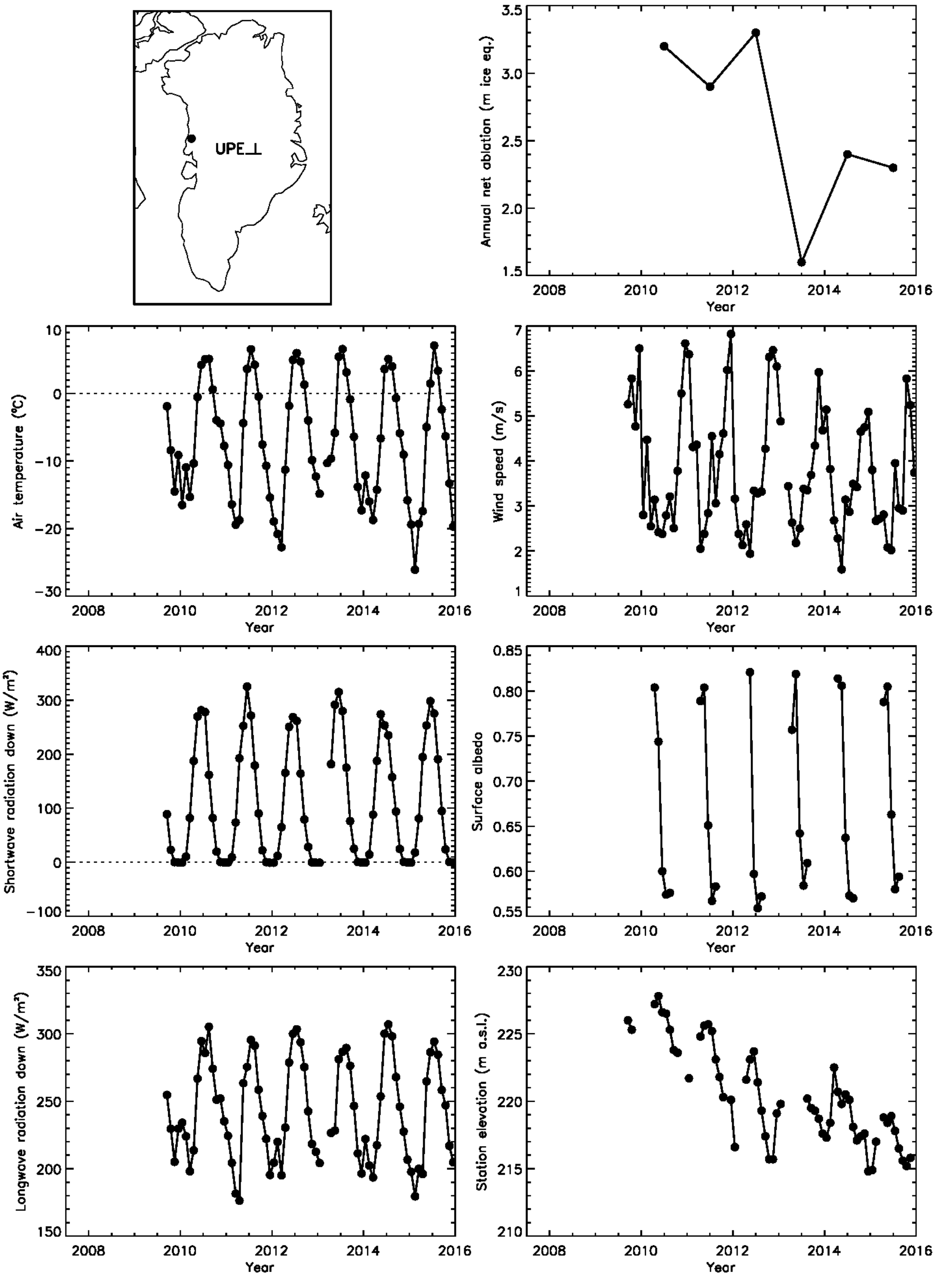
UPE_L
Annual net ablation (m ice eq.)
Air temperature (°C)
Wind speed (m/s)
Shortwave radiation down (W/m²)
Surface albedo
Longwave radiation down (W/m²)
Station elevation (m a.s.l.)
Year

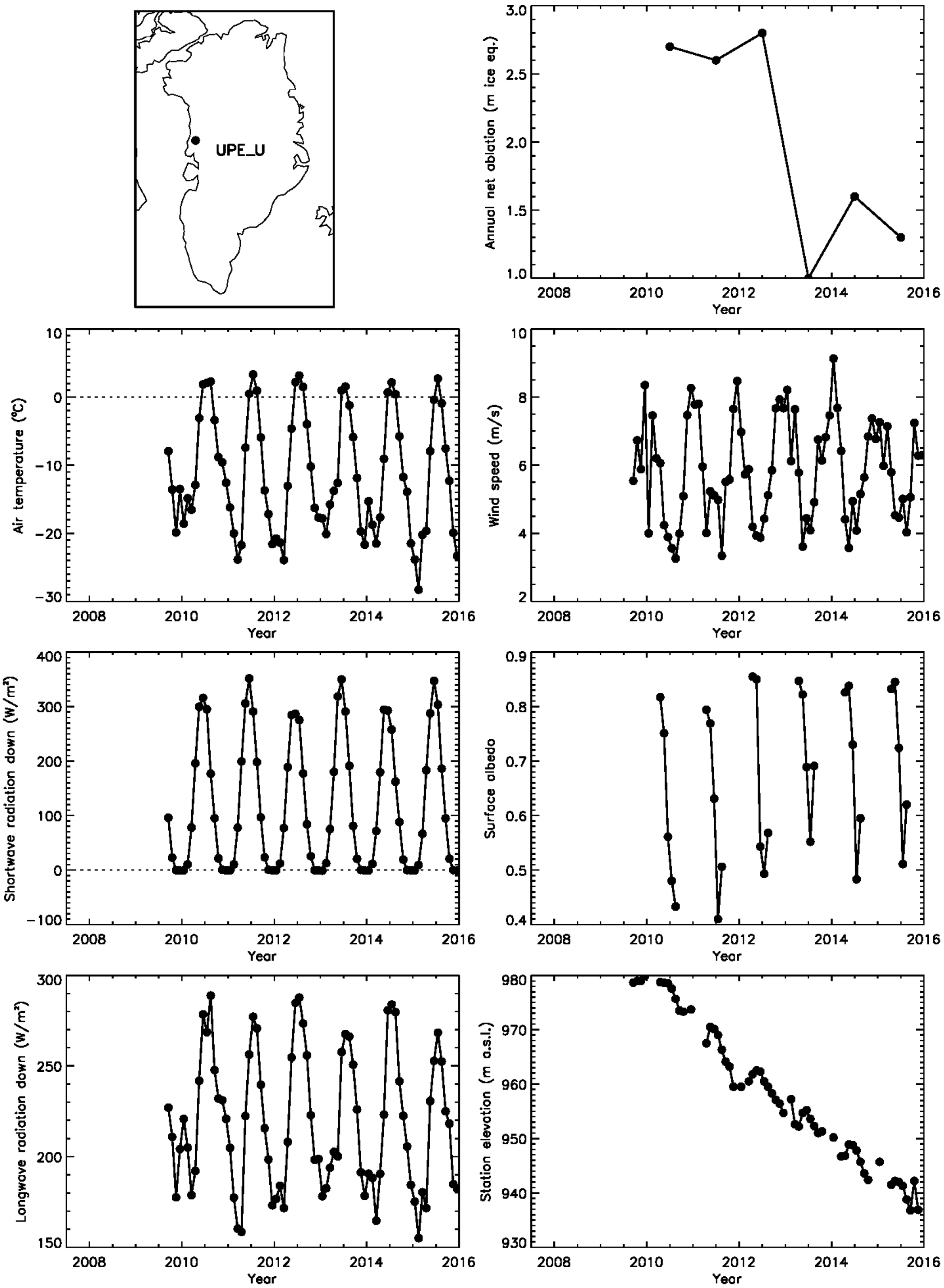
UPE_U
Annual net ablation (m ice eq.)
Air temperature (°C)
Wind speed (m/s)
Shortwave radiation down (W/m²)
Surface albedo
Longwave radiation down (W/m²)
Station elevation (m a.s.l.)
Year

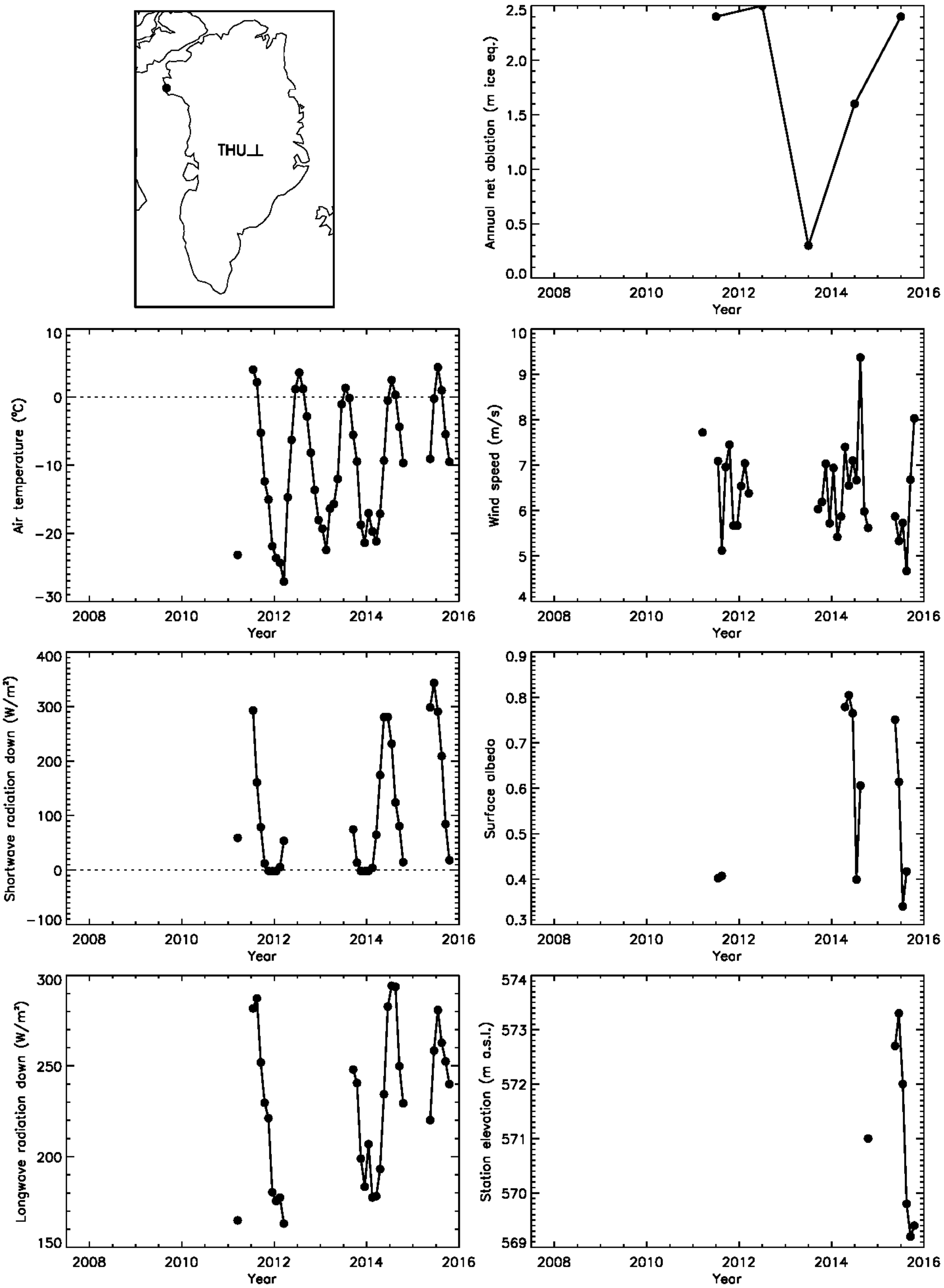
THU_L
Annual net ablation (m ice eq.)
Air temperature (°C)
Wind speed (m/s)
Shortwave radiation down (W/m²)
Surface albedo
Longwave radiation down (W/m²)
Station elevation (m a.s.l.)
Year

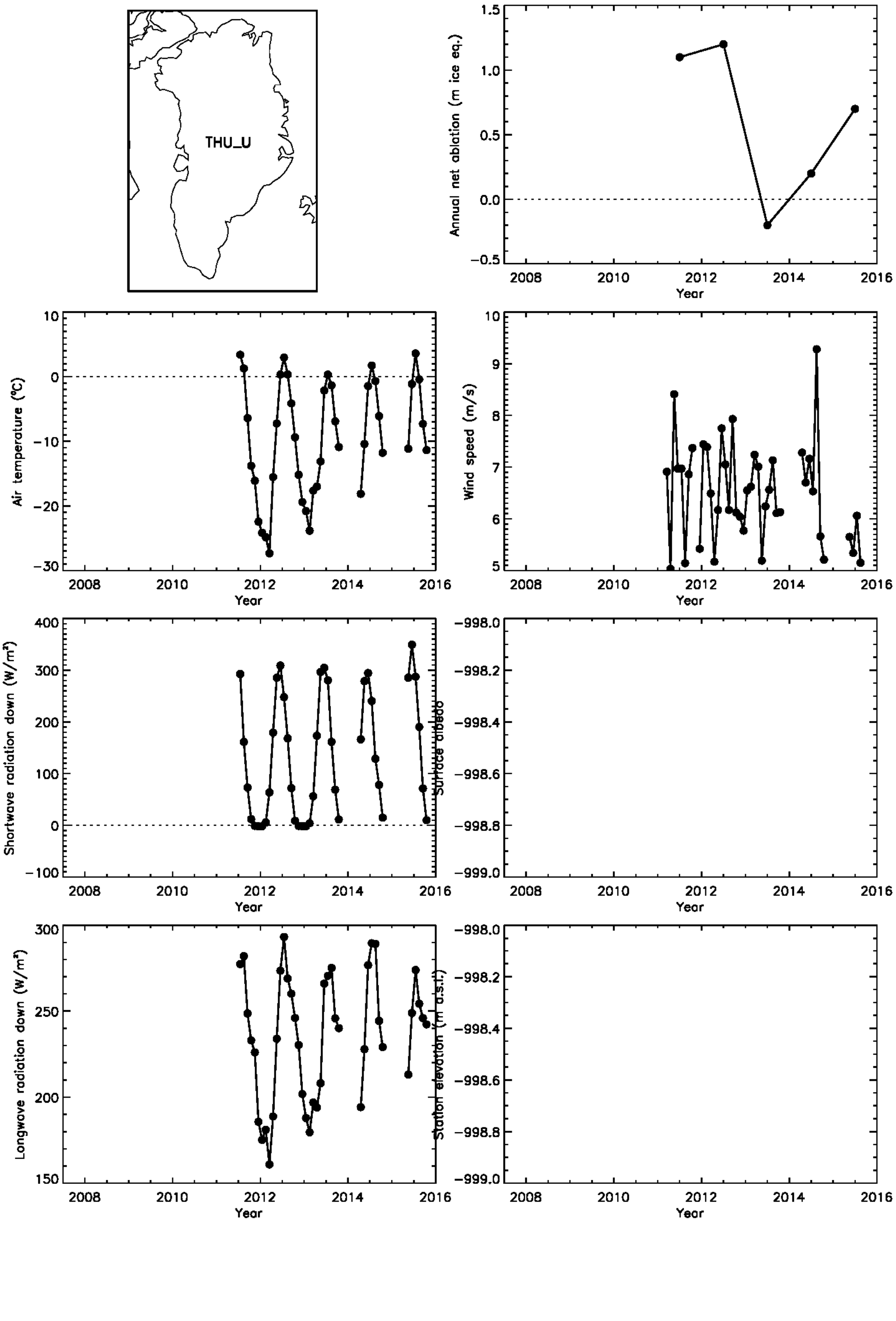
THU_U
Annual net ablation (m ice eq.)
Air temperature (°C)
Wind speed (m/s)
Shortwave radiation down (W/m²)
Surface albedo
Longwave radiation down (W/m²)
Station elevation (m a.s.l.)
Year
2008
2010
2012
2014
2016

Appendix B: Minutes from PROMICE advisory board meeting 2015

Climate Days conference, Ilulissat, 4 June 2015, 17:00

Attendees: Signe Bech Andersen, Søren Rysgaard, Jens Hesselbjerg Christensen, Aslak Grindsted, Louise Sandberg Sørensen, Sebastian Simonson, Andreas Ahlstrøm, Christine Hvidberg, Naja Mikkelsen, Dirk van As, Jakob Abermann, Dorthe Petersen, Jason Box, René Forsberg

Welcome by Signe.

Repeating the main points made at the 2014 meeting:

- AWS data is properly processed and useful for modelers and others.
- The flight lines for flux gate determination are too high up the ice sheet (a large correction for SMB and volume change is needed), but the tracks are kept there for good bedrock returns and the fact that in monitoring it's valuable to stick to the routine.
- Communication: spread the PROMICE results better. Yearly report? Jason: external review improves credibility. Jakob: combine with GEM's Arctic report card? Christine: GEUS publication? Jason: yes, special issue? Jens: more than just a report card? Søren: why report needed? Signe: needed for providing feedback to politicians and for use in scientific community. Søren: broader branding? Rene: as long as it is focused on glaciology. Signe: way to go is to have an annual citable report. Jason: Polar Portal, external review. Check with Morten. Will follow up on it. Naja: Don't ask Morten what is needed, but tell what you want yourself. Andreas: the PROMICE report is more narrow than ARC because it's only about Greenland. Rene: Plus sea ice, is what Greenlanders want. Jens and Christine: collaboration between DK groups is important. Naja: get written advice on PROMICE course from Greenland, also to visualize importance of PROMICE also in Greenland.

Individual comments:

- Søren: AWS are important to get freshwater running into fjords and fjord circulation. Still struggling to understand fjord circulation, and thus ice-ocean interaction. Need more simple, low cost AWS for wind along fjords. Low cost. Further instrumentation such as CTD can be provided to easily insert into fjord on PROMICE helicopter flights.
- Jens: PROMICE does monitoring, not conventional science. Better stick to the monitoring, do it well, do outreach, improve as we go along.
- Christine: put AWS in the southeast where measurements are needed? Signe: would be too much for PROMICE, better stick to mass *loss*.
- Louise: How do you track PROMICE publications to show project impact? Signe and Dirk: terms of use list ways to refer to PROMICE. Since last year the terms of use are more visibly included in data downloads.
- Sebastian: Great that AWS data are easily available.
- Christine: 1) Polar Portal is good. 2) Make data usage more visible online. 3) Improve coordination with CIC.
- Naja: Consider a Weekend Avisen article about PROMICE, flagging that PROMICE data are used at this meeting. Also publish in Greenlandic media (Suluk, …?) to inform GL policy makers. GL media are always looking for such news. Mention Isskolen. (Related comment: distribute Isskolen on DVD in Greenland where internet connectivity is poor.)

- Dorthe: Horst Machguth's PROMICE mass balance database is very useful.
- Rene: More outreach, in Polar Portal and anywhere else.

Signe closes meeting at 18:00.

Appendix C – Peer reviewed scientific publications from the PROMICE team

This appendix details the scientific results produced by PROMICE team members with relation to their activities in PROMICE. 20 peer reviewed scientific publications from the PROMICE team were published in 2015. Publications marked with * have been cited in the 2014 IPCC AR5 report.

2015

1. Charalampidis C and Van As D (2015) Observed melt-season snowpack evolution on the Greenland ice sheet. Geol. Surv. Denmark Greenland Bull., 33, 65-68
2. Charalampidis, C., van As, D., Box, J. E., van den Broeke, M. R., Colgan, W. T., Doyle, S. H., Hubbard, A. L., MacFerrin, M., Machguth, H., and Smeets, C. J. P. P. (2015) Changing surface–atmosphere energy exchange and refreezing capacity of the lower accumulation area, West Greenland, The Cryosphere, 9, 2163-2181, doi:10.5194/tc-9-2163-2015.
3. Citterio M, Van As D, Ahlstrøm AP, Andersen ML, Andersen SB, Box JE, Charalampidis C, Colgan WT, Fausto RS, Nielsen S and Veicherts M (2015) Automatic weather stations for basic and applied glaciological research. Geol. Surv. Denmark Greenland Bull., 69-72
4. Colgan, W., Abdalati, W., Citterio, M., Csatho, B., Fettweis, X., Luthcke, S., Moholdt, G., Simonsen, S.B., Stober, M. (2015) Hybrid glacier Inventory, Gravimetry and Altimetry (HIGA) mass balance product for Greenland and the Canadian Arctic, Remote Sensing of Environment, volume 168, issue, pp. 24 - 39
5. Colgan, W., J. Box, M. Andersen, X. Fettweis, B. Csatho, R. Fausto, D. van As and J. Wahr (2015) Greenland high elevation mass balance: Inference and implication of reference period (1961-1990) imbalance. Annals of Glaciology. 70: 70A967.
6. Dow, C. B. Kulessa, I. C. Rutt, V.C.Tsai, S. Pimentel, SH.Doyle, D.vanAs, K. Lindbäck, R. Pettersson, G.A. Jones, and A. Hubbard (2015). Modeling of subglacial hydrological development following rapid supraglacial lake drainage. J. Geophys. Res., 120, 1127–1147,doi:10.1002/2014JF003333
7. Doyle, S.H., A. Hubbard, R.S.W. van de Wal, J.E. Box, D. van As, K. Scharrer, T.W. Meierbachtol, P.C. J. P. Smeets, J.T. Harper, E. Johansson, R.H. Mottram, A.B. Mikkelsen, F. Wilhelms, H. Patton, P. Christoffersen, Bryn Hubbard (2015) Amplified melt and flow of the Greenland ice sheet driven by late-summer cyclonic rainfall, Nature Geoscience, 8, pages 647-653, doi:10.1038/ngeo2482
8. Fausto RS, Van As D, Antoft JA, Box JE, Colgan W and PROMICE project team (2015) Greenland ice sheet melt area from MODIS (2000-2014). Geol. Surv. Denmark Greenland Bull., 33, 57-60
9. Johansson E, Berglund S, Lindborg T, Petrone J, Van As D, Gustafsson L-G, Næslund J-O and Laudon H (2015) Hydrological and meteorological investigations in a periglacial lake catchment near Kangerlussuaq, west Greenland presentation of a new multi-parameter dataset. Earth Syst. Sci. Data, 7, 93-108 (doi:10.5194/essd-7-93-2015)
10. Kobashi, T., J. E. Box, B. M. Vinther, K. Goto-Azuma, T. Blunier, J. W. C. White, T. Nakaegawa, and C. S. Andresen (2015), Modern solar maximum forced late 20th century Greenland cooling, Geophys. Res. Lett., 42, doi:10.1002/2015GL064764.
11. Kuipers Munneke, P., Ligtenberg, S. R. M., Noël, B. P. Y., Howat, I. M., Box, J. E., Mosley-Thompson, E., McConnell, J. R., Steffen, K., Harper, J. T., Das, S. B., and van den Broeke, M. R. (2015), Elevation

change of the Greenland Ice Sheet due to surface mass balance and firn processes, 1960–2014, The Cryosphere, 9, 2009-2025, doi:10.5194/tc-9-2009-2015.

12. Langen, P.L., R.H. Mottram, J.H. Christensen, F. Boberg, C.B. Rodehacke, M. Stendel, D. van As, A.P. Ahlstrøm, J. Mortensen, S. Rysgaard, D. Petersen, K.H. Svendsen, G. Adalgeirsdottir, and J. Cappelen (2015), Quantifying Energy and Mass Fluxes Controlling Godthåbsfjord Freshwater Input in a 5-km Simulation (1991Ð2012), J. Climate, 28, 3694D3713. doi: http://dx.doi.org/10.1175/JCLI-D-14-00271.1.
13. Lindbäck K, Pettersson R, Hubbard AL, Doyle SH, Van As D, Mikkelsen AB and Fitzpatrick AA (2015), Subglacial water drainage and piracy beneath the Greenland Ice Sheet, Geophys. Res. Lett., 42*,* 7606–7614*, doi:*10.1002/2015GL065393*.*
14. Masson-Delmotte, V., Steen-Larsen, H. C., Ortega, P., Swingedouw, D., Popp, T., Vinther, B. M., Oerter, H., Sveinbjornsdottir, A. E., Gudlaugsdottir, H., Box, J. E., Falourd, S., Fettweis, X., GallŽe, H., Garnier, E., Gkinis, V., Jouzel, J., Landais, A., Minster, B., Paradis, N., Orsi, A., Risi, C., Werner, M., and White, J. W. C. (2015), Recent changes in north-west Greenland climate documented by NEEM shallow ice core data and simulations, and implications for past-temperature reconstructions, The Cryosphere, 9, 1481-1504, doi:10.5194/tc-9-1481-2015, 2015.
15. Rahmstorf, S., J.E. Box, G. Feulner, M.E. Mann, A. Robinson, S. Rutherford and E.J. Schaffernicht (2015), Exceptional twentieth-century slowdown in Atlantic Ocean overturning circulation, Nature Climate Change, 5, 475-480 doi: 10.1038/nclimate2554
16. Ryan, J. C., Hubbard, A. L., Box, J. E., Todd, J., Christoffersen, P., Carr, J. R., Holt, T. O., and Snooke, N.(2015), UAV photogrammetry and structure from motion to assess calving dynamics at Store Glacier, a large outlet draining the Greenland ice sheet, The Cryosphere, 9, 1-11, doi:10.5194/tc-9-1-2015, 2015.
17. Stibal M, Gözdereliler E, Cameron KA, Box JE, Stevens IT, Gokul JK, Schostag M, Zarsky JD, Edwards A, Irvine-Fynn TD and Jacobsen CS (2015). Microbial abundance in surface ice on the Greenland Ice Sheet. Front. Microbiol. 6:225. doi: 10.3389/fmicb.2015.00225
18. Tedesco, M., J.E. Box, J. Cappelen, R. S. Fausto, X. Fettweis, K. Hansen, T. Mote, C.J.P.P. Smeets, D. van As, R.S.W. van de Wal, J. Wahr (2015), Greenland, [in Arctic Report Card 2015], M. Jeffries and J. Richter-Menge (Eds.)
19. Tedesco, M., J.E. Box, J. Cappelen, X. Fettweis, T. Mote, R S.W. van de Wal, M. van den Broeke, C.J.P.P. Smeets, and J. Wahr, (2015), Greenland Ice Sheet, [in “State of the Climate in 2014”]. Bull. Amer. Meteor. Soc., 96 (7), S137-S139.
20. Zemp, M. and 38 others (2015) Historically unprecedented global glacier decline in the early 21st century, Journal of Glaciology, Vol. 61, No. 228, 745Ð762, doi: 10.3189/2015JoG15J017.

2014

21. Andersen, ML. Stenseng, H. Skourup, W. Colgan, S. Khan, S. Kristensen, S. Andersen, J. Box, A. Ahlstrøm, X, Fettweis and R. Forsberg. (2014). Basin-scale partitioning of Greenland ice sheet mass balance components (2007–2011). Earth and Planetary Science Letters. 409: 89-95. doi:10.1016/j.epsl.2014.10.015
22. Andersen ML, Andersen SB, Stenseng L, Skourup H, Colgan W, Kristensen SS, Merryman Boncori JP,

Ahlstrøm AP, Fettweis X, Forsberg R, Citterio M, Box JE, Van As D and Fausto RS (2014) Mass loss from an ice-sheet drainage basin in West Greenland. Geol. Surv. Denmark Greenland Bull., 31, 87-90

23. Andersen ML, Stenseng L, Skourup H, Colgan W, Khan SA, Kristensen SS, Andersen SB, Box JE, Ahlstrøm AP, Fettweis X and Forsberg R (2014) Basin-scale partitioning of Greenland ice sheet mass balance components (2007–2011). Earth Planetary Sci. Lett., 409, 89-95, doi:10.1016/j.epsl.2014.10.015)

24. Colgan W, Box JE, Fausto RS, Van As D, Barletta VR and Forsberg R (2014) Surface albedo as a proxy for the mass balance of Greenland's terrestrial ice. Geol. Surv. Denmark Greenland Bull., 31, 91-94

25. Davis, J.L.,J. De Juan Verger, M.Nettles, P.Elo´Segui, M.L.Andersen, 2014, Evidence for non-tidal diurnal velocity variations of Helheim Glacier, East Greenland, Journal of Glaciology, Vol. 60, No. 224, 2014 doi: 10.3189/2014JoG13J230

26. Doyle SH, Hubbard A, Fitzpatrick AAW, Van As D, Mikkelsen AB, Pettersson R and Hubbard B (2014) Persistent flow acceleration within the interior of the Greenland Ice Sheet. Geophys. Res. Let., 41 (3), 899-905 (doi:10.1002/2013GL058933)

27. Fitzpatrick AAW, Hubbard AL, Box JE, Quincey DJ, van As D, Mikkelsen APB, Doyle SH, Dow CF, Hasholt B and Jones GA (2014) A decade (2002–2012) of supraglacial lake volume estimates across Russell Glacier, West Greenland. Cryosph., 8, 107-121 (doi: 10.5194/tc-8-107-2014)

28. Lea JM, Mair DWF, Nick FM, Rea BR, Van As D, Morlighem M, Nienow PW and Weidick A (2014) Fluctuations of a Greenlandic tidewater glacier driven by changes in atmospheric forcing: observations and modelling of Kangiata Nunaata Sermia, 1859–present. Cryosph., 8, 2031-2045 (doi:10.5194/tc-8-2031-2014)

29. Lea JM, Mair DWF, Nick FM, Rea BR, Weidick A, Kjær KH, Morlighem M, Van As D and Schofield JE (2014) Terminus-driven retreat of a major southwest Greenland tidewater glacier during the early 19th century: insights from glacier reconstructions and numerical modelling. J. Glac., 60 (220), 333-344 (doi:10.3189/2014JoG13J163)

30. Mernild SH, Malmros JK, Yde JC, Wilson R, Knudsen NT, Hanna E, Fausto RS and Van As D (2014) Albedo decline on Greenland's Mittivakkat Gletscher in a warming climate. Int. J. Climatol. (doi:10.1002/joc.4128)

31. Tedesco, M., J E. Box, J. Cappelen, X. Fettweis, T.S. Jensen, T. Mote, A.K. Rennermalm, L.C. Smith, R.S.W. van de Wal, and J. Wahr, 2014, Greenland Ice Sheet, [in "State of the Climate in 2013"]. Bull. Amer. Meteor. Soc., 95 (7), S5-S49.

32. Van As D, Andersen ML, Petersen D, Fettweis X, Van Angelen JH, Lenaerts JTM, Van den Broeke MR, Lea JM, Bøggild CE, Ahlstrøm AP and Steffen K (2014) Increasing meltwater discharge from the Nuuk region of the Greenland ice sheet and implications for mass balance (1960-2012). J. Glac., 60 (220), 314-322 (doi: 10.3189/2014JoG13J065)

33. Van As D, Fausto RS, Steffen K and PROMICE project team (2014) Katabatic winds and piteraq storms: observations from the Greenland ice sheet. Geol. Surv. Denmark Greenland Bull., 31, 83-86

2013

34. Ahlstrøm A.P., S.B. Andersen, M.L. Andersen, H. Machguth, F.M. Nick, I. Joughin, C.H. Reijmer, R.S.W. Van de Wal, J.P. Merryman Boncori, J.E. Box, M. Citterio, D. Van As, R.S. Fausto, A. Hubbard (2013): 'Seasonal velocities of eight major marine-terminating outlet glaciers of the Greenland ice sheet from continuous in situ GPS instruments', Earth Syst. Sci. Data, 5, 277-287, doi:10.5194/essd-5-277-2013.
35. *Bolch, T., L.S. Sørensen, N. Mölg, H. Machguth and F. Paul. 2013. Changes of Greenland's local glaciers and ice caps observed from ICEsat. Geophysical Research Letters, 40(5) 875-881; doi:10.1002/grl.50270
36. *Citterio, M. & Ahlstrøm, A.P. 2013: Brief communication "The aerophotogrammetric map of Greenland ice masses". The Cryosphere 7, 445-449.
37. Colgan, W., Abdalati, W., Citterio, N., Csatho, B. Fettweis, X., Luthcke, S., Moholdt, G. & Stober, M. 2013: Hybrid inventory, gravimetry and altimetry (HIGA) mass balance product for Greenland and the Canadian Arctic. The Cryosphere Discussions 8, 537-580.
38. Colgan, W., Luthcke S., Abdalati, W. & Citterio, M. 2013: Constraining GRACE-derived cryosphere-attributed signal to ireegularly shaped ice-covered areas. The Cryosphere 7, 1901-1914.
39. Fausto, R.S., Colgan, W. & Langen, P.L. 2013: Real-Time Changes in Arctic Ice Presented in Online Portal. EOS transactions American Geophysical Union 94(44), 397-398.
40. Fitzpatrick A.A.W., Hubbard, A., Joughin, I., Quincey, D.J., Van As, D., Mikkelsen, A.P.B., Doyle, S.H., Hasholt, B., Jones, G.A 2013: Ice flow dynamics and surface meltwater flux at a land-terminating sector of the Greenland Ice Sheet. Journal of Glaciology 59(216), 687-696.
41. *Machguth, H., P. Rastner, T. Bolch, N. Mölg and L.S. Sørensen. 2013. Future sea level rise contribution of Greenland's glaciers and ice caps. Environmental Research Letters, 8 025005 doi:10.1088/1748-9326/8/2/025005
42. Mernild, S.H. , Knudsen, N.T., Yde, J.C., Hoffman, M.J., Limpscomb, W.H., Hanna, E., Malmros, J.K. & Fausto, R.S. 2013: Thinning and slowdown from Greenland¿s Mittivakkat Gletscher. Journal of glaciology 59(216), 11.
43. *Nick, F.M., Vieli, A., Andersen, M.L., Payne, T. Edwards, T., Joughin, I., Pattyn, F. & van der Wal, R.S.W. 2013: Contributions from the Greenland marine outlet glaciers to global sea level rise as climate continues to warm. Nature 497,235–238,doi:10.1038/nature12068
44. Rennermalm, A.K., Smith, L.C., Chu, V.W., Box, J.E., Forster, R.R., Van den Broeke, M.R., Van As, D. & Moustafa, S.E. 2013: Evidence of meltwater retention within the Greenland ice sheet. The Cryosphere 7, 1433-1445.
45. Simonsen, S. B; Stenseng, L; Adalgeirsdottir, G.; Fausto, R. S.; Hvidberg, C. S.; Lucas-Picher, P Assessing a multilayered dynamic firn-compaction model for Greenland with ASIRAS radar measurements. Journal of Glaciology, Vol. 59, No. 215, 2013, p. 545-558.
46. Van As, D., Fausto, R.S., Colgan, W.T., Box. J.E., Ahlstrøm, A.P., Andersen, S.B., Andersen, M.L., Charalampidis, C., Citterio, M., Edelvang, K., Jensen, T.S., Larsen, S.H., Machguth, H., Nielsen, S.,

Veicherts, M. & Weidick, A. 2013: Darkening of the Greenland ice sheet due to the melt-albedo feedback observed at PROMICE weather stations. In: Bennike, O., Garde, A.A, & Watt, W.S.(eds): Review of Survey Activities 2012. Geological Survey of Denmark and Greenland Bulletin 28, 69-72.

2012

47. *Andresen CS, Straneo F, Ribergaard MH, Bjørk AA, Andersen TJ, Kuijpers A, Nørgaard-Pedersen N, Kjær KH, Schjøth F, Weckström K and Ahlstrøm AP (2012) Rapid response of Helheim Glacier in Greenland to climate variability over the past century. Nature Geosc., 5, 37-41 (doi: 10.1038/ngeo1349)
48. Banwell AF, Arnold N, Willis I, Tedesco M and Ahlstrøm A (2012) Modelling supraglacial water routing and lake filling on the Greenland Ice Sheet. J. Geophys. Res., 117, F0401 (doi: 10.1029/2012JF002393)
49. Banwell AF, Willis I, Arnold N, Messerli A, Rye C and Ahlstrøm A (2012) Calibration and validation of a high resolution surface mass balance model for Paakitsoq, west Greenland. J. Glac., 58 (212), 1047-1062 (doi: 10.3189/2012JoG12J034)
50. Fausto , R.S., S.H. Mernild, B. Hasholt, A.P. Ahlstrøm and N.T. Knudsen. 2012. Modeling suspended sediment concentration and transport for Mittivakkat Glacier, Southeast Greenland. Arctic, Antarctic and Alpine Research Vol. 44., No. 3, 306-318.
51. Fausto, R.S., D. Van As, A.P. Ahlstrøm, S.B. Andersen, M.L. Andersen, M. Citterio, K. Edelvang, et al. 2012. Ablation Observations for 2008–2011 from the Programme for Monitoring of the Greenland Ice Sheet (PROMICE). Geological Survey of Denmark and Greenland Bulletin 26, 73–76.
52. Fausto RS, Van As D, Ahlstrøm AP and Citterio M (2012) Assessing the accuracy of Greenland ice sheet surface ablation measurements by pressure transducer. J. Glac., 58 (212), 1144-1150 (doi: 10.3189/2012JoG12J075)
53. Fausto R.S., D. van As and the PROMICE team. 2012. Ablation observations for 2008–2011 from the Programme for Monitoring of the Greenland Ice Sheet (PROMICE). Geol. Surv. Denmark Greenland Bull., 26, 73-76.
54. Jiskoot, H., D. Juhlin, H. St Pierre, and M. Citterio. 2012. Tidewater Glacier Fluctuations in Central East Greenland Coastal and Fjord Regions (1980s–2005). Annals of Glaciology 53, no. 60, 35–44.
55. *Kargel, J.S., A.P. Ahlstrøm, R.B. Alley, J.L. Bamber, T.J. Benham, J.E. Box, C. Chen, M. Citterio, et al. 2012. Brief Communication: Greenland's Shrinking Ice Cover: 'Fast Times' but Not That Fast. The Cryosphere 6, no. 3, 533–537.
56. *Leclercq, P.W., A. Weidick, F. Paul, T. Bolch, M. Citterio, and J. Oerlemans.(2012) Brief Communication: Historical Glacier Length Changes in West Greenland. The Cryosphere Discussions 6, no. 4, 3491–3501.
57. Mernild, S.H., N.T. Knudsen, J.C. Yde, M.J. Hoffman, W.H. Limpscomb, E. Hanna, R.S. Fausto and J.K. Malmros. 2012. Retreat, thinning, and slowdown from Greenland's Mittivakkat Gletscher. The Cryosphere Discuss., 6, 2005-2036.
58. Mikkelsen et al. In preparation. Meltwater runoff and ice sheet velocity response during the new record melt year 2012 in southwest Greenland.
59. Nick, F.M., A. Luckman, A. Vieli, C.J. van der Veen, D. van As, R.S.W. van de Wal, F. Pattyn, A.L. Hubbard and D. Floricioiu. 2012. The response of Petermann Glacier, Greenland, to large calving events, and its future stability in the context of atmospheric and oceanic warming. Journal of Glaciology 58 (208), 229-239.
60. Nick F. M., A. Vieli, M. L. Andersen, T. Payne, T. Edwards, I. Joughin, , F. Pattyn, and R.S.W. van der Wal. Under revision, 2012. Contributions from the Greenland marine outlet glaciers to global sea

level rise as climate continues to warm. Nature 497, 235-238 (doi. 10.1038/nature12068).
61. *Rastner, P., T. Bolch, N. Mölg, H. Machguth and F. Paul. 2012. The first complete glacier inventory for entire Greenland. The Cryosphere., 6, 1483-1495 (doi: 10.5194/tc-6-1483-2012)
62. Simonsen, S.B., L. Stenseng, G. Adalgeirsdottir, R.S. Fausto and C.S. Hvidberg. Submitted, 2012. Assessing a multi-layered dynamic firn compaction model for Greenland with ASIRAS radar measurements. Journal of Glaciology.
63. van As, D., A.L. Hubbard, B. Hasholt, A.B. Mikkelsen, M.R. van den Broeke and R.S. Fausto. 2012. Large surface meltwater discharge from the Kangerlussuaq sector of the Greenland ice sheet during the record-warm year 2010 explained by detailed energy budget observations. Cryosphere 6, 199-209.
64. Weidick, A., O. Bennike, M. Citterio and N. Nørgaard-Pedersen. 2012. Neoglacial and historical changes in southern West Greenland, with special emphasis on the area around Kangersuneq fjord. Geological Survey of Denmark and Greenland Bulletin 27, 68 pp.

2011

65. Andersen, M.L., M. Nettles, T.B. Larsen, P. Elosegui, G.S. Hamilton and L.A. Stearns. 2011. Quantitative estimates of velocity sensitivity to surface melt variations at a large Greenland outlet glacier. Journal of Glaciology 57 (204), 609-620.
66. Box , J.E., A. Ahlstrøm, J. Cappelen, X. Fettweis, D. Decker, T. Mote, D. van As, R.S.W. van de Wal, B. Vinther and J. Wahr. 2011. Greenland [in "State of the Climate in 2010"]. Bull. Amer. Meteor. Soc. 92 (6), S161-171.
67. Brown, K.J., H. Seppä, G. Schoups, R.S. Fausto, P. Rasmussen and H.J.B Birks. 2011. A spatio-temporal reconstruction of Holocene temperature change in southern Scandinavia. The Holocene, DOI: 10.1177/0959683611414926.
68. Fausto, R.S., A.P. Ahlstrøm, D. van As and K. Steffen. 2011. Present-day temperature standard deviation parameterization for Greenland. J. Glaciol. 57 (206), 1181-1183.
69. van As, D.. 2011. Warming, glacier melt and surface energy budget from weather station observations in the Melville Bay region of northwest Greenland. Journal of Glaciology 57 (202), 208-220.
70. Van As, D., R.S. Fausto, A.P. Ahlstrøm, S.B. Andersen, M.L. Andersen, M. Citterio, K. Edelvang, et al. 2011. Programme for Monitoring of the Greenland Ice Sheet (PROMICE): First Temperature and Ablation Record. Geological Survey of Denmark and Greenland Bulletin 23, 73–76.
71. Van As, D., R.S. Fausto, A.P. Ahlstrøm, S.B. Andersen, M.L. Andersen, M. Citterio, K. Edelvang, P. Gravesen, H. Machguth, F.M. Nick, S. Nielsen and A. Weidick. 2011. Temperature and ablation records from the Programme for Monitoring of the Greenland Ice Sheet (PROMICE). Geological Survey of Denmark and Greenland Bulletin 23, 73-76.
72. van As, D., R.S. Fausto and the PROMICE team. 2011. Programme for Monitoring of the Greenland Ice Sheet (PROMICE): first temperature and ablation records. Geol. Surv. Denmark Greenland Bull. 23, 73-76.
73. Weidick A. & Citterio M. 2011. The ice-dammed lake Isvand, West Greenland, has lost its water. Journal of Glaciology 57(201), 186-188.

2010

74. Andersen, M.L., T.B. Larsen, M. Nettles, P. Elosegui, D. van As, G.S. Hamilton, L.A. Stearns, J.L. Davis, A.P. Ahlstrøm, J. de Juan, G. Ekström, L. Stenseng, S.A. Khan, R. Forsberg and D. Dahl-Jensen. 2010. Spatial and temporal melt variability at Helheim Glacier East Greenland, and its effect on ice dynamics. Journal of Geophysical Research 115, 18 pp. doi:10.1029/2010JF001760.
75. de Juan, J., P. Elosegui, M. Nettles, T.B. Larsen, J.L. Davis, G.S. Hamilton, L.A. Stearns, M.L. Andersen, G. Ekström, A.P. Ahlstrøm, L. Stenseng, S.A. Khan and R. Forsberg. 2010. Sudden increase in tidal response linked to calving and acceleration at a large Greenland outlet glacier. Geophysical Research Letters 37 (12501), 5 pp., doi:10.1029/2010GL043289.
76. Mernild, S.H., I.M. Howat, Y. Ahn, G.E. Liston, K. Steffen, B.H. Jakobsen, B. Hasholt, B. Fog, and D. van As. 2010. Freshwater flux to Sermilik Fjord, SE Greenland. Cryosphere 4, 453-465.
77. *Nick, F.M., C.J. van der Veen, A. Vieli, and D.I. Benn. 2010. A physically based calving model applied to marine outlet glaciers and implications for the glacier dynamics. Journal of Glaciology 56 (199), 781-794.
78. van As, D. 2010. Changes in temperature and glacier melt from weather station observations in the Melville Bay region of North-West Greenland. J. Glaciol. 57 (202), 208-220.

2009

79. Citterio M., R.H. Mottram, S.H. Larsen and A.P. Ahlstrøm. 2009. Glaciological investigations at the Malmbjerg mining prospect, central East Greenland. Geological Survey of Denmark and Greenland Bulletin 17, 73-76.
80. Citterio, M., F. Paul, A.P. Ahlstrøm, H.F. Jepsen and A. Weidick. 2009. Remote sensing of glacier change in West Greenland: accounting for the occurence of surge-type glaciers. Annals of Glaciology 50(53), 70-80.
81. Dawes, P.R. and D. van As. 2009. An advancing glacier in a recessive ice regime: Berlingske Bræ, North-West Greenland. In: Bennike, O., Garde, A.A. & Watt, W.S. (eds): Review of Survey activities 2009. Geological Survey of Denmark and Greenland Bulletin 20, 79-82.
82. Fausto, R.S., A.P. Ahlstrøm, D. van As, C.E. Bøggild and S.J. Johnsen. 2009. A new present-day temperature paramerization for Greenland. Journal of Glaciology 55(189), 95-105.
83. Fausto, R.S., A.P. Ahlstrøm, D. van As, S.J. Johnsen, P.L. Langen and K. Steffen. 2009. Improving surface boundary conditions with focus on coupling snow densification and meltwater retention in large-scale ice-sheet models of Greenland. Journal of Glaciology 55(193), 869-878.
84. Mottram, R., C. Nielsen, A.P. Ahlstrøm, N. Reeh, S.S. Kristensen, E.L. Christensen, R. Forsberg, and L. Stenseng. 2009. A new regional high-resolution map of basal and surface topography for the Greenland ice sheet margin at Paakitsoq, West Greenland. Annals of Glaciology 50 (51), 105-111.
85. *Nick, F.M., A. Vieli, I.M. Howat, and I. Joughin. 2009. Large-scale changes in Greenland outlet glacier dynamics triggered at the terminus. Nature Geoscience 2, 110-114.
86. van As, D., C.E. Bøggild, S. Nielsen, A.P. Ahlstrøm, R.S. Fausto, S. Podlech, M.L. Andersen. 2009. Climatology and ablation at the South Greenland ice sheet margin from automatic weather station observations. Cryosphere Disc. 3 (1), 117-158.

2008

87. Ahlstrøm, A.P. and the PROMICE project team 2008. A new programme for monitoring the mass loss of the Greenland ice sheet. In: Bennike, O. & Higgins, A.K.(eds): Review of Survey activities 2007. Geological Survey of Denmark and Greenland Bulletin 15, 61-64.
88. Ahlstrøm A.P., P. Gravesen, S.B. Andersen, D. van As, M. Citterio, R.S. Fausto, S. Nielsen, H.F. Jepsen, S.S. Kristensen, E.L. Christensen, L. Stenseng, R. Forsberg, S. Hanson, D. Petersen and the PROMICE Project Team. 2008. A new programme for monitoring the mass loss of the Greenland ice sheet. Geological Survey of Denmark and Greenland Bull. 15, 61-65.
89. Nettles, M., T.B. Larsen, P. Elosegui, G.S. Hamilton, L.A. Stearns, A.P. Ahlstrøm, J.L. Davis, M.L. Andersen, J. de Juan, S.A. Khan, L. Stenseng, G. Ekström and R. Forsberg. 2008. Step-wise changes in glacier flow speed coincide with calving and glacial earthquakes at Helheim Glacier, Greenland. Geophysical Research Letters 35, L24503, 5 pp. doi:10.1029/2008GL036127.
90. Smelror, M., A. Ahlstrøm, L. Ekelund, J.M. Hansen, K. Nenonen and A.K. Mortensen. 2008. The Nordic geological surveys: Geology for society in practice. Episodes 31(1), 193-200.

2007

91. Ahlstrøm, A.P., C.E. Bøggild, O.B. Olesen, D. Petersen and J.J. Mohr. 2007. Mass balance of the Amitsulôq ice cap. Glacier Mass Balance Changes and Meltwater Discharge. IAHS Red Books 318, 107-115 International Association of Hydrological Sciences. IAHS Press.
92. Fausto, R.S., C. Mayer and A.P. Ahlstrøm. 2007. Satellite derived surface type and melt area of the Greenland ice sheet using MODIS data from 2000 to 2005. Annals of Glaciology 46, 35-42.
93. Weidick, A. & O. Bennike. 2007. Quaternary glaciation history and glaciology of Jakobshavn Isbræ and the Disko Bugt region, West Greenland: a review. Geological Survey of Denmark and Greenland Bulletin 14, 78 pp.

Programme for Monitoring of the Greenland Ice Sheet
No 8 • 2015

Survey of Greenland Glacier area changes

The 45 largest marine terminating glaciers in Greenland are annually surveyed by PROMICE to measure their frontal positions. The results indicate not only a widespread ice area loss, they also reinforce that these glaciers are sensitive indicators of climate change. We find statistical evidence that surface melting is important for glacier area change.

Marine-terminating glaciers

Marine-terminating glaciers are the outlets via which the inland ice sheet discharges to the ocean. When a glacier front is stationary, the iceberg calving (by area) is balanced by the seaward motion of the ice.

Survey work

PROMICE includes an annual survey of the front position of now 45 of the widest (and fastest) marine-terminating glaciers in Greenland.

The survey involves manually digitizing the glacier fronts in satellite imagery. We must be diligent searching for cloud free images. The survey began with the launch of Landsat 7 in 1999 and is still running. We update the survey in September each year.

Net ice loss

The surveyed glaciers have collectively lost an area of 1799 km^2, twenty times the area of Manhattan Island, New York or Copenhagen (88.25 km^2) or three times the area of Bornholm (588 km^2).

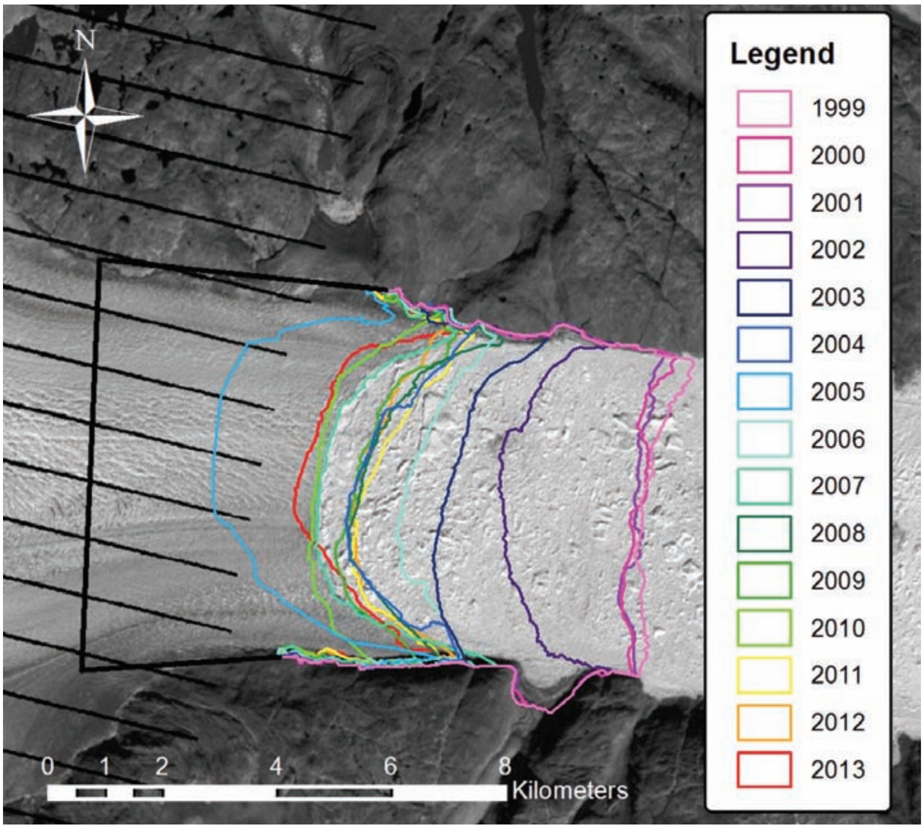

Fifteen frontal positions of Helheimgletscher in the period 1999–2013. The background image is from Landsat 7, 19 August 2007.

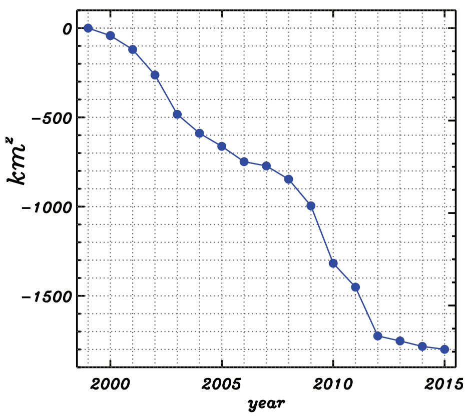

Cumulative net area change at the 45 of the widest and fastest marine-terminating glaciers of the Greenland ice sheet (after Jensen et al. (submitted) and Box & Decker 2011).

Climate Sensitivity

Greenland glacier fronts indicate the climate by advancing in the cold season and retreating in the warm season. The winter advance can produce a seasonal floating ice shelf that is lost the following warm season. The springtime retreat is promoted by surface melting producing liquid water draining down into crevasses driving a process called *hydrofracture* that can quickly disintegrate ice shelves.

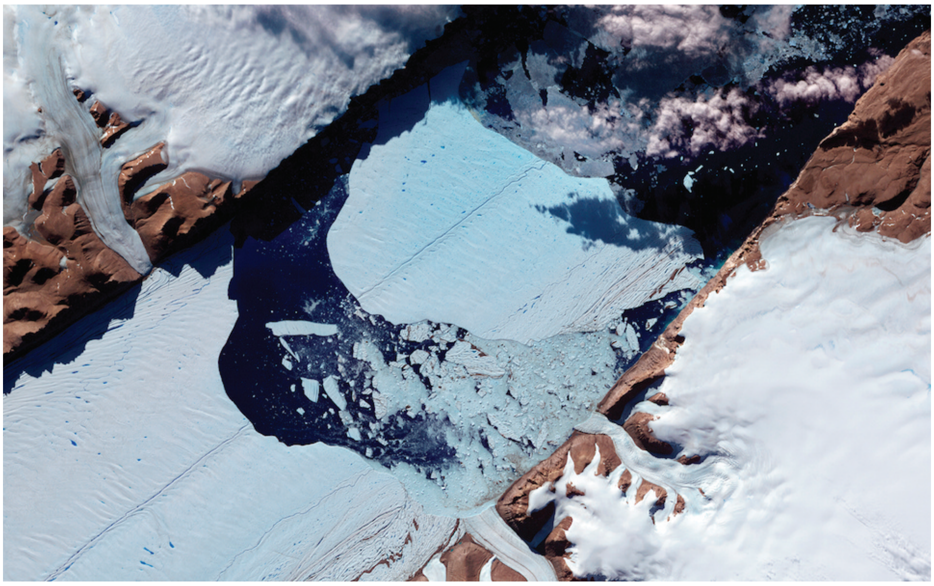

Confirming that a massive 140 km² calving like this one that occurred at Petermann Gletscher in the record warm summer of 2012, was the result of warm weather is difficult as it would require direct observations of hydrofracture like those conducted at Store Gletscher by GEUS. Photo: NASA.

Installation of (left) crevasse water monitor float and (right) crevasse strain gauge at Store Gletscher.

The PROMICE project measures the glacier front positions each year at the end of summer when the they have retreated most to be able to use them as climate indicators.

We find a significant statistical correlation between the date of seasonal minimum glacier front position and glacier latitude indicating that the calving season is shorter in north Greenland, consistent with a shorter melt season.

Further indication that surface melting is part of the ice area change story is that summer air temperatures correlate with the glacier area changes. At all 11 DMI stations we find a correlation consistent with the warmer the summer air temperature, the greater the net ice area loss at the 45 surveyed glaciers. At 4 of the 11 sites, the confidence in that correlation is above 95%. At 7 of the 11 sites, the confidence in that correlation is above 80%.

Work Cited

Box, J.E. & Decker, D.T. 2011: Greenland marine-terminating glacier area changes: 2000-2010. Ann. Glaciol. **52**, 91–98, http://dx.doi.org/10.3189/172756411799096312

Jensen, T., Box, J.E. & Hvidberg, C. A sensitivity study of yearly Greenland ice sheet marine terminating outlet glacier changes: 1999-2013, Journal of Glaciology, 15J085, submitted 30 Nov., 2015.

Further information

http://www.promice.dk

PROMICE

PROMICE is financed by the Ministry of Energy, Utilities and Climate through the climate support programme DANCEA (Danish Cooperation for Environment in the Arctic), which is managed by the Danish Energy Agency.

- The purpose of PROMICE is to monitor the mass loss of the Greenland ice sheet, both the melting on the surface and the volume of icebergs discharged into the sea
- PROMICE is headed in Denmark by GEUS in cooperation with DTU Space and Asiaq in Greenland. Furthermore the programme collaborates with the Danish Meteorological Institute and foreign universities and authorities.
- Read more about PROMICE on promice.org, where you can find photos and videos, get direct access to measuring data from the ice sheet and the PROMICE outreach material. On the website you can also subscribe to our newsletter.
- Information can also be found on porlarportal.org a new website where Danish research institutions display the results of their monitoring of the Greenland ice sheet and the sea ice in the Arctic.

Authors
J.E. Box & K. Hansen
Geological Survey of Denmark and Greenland, Copenhagen, Denmark

Editor
Signe Bech Andersen, senior researcher, GEUS.

Layout
Henrik Klinge Pedersen, GEUS.

Geological Survey of Denmark and Greenland
Øster voldgade 10
DK-1350 Copenhagen K
Denmark

Technical University of Denmark
Anker Engelunds Vej 1, 101A
DK-2800 Kgs. Lyngby
Denmark

Asiaq
Qatserisut 8, P.O. Box 1003
3900 Nuuk
Greenland

Ministry of Energy, Utilities and Climate
Stormgade 10–12
DK-1470 Copenhagen K
Denmark

Danish Energy Agency
Amaliegade 44
DK-1256 Copenhagen K
Denmark

Programme for Monitoring of the Greenland Ice Sheet

No 9 • 2015

How meltwater can create an ice lid in the snow blanket over the Greenland ice sheet

Cores extracted from multi-year snow on the Greenland ice sheet give new insights into its capability to store meltwater through refreezing. This refreezing process was previously believed to be an efficient buffer absorbing meltwater, thus delaying sea-level rise – however, now we find this is not always the case.

What started as a mission to learn more about physical processes in multi-year snow (firn) blanketing the large interior of the Greenland ice sheet, turned into a large, in-depth study on how meltwater refreezes in firn. It took three expeditions to Greenland to gather all the evidence we needed. In spring 2012, the GEUS glaciology group coordinated a week-long expedition to the accumulation area of the ice sheet, at 1840 m above sea level, east of Kangerlussuaq (Fig. 1). Central to the campaign was to install thermistor strings in the firn and to extract as many firn cores as time would allow (Fig. 2) to be able to determine energy and mass fluxes into the firn. The site had already been monitored using mass-balance stakes (Utrecht University) and a weather station (GEUS) in the previous years.

We anticipated finding firn with some ice layers, the site being located high enough in the ice sheet interior for annual snowfall to be larger than melt, but low enough for substantial melting to occur in summer. Yet we found evidence of large melting in previous years judging from a layer of six metres of mostly solid ice (refrozen meltwater), concealed by roughly one metre of snow on top. It soon became evident that we had to return the year after to find out how far

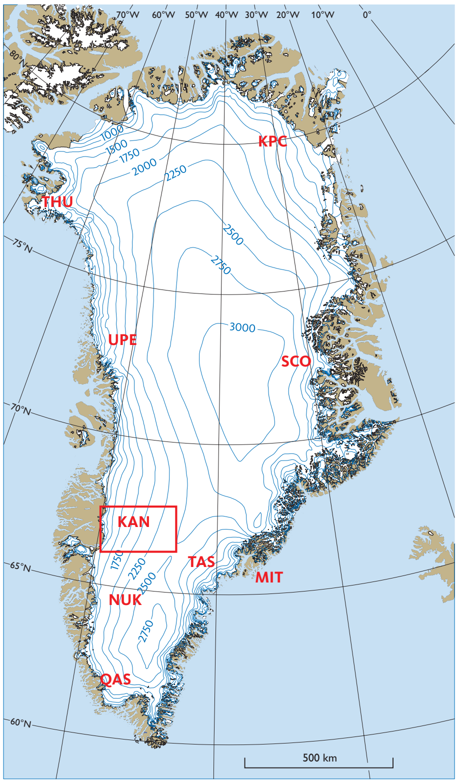

Figure 1. The region of core extractions (red box) and the regions with PROMICE weather stations (red lables).

these ice layers stretched horizontally, and what they meant for the capability of the ice sheet to store meltwater in the cold firn underneath this ice lid. It proved the start of a fruitful collaboration with the Cooperative Institute for Research in Environmental Sciences (CIRES) in Boulder, USA.

We did not have to wait long to learn about some of the consequences of the ice layer. In July 2012 the Greenland ice sheet was hit by the most widespread melting event in recorded history, with melt occurring even in the highest and generally coldest regions. The surface at our drill site was marked with a well-developed network of channels transporting meltwater to lower elevations (Fig. 3), in a region where meltwater had not lingered at the surface in summers before, but had always percolated into the firn. We suspected that the thick ice layers were preventing meltwater from refreezing locally, and urging it to flow towards the ocean.

The 2013 spring expedition set out to drill more firn cores, to a greater depth (up to 20 m), and for a larger region of the ice sheet (Fig. 1). Ground-penetrating radar was used in between the drill sites to confirm that our cores were representative of a larger region. Our scientific goals thus required us to move around with our tent camp making use of snow mobiles. In spite of harsh conditions including several storms and temperatures dropping to –40°C, the expedition was a great success.

The newly obtained data did not only confirm that the ice layers were vast and thick, but also that relatively great quantities of meltwater in 2012 could not find efficient passage through this ice lid into the porous space between the ice grains below. Thus the underlying firn is largely sealed, and it can no longer efficiently absorb meltwater, which instead runs into the sea, contributing to sea level rise. Yet previous findings on the ice sheet, predating the 2010 and 2012 high melt years, had suggested the likelihood of meltwater percolating and refreezing locally until all pore space in the firn had been filled. We added temporal perspective by also extracting firn cores at locations where other cores were drilled in the 1990s. From these we concluded that great changes occurred in the firn over this period, attributal only to an increase in local temperatures, increasing melting and the formation of ice layers in firn.

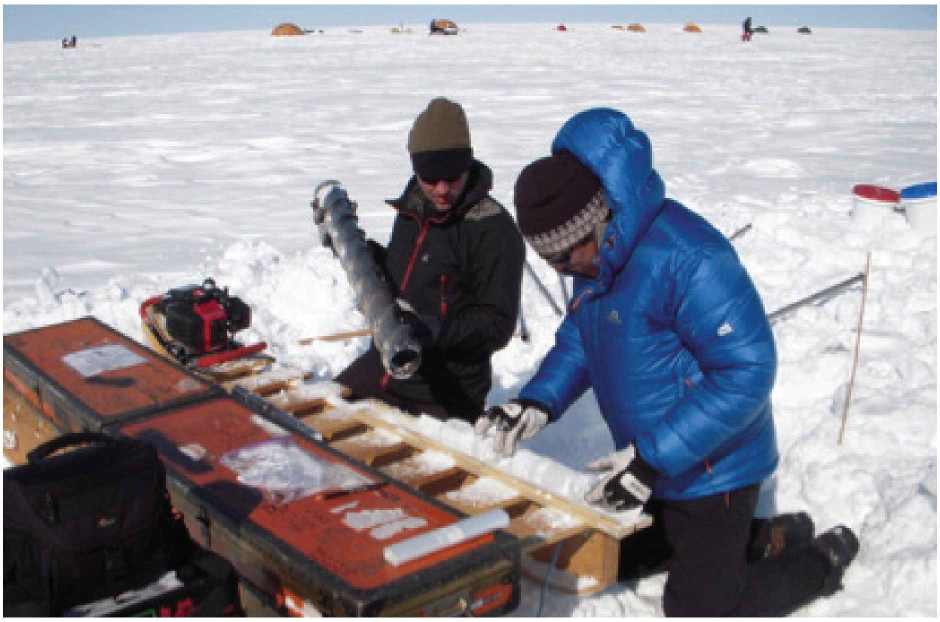

Figure 2. M. MacFerrin (CIRES) and H. Machguth (then GEUS) processing a segment of a firn core in May 2012. The camp is visible in the background.

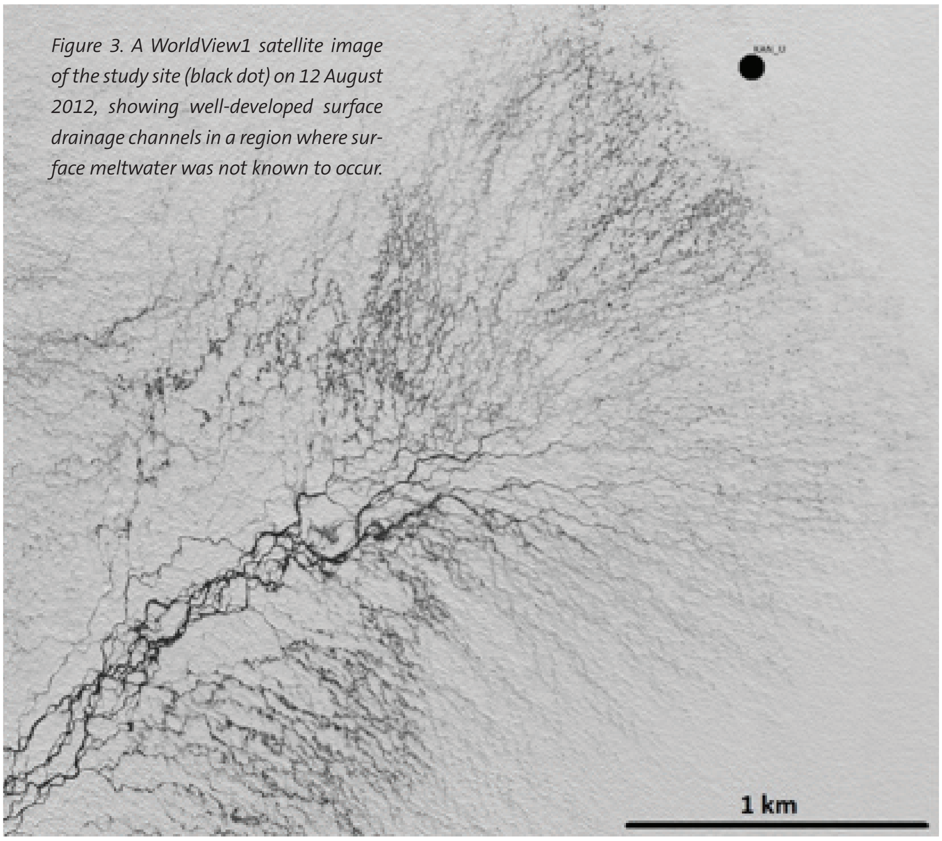

Figure 3. A WorldView1 satellite image of the study site (black dot) on 12 August 2012, showing well-developed surface drainage channels in a region where surface meltwater was not known to occur.

These findings formed the basis of a study published in Nature Climate Change (Machguth et al. 2015), and supported several other studies of Greenland firn (e.g. Charalampidis et al. 2015). In 2015 another expedition took place, adding even more perspective, and with the potential to investigate firn processes over the entire Greenland ice sheet in a CIRES-run project named FirnCover. All three expeditions were done in tight collaboration between CIRES (funded by NASA) and GEUS. GEUS involvement relied on contributions from the projects GAP, REFREEZE, RETAIN, Svali and PROMICE.

Work Cited

Charalampidis, C., Van, As D., Box, J.E., Van den Broeke, M.R., Colgan, W.T., Doyle, S.H., Hubbard, A.L., MacFerrin, M., Machguth, H. & Smeets, C. 2015: Changing surface–atmosphere energy exchange and refreezing capacity of the lower accumulation area, West Greenland. Cryosph. 9, 2163-2181 (doi:10.5194/tc-9-2163-2015)

Machguth H, MacFerrin M, Van As D, Box JE, Charalampidis C, Colgan W, Fausto RS, Meijer HAJ, Mosley-Thompson E and Van de Wal RSW (2016) Greenland meltwater storage in firn limited by near-surface ice formation. Nature Clim. Change (doi:10.1038/nclimate2899)

Further information

http://www.promice.dk
http://www.undergroundchannel.dk/an-icelid-more-greenland-meltwater

PROMICE

PROMICE is financed by the Ministry of Energy, Utilities and Climate through the climate support programme DANCEA (Danish Cooperation for Environment in the Arctic), which is managed by the Danish Energy Agency.

- The purpose of PROMICE is to monitor the mass loss of the Greenland ice sheet, both the melting on the surface and the volume of icebergs discharged into the sea
- PROMICE is headed in Denmark by GEUS in cooperation with DTU Space and Asiaq in Greenland. Furthermore the programme collaborates with the Danish Meteorological Institute and foreign universities and authorities.
- Read more about PROMICE on promice.org, where you can find photos and videos, get direct access to measuring data from the ice sheet and the PROMICE outreach material. On the website you can also subscribe to our newsletter.
- Information can also be found on porlarportal.org a new website where Danish research institutions display the results of their monitoring of the Greenland ice sheet and the sea ice in the Arctic.

Authors
Dirk van As (GEUS), Horst Machguth (UZH, Switzerland) and Mike MacFerrin (CIRES, USA)

Editors
Signe Bech Andersen, senior researcher, GEUS.
Jane Holst, GEUS.

Layout
Henrik Klinge Pedersen, GEUS.

Geological Survey of Denmark and Greenland
Øster voldgade 10
DK-1350 Copenhagen K
Denmark

Technical University of Denmark
Anker Engelunds Vej 1, 101A
DK-2800 Kgs. Lyngby
Denmark

Asiaq
Qatserisut 8, P.O. Box 1003
3900 Nuuk
Greenland

Ministry of Energy, Utilities and Climate
Stormgade 10–12
DK-1470 Copenhagen K
Denmark

Danish Energy Agency
Amaliegade 44
DK-1256 Copenhagen K
Denmark

Automatic weather stations for basic and applied glaciological research

Michele Citterio, Dirk van As, Andreas P. Ahlstrøm, Morten L. Andersen, Signe B. Andersen, Jason E. Box, Charalampos Charalampidis, William T. Colgan, Robert S. Fausto, Søren Nielsen and Martin Veicherts

Since the early 1980s, the Geological Survey of Denmark and Greenland (GEUS) glaciology group has developed automatic weather stations (AWSs) and operated them on the Greenland ice sheet and on local glaciers to support glaciological research and monitoring projects (e.g. Olesen & Braithwaite 1989; Ahlstrøm *et al.* 2008). GEUS has also operated AWSs in connection with consultancy services in relation to mining and hydropower pre-feasibility studies (Colgan *et al.* 2015). Over the years, the design of the AWS has evolved, partly due to technological advances and partly due to lessons learned in the field. At the same time, we have kept the initial goal in focus: long-term, year-round accurate recording of ice ablation, snow depth and the physical parameters that determine the energy budget of glacierised surfaces. GEUS has an extensive record operating AWSs in the harsh Arctic environment of the diverse ablation areas of the Greenland ice sheet, glaciers and ice caps (Fig. 1). The current GEUS-type AWS (Fig. 2) records meteorological, surface and sub-surface variables, including accumulation and ablation, as well as for example ice velocity. A large part of the data is transmitted by satellite near real-time to support ongoing applications, field activities and the planning of maintenance visits. The data have been essential for assessing the impact of climate change on land ice. The data are also crucial for calibration and validation of satellite-based observations and climate models (van As *et al.* 2014).

The current version of the GEUS AWS was developed in 2007 (sensors and tripod) and in 2008 (data logger, satellite data telemetry and power management) coinciding with the establishment of the Programme for the Monitoring of the Greenland ice sheet (PROMICE; Ahlstrøm *et al.* 2008) and the GlacioBasis Programme monitoring an ice cap in A.P. Olsen Land in North-East Greenland (APO; Fig. 1). In con-

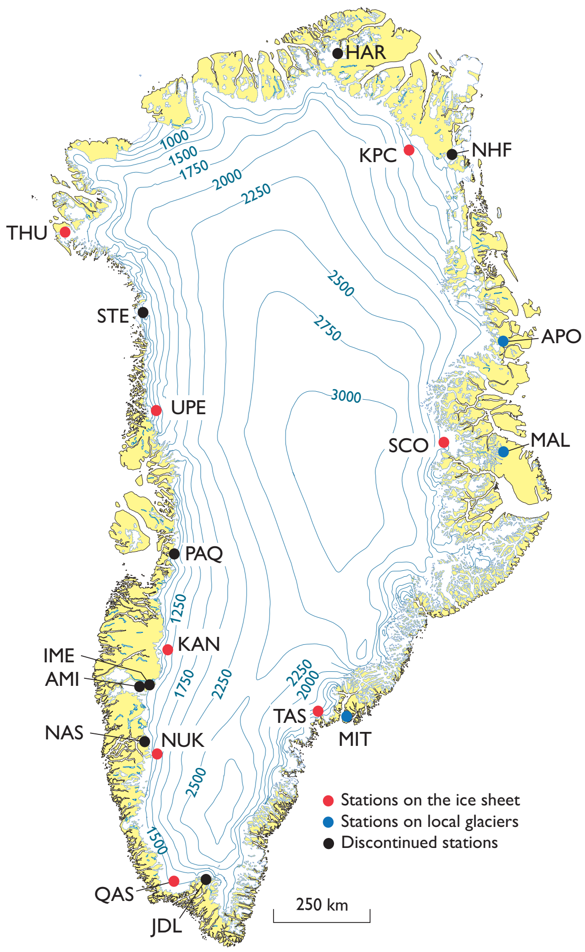

Fig. 1. Sites monitored by the Geological Survey of Denmark and Greenland with automatic weather stations. The currently active sites on the Greenland ice sheet (red dots) consist of transects with two or three stations at different elevations. QAS: Qassimiut (2000–). NUK: Qamanaarsuup Sermia, Nuuk (1979–1989, 2008–). KAN: Kangerlussuaq (2008–). UPE: Upernavik (2008–). THU: Tuto Ramp, Thule (2008–). KPC: Kronprins Christian Land (1993–1994, 2008–). SCO: Violin Gletscher near Scoresby Sund (2008–). TAS: Tasiilaq (2004–). Currently active sites on local glaciers (blue dots), with one to three AWS per site are APO: ice cap in A.P. Olsen Land (2008–). MAL: Malmbjerg (2008–). MIT: Mittivakkat glacier (1995–). Sites where GEUS had automatic weather stations in the past (black dots), some of which in cooperation with the former Greenland Technical Organisation: JDL: Nordbogletscher, Johan Dahl Land (1977–1983). AMI Amitsuloq Ice Cap (1981–1990). PAQ: Pakitsoq (1984–1987). NAS: Narsap Sermia (2003–2006). ISO: Isortuarsuup Tasia (1984–1987). NHF: Nioghalvfjerdsfjorden (1996–1997). HAR: Hare Gletscher (1994–1995). STE: Steenstrup Gletscher (2004–2008). IME: Imersuaq (1999–2002). STS: Storstrømmen (1989–1994).

nection with consulting work, the first AWS with the new design (MAL; Fig. 1) was installed in 2008 for Quadra Mining Ltd., Vancouver, Canada (now KGHM International Ltd., Lubin, Poland) near the Malmbjerg molybdenum occurrence in Stauning Alper, central East Greenland (Citterio *et al.* 2009), followed in 2008 and 2009 by three more stations on the ice sheet in the Kangerlussuaq region (KAN, Fig. 1). These stations are part of the Greenland Analogue Project (GAP; van As *et al.* 2012) for SKB, the Swedish Nuclear Fuel and Waste Management Company (Stockholm, Sweden) and Posiva Oy (Olkiluoto, Eurajoki, Finland).

The GEUS AWS model in use now is a reliable tool that is adapted to the environmental and logistical conditions of polar regions. It has a proven record of more than 150 station-years of deployment in Greenland since its introduction in 2007–2008, and a success rate of *c.* 90% defined as the fraction of months with more than 80% valid air-temperature measurements over the total deployment time of the 25 stations in the field. The rest of this paper focuses on the technical aspects of the GEUS AWS, and provides an overview of its design and capabilities.

Station requirements

The GEUS AWS is the fundamental component of a monitoring network which can include numerous stations, a satellite data link, and a receiving database where telemetry data are decoded and validated before further analysis and dissemination. The cost-effective AWS delivers timely research-quality data year-round from glacier ablation areas in remote locations. The AWS must therefore require little maintenance, with a target of maximum one visit per year. Power generation and battery capacity must be sufficient to operate through the polar night. Data quality must be assured by accurate measurement techniques including aspiration of radiation shields and tilt correction of (shortwave) radiometer measurements. The mechanical construction of the station must keep the sensors at a constant height above the ice surface, which can ablate more than 9 m of ice per year in South Greenland (van As *et al.* 2011), and the station must be able to survive burial in snow in the winter months. Timeliness of data availability and the assessment of station health demand satellite data telemetry both in summer and winter. To our knowledge, no other commercially available AWS satisfies all these requirements.

Sensors, data logger and telemetry

The GEUS AWS can be fitted with any sensor, but the standard AWS measures air temperature and humidity,

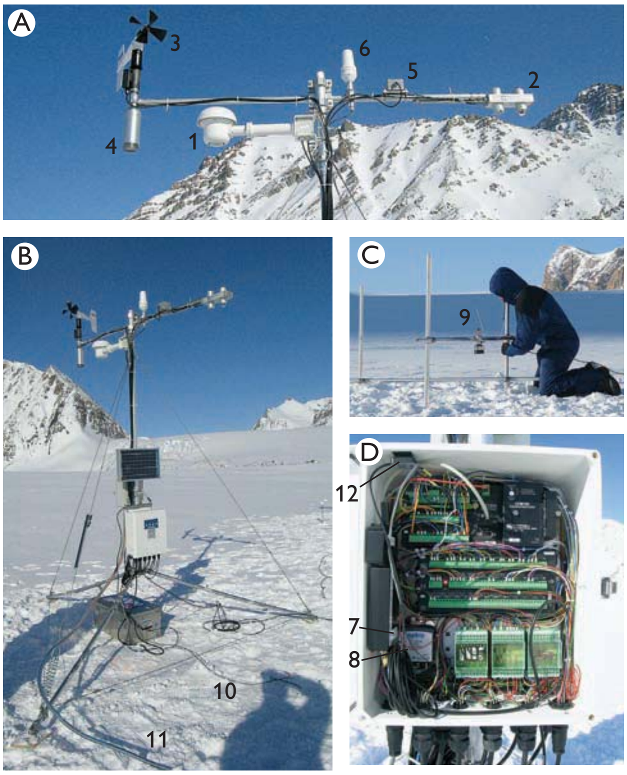

Fig. 2. Standard sensor suite of the automatic weather station on Arcturus Gletscher at the Malmbjerg molybdenum prospect. **A**: The main instrument boom. **B**: The tripod and the sites of the thermistor string and pressure-transducer assembly drilled into the ice. **C**: The sonic ranger- stake frame drilled into the ice. **D**: The inside of the data logger enclosure. The numbers refer to the list in Table 1.

wind speed and direction, atmospheric pressure, downward and reflected solar shortwave radiation, downward and upward longwave radiation, subsurface (ice) temperatures, snow depth, ice ablation, GPS position, as well as diagnostic parameters such as battery voltage and ventilator power consumption, and 2-axes station tilt necessary for correcting shortwave radiation measurements. Table 1 lists sensor types, their measurement heights and uncertainty as specified by the manufacturers.

The GEUS AWS is designed to minimise measurement errors where possible, for instance by actively aspirating the radiation shield inside which air-temperature and humidity sensors are located. Successful error detection and management increases with user experience and specialist knowledge.

Two of the sensors listed in Table 1 are designed and manufactured in-house at GEUS for use on ice: the 8-levels thermistor string and the pressure transducer assembly (PTA) that measure ice ablation (Fausto *et al.* 2012). The PTA works by relating decrease of bottom hydraulic pressure (corrected for atmospheric pressure), measured inside an antifreeze-mixture filled hose drilled into the ice, to surface

Table 1. Current sensors used on a standard GEUS automatic weather station

	Parameter and sensor height	Manufacturer, type and sensor accuracy
1.	Air temperature and relative humidity, 2.7 m	Rotronic MP102H with Pt100 and HC2-S3 probe (±0.1 K, ± 0.8% rh, at 23°C ± 5 K), housed in a RS12T aspirated shield
2.	Radiation (downward and reflected solar shortwave, downward and upward longwave; 2.9 m)	Kipp & Zonen CNR1 (uncertainty in daily totals < 10%) or CNR4 (uncertainty in daily totals < 5% shortwave, < 10% longwave)
3.	Wind speed and direction, 3.1 m	R.M. Young 05103-5 (± 0.3 ms^{-1} or 1%, ± 3°, non-riming conditions)
4.	Snow depth	Campbell Scientific SR50 or SR50A (± 1 cm or 0.4%)
5.	2-axes radiometer tilt	HL Planar NS-25/E2 in GEUS assembly (± 0.2°)
6.	Iridium satellite antenna	Iridium AT1621-142 quad-helix
7.	Iridium SBD modem	u-blox NEO module
7.	Iridium SBD modem	NAL Research SBD-9601 or SBD-9602
8.	Atmospheric pressure	Setra model 278 (± 2.5 hPa, at –40 to 60°C)
9.	Ice ablation and snow depth	Campbell Scientific SR50 or SR50A (± 1 cm or 0.4%)
10.	Subsurface temperature profile	GEUS thermistor string with 8 RS Components thermistors 151-243 (± 0.2°C, at 0°C)
11.	Ice ablation	GEUS PTA with Ørum & Jensen Elektronik NT1400 or NT1700 (± 2.5 cm)
12.	GPS antenna	Trimble P/N 56237-40 active ceramic patch

The numbers refer to Fig. 2 where the positions of the sensors on an automatic weather station are shown.The heights of the sensors above the surface are indicative. The accurate heights are measured before and after every maintenance visit.

lowering due to ice ablation. Both the PTA and the thermistor string can easily be interfaced to most data loggers.

All analog and digital sensors are connected to a Campbell CR1000 data logger housed in a watertight enclosure together with a Campbell AM16/32A analog multiplexer and supporting circuitry. The logger is programmed to record in 10-minute cycles throughout the year. The only exception is the GPS, which is not needed at such a high rate and is activated less frequently in order to economise power. The Campbell CR1000 data logger is an established platform that is widely used in polar climates both in the Arctic and in Antarctica (Lazzara *et al.* 2012). The multiplexer is configured to support half-bridge measurement of thermistors from up to four 8-level thermistor strings (only one is normally used), in addition to 32 single-ended or 16 differential analog measurements (only six of each type are normally used), providing large flexibility for customised sensor suites.

The main local data storage is a removable flashcard rated for operation over extended temperature ranges. For reference, a 256 MB card will log in excess of 7 years of 10-minute records. To provide redundancy of data storage, the internal logger memory is configured to store 1-hour average records

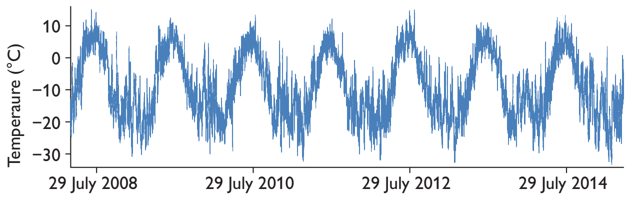

Fig. 3. An example of 10-minute observations of air temperatures from 2008 to 2015 from the APO_M station on an ice cap in A.P. Olsen Land in North-East Greenland.

and can hold in excess of one year of data as a backup for the flashcard. Data can be retrieved during on-site maintenance by swapping the flashcard or downloading its content to a laptop. The robustness of the system is illustrated in Fig. 3 by an uninterrupted 2008–2015 time series from the APO_M station in North-East Greenland, the first AWS built entirely according to the current GEUS design. After seven years in the field, this station still employs the original electronics, telemetry, battery and tripod hardware although sensors have been periodically replaced according to a scheduled recalibration plan.

Satellite data telemetry can transmit up to 340 bytes per message through the Iridium short burst of data (SBD) service. The program running on the CR1000 data logger implements a full software handshake with the transmitter to ensure that a satellite is in view and that data are correctly transferred from the logger to the transmitter and the Iridium satellite. If no acknowledgement of successful transmission is received from the satellite, the data logger will retry the transmission once, or queue the unsent message for delivery at a later time, depending on Iridium service availability. This mode of operation ensures a low rate of message loss and relatively low power consumption by avoiding unnecessary transmission attempts. The stations binary-encode data before transmission, reducing data transmission costs by about 2/3. Further transmission costs can be saved by transmitting the less transient variables at longer intervals.

Power

The long polar night and low temperatures exert a strong influence on the AWS design. The AWS operates on solar power and rechargeable sealed lead-acid batteries for a nominal total of 112 Ah at 12 V. The power system is composed of the main unregulated 12 V power rail permanently supplying the data logger directly from the batteries, two 12 V unregulated rails controlled by software through two external solid-state switches, and one switched 5 V regulated rail under direct data logger control. This arrangement allows independent powering up of the radiation shield aspirator fan, the GPS and satellite transmitter, the 5 V loads of the sonic rangers, temperature and humidity sensors, tilt meter and multiplexer. A single 10 W solar panel is wired to the main 12 V rail through a power Schottky diode to prevent that the solar panel drains the battery during the winter months, and to eliminate the need for a charge regulator, which occasionally failed in previous AWS designs.

A software-controlled low-power mode is activated when battery voltage under load falls below a configurable threshold (set to 11.5 V), which is never reached in normal circumstances. In low-power mode, operation continues almost as normal, but the most power-demanding functions (aspiration fan, satellite telemetry and GPS) are deactivated. The low-power mode is exited once solar charging brings the battery sufficiently above the voltage threshold. The software can be configured for polar day and night operation, for instance to reduce data transmission rates during winter. The typical monthly power requirements of a GEUS AWS as configured for PROMICE is 17 Ah in summer, 11 Ah in winter and 1.3 Ah in low-power mode.

Tripod and sonic ranger frame

The tripod is constructed from 1″ and 1.5″ aluminium tubes with steel wires connecting legs and mast in a tetrahedral structure for a stable free-floating tripod. Most of the sensors are fixed to a horizontal boom at *c.* 2.9 m above surface. The battery box, which weighs *c.* 50 kg, is suspended under the mast to improve station stability by increasing the AWS mass and lowering the centre of gravity. The tripod can be folded and transported in a small helicopter. During maintenance visits, which normally take 3–4 hours and include replacements of sensors due for recalibration, re-drilling of sensors and occasional repairs, the tripod can be easily tilted so that it does not have to be disassembled. The sonic ranger frame is also built from 1″ aluminium tubes, and its three vertical legs are drilled into the ice a few metres away from the AWS tripod.

Concluding remarks

The GEUS AWS has been developed, produced and deployed operationally by GEUS, and supplied to partners within Denmark and abroad. It is a proven solution for a wide range of basic and applied glaciological research in Arctic and alpine settings and is available through research collaborations or commercial sale. The standard design can accommodate significant expansion of the sensor suite. The GEUS AWS is readily available and supported as a stand-alone or as a component of wider services including field deployment, maintenance, training and data management and analysis.

Acknowledgements

We thank Ole B. Olesen, Carl E. Bøggild, Wim Boot, Peer Jørgensen, and other people who were instrumental in the technical development of the GEUS AWS over the years. The PROMICE and GlacioBasis monitoring programmes are funded by the Danish Energy Agency (ENS).

References

Ahlstrøm, A.P. and the PROMICE project team 2008: A new programme for monitoring the mass loss of the Greenland ice sheet. Geological Survey of Denmark and Greenland Bulletin **15**, 61–64.

Citterio, M., Mottram, R., Larsen, S.H. & Ahlstrøm, A.P. 2009: Glaciological investigations at the Malmbjerg mining prospect, central East Greenland. Geological Survey of Denmark and Greenland Bulletin **17**, 73–76.

Colgan, W., Thomsen, H.H. & Citterio, M. 2015: Unique applied glaciology challenges of proglacial mining. Geological Survey of Denmark and Greenland Bulletin **33**, 61–64.

Fausto, R.S., van As, D., Ahlstrøm, A.P. & Citterio, M. 2012: Assessing the accuracy of Greenland ice sheet ice ablation measurements by pressure transducers. Journal of Glaciology **58**, 1144–1150.

Lazzara, M.A., Weidner, G.A., Keller, L.M., Thom, J.E. & Cassano, J.J. 2012: Antarctic automatic weather station program: 30 years of polar observation. Bulletin of the American Meteorological Society **93**, 1519–1537.

Olesen, O.B. & Braithwaite, R.J. 1989: Field stations for glacier-climate research, West Greenland. In: Oerlemans, J. (ed.): Glacier fluctuations and climatic change, 207–218. Dordrecht: Kluwer Academic Publishers.

Van As, D., Fausto, R.S. & the PROMICE project team 2011: Programme for monitoring of the Greenland Ice Sheet (PROMICE): first temperature and ablation records. Geological Survey of Denmark and Greenland Bulletin **23**, 73–76.

Van As, D., Hubbard, A.L., Hasholt, B., Mikkelsen, A.B., van den Broeke, M.R. & Fausto, R.S. 2012: Large surface meltwater discharge from the Kangerlussuaq sector of the Greenland Ice Sheet during the record-warm year 2010 explained by detailed energy balance observations. The Cryosphere **6**, 199–209.

Van As, D. *et al.* 2014: Increasing meltwater discharge from the Nuuk region of the Greenland ice sheet and implications for mass balance (1960–2012). Journal of Glaciology **60**, 314–322

Authors' address
Geological Survey of Denmark and Greenland, Øster Voldgade 10, DK-1350 Copenhagen K, Denmark. E-mail: *mcit@geus.dk*